STRUCTURAL FIRE PERFORMANCE OF FIBER REINFORCED HSC COLUMNS USING OPENSEES SOFTWARE

by

Saif ur Rehman

(NUST201362915MSCEE15213F)

A Thesis

Submitted in partial fulfillment of the requirements of the degree of

Master of Science

In

National Institute of Civil Engineering

National University of Science and Technology

Islamabad, Pakistan

April 2017

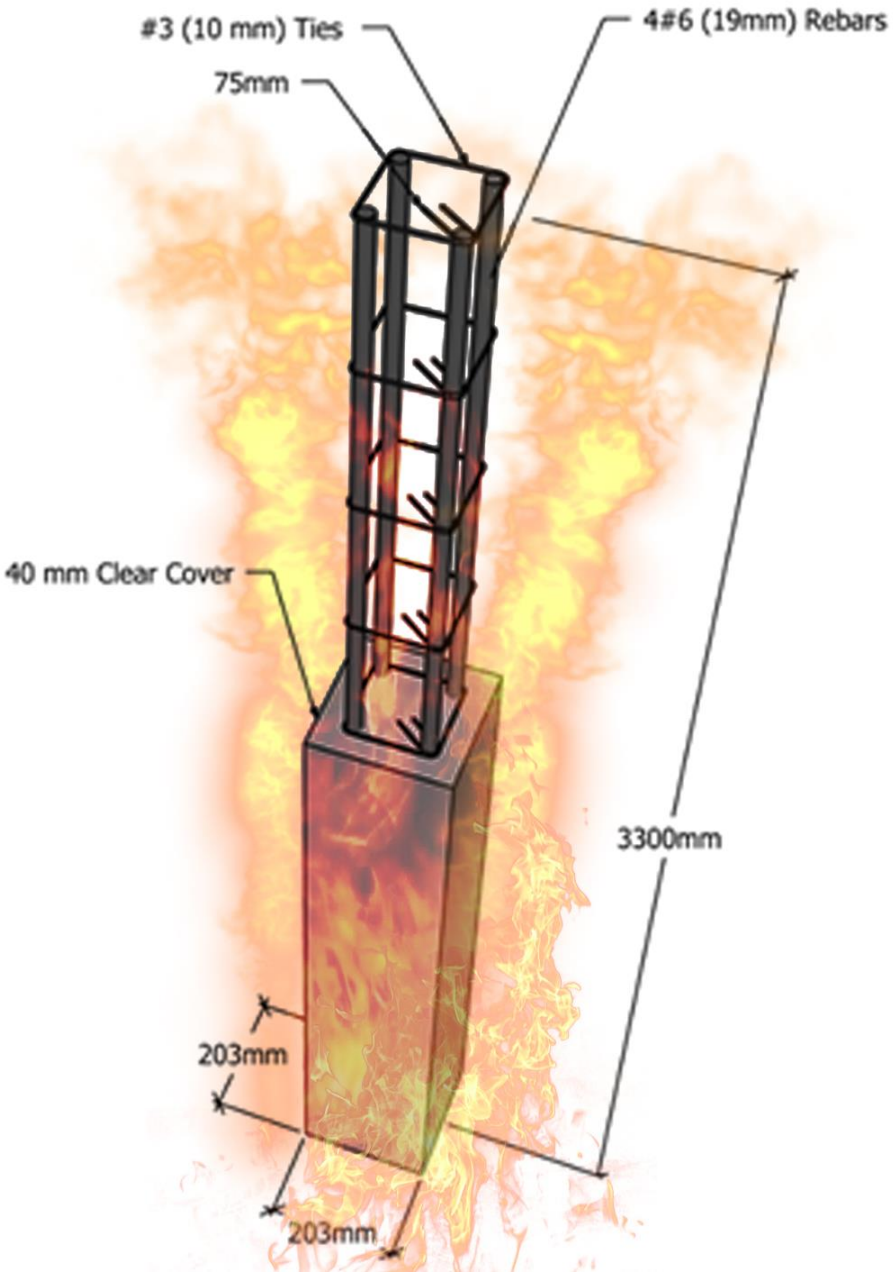

FIBRE REINFORCED HSC COLUMN UNDER FIRE

This is to certify that the

thesis titled

STRUCTURAL FIRE PERFORMANCE OF FIBER REINFORCED HSC COLUMNS USING OPENSEES SOFTWARE

submitted by

topo

Saif ur Rehman

NUST201363915MSCEE15213F

has been accepted towards the partial fulfillment

of the requirements for the degree

of

Master of Science

in

Structural Engineering

_____

Dr. Syed Hassan Farooq (Advisor)
Associate Professor
NUST Institute of Civil Engineering (NICE)
School of Civil and Environmental Engineering (SCEE)
National University of Sciences and Technology (NUST), Islamabad, Pakistan

DEDICATED TO

MY FAMILY AND PARENTS

ACKNOWLEDGEMENTS

All praise be to ALLAH the Almighty the Exalted, the Lord of all the worlds and gratitude to the last Prophet MUHAMMAD (PBUH).

This acknowledgement will hardly justify my sense of profound veneration for my revered supervisor ***Dr. Syed Hassan Farooq*** for his indelible help, unprecedented motivation, constructive criticism and perceptive encouragement.

I am highly honored to ***Prof. Dr. Syed Ali Rizwan*** for his expert guidance during my MS program and research. I also sincerely thank other committee members for their valuable suggestions, thoughtful criticism and sustained encouragement during pursuance of my research.

I have great regards and immense gratitude to my colleagues Shahzada Khurram and Muhammad Safdar for their whole hearted and ever available help, moral support and comradeship.

I am grateful to all the faculty and staff of National Institute of Civil Engineering for their guidance and support in every aspect for the completion of this thesis. I am grateful to National University of Sciences and Technology for the financial support of the complete research work.

I extend special thanks to my family for their help and strength owing to which I could work peacefully.

Saif ur Rehman

ABSTRACT

Fire testing / fire performance evaluation of reinforced concrete structures is a time, effort and resource heavy discourse. Analytical approach to establish fire resistance rating and fire performance of reinforced concrete (RC) structures is a viable alternative and helps to simulate the fire response of structures. OpenSees (Open System for Earthquake Engineering Simulation) is an object oriented software framework used to create finite element applications and then simulate the response of structural systems subjected to earthquake. The OpenSees developers group in School of Engineering, University of Edinburgh have successfully conducted the research to add structures-in-fire modelling capability into the OpenSees framework by utilizing its well-designed software architecture (Jiang, Jiang, Kotsovinos, Zhang, Usmani, McKenna and Li, 2013). By adopting object-oriented programming paradigm, the software structure is consistent with that of OpenSees, which made it possible to reuse some of the existing components of software whereby introducing fire related components in it.

At present, the use of high performance concrete (HPC) is becoming more popular due to the improvements in structural performance such as high strength and durability that it can provide compared to conventional NSC (Kodur and Dwaikat, 2008). However, OpenSees modeling module lacks material properties of many concrete types such as High Performance Concrete (HPC) and Fiber Reinforced Concrete (FRC). Thus, there is a dire need to incorporate such material properties in existing OpenSees Software and make it a more versatile tool to simulate behavior of all types of concrete infrastructures.

TABLE OF CONTENTS

ACKNOWLEDGEMENTS v
ABSTRACT
TABLE OF CONTENTS vii
LIST OF TABLES xii
CHAPTER 1 1
INTRODUCTION 1
1.1 General 1
1.2 Problem Statement 1
1.3 Methodology 2
1.4 Objectives 3
1.5 Scope and Limitation 3
1.6 Significance 4
1.6 Thesis Organisation 4
CHAPTER 2 6
LITERATURE REVIEW 6
2.1 General 6
2.2 Properties that effect Concrete at Elevated Temperature 6
2.3 Thermal Properties of Concrete at Elevated Temperatures 7
2.3.1 General 7
2.3.2 Thermal Conductivity 7
2.3.3 Specific Heat 9
2.3.4 Thermal Expansion 11
2.3.5 Mass Loss 13
2.3.6 Summary 15
2.4 Mechanical Properties of Concrete 16
2.4.1 General 16
2.4.2 Compressive Strength 16
2.4.3 Tensile Strength 21
2.4.4 Modulus of Elasticity 26
2.4.5 Stress Strain Curves 28

CHAPTER 3 33
Analytical Element Modelling 33
3.1 General 33
3.2 Modification of Open Sees 33
3.2.1 Existing material Library of Open Sees 33
3.2.2 Incorporating New Concrete Material in Open Sees 37
3.2.3 Relationship for Thermal Properties 37
3.2.3.1 Relations for Thermal Conductivity 38
3.2.3.2 Relations for Specific Heat 38
3.2.3.3 Relations for Thermal Expansion 38
3.2.3.4 Relations for Mass Loss 39
3.2.4 Relationships for Mechanical Properties 39
3.2.4.1 General 39
3.2.4.2 Relations for Compressive Strength 40
3.2.4.3 Relations for Splitting Tensile Strength 40
3.2.4.4 Relations for Elastic Modulus 41
3.2.4.5 Summary of Thermal properties of HSC at elevated temperature 41
3.2.5 Input file of Concrete02thermalHCC 42
3.2.6 Adding new material Code in OpenSees 42
3.2.7 Testing the New Material Code 42
3.3 Modelling of RCC Columns in OpenSees 42
3.3.1 Writing Input File of OpenSees for RCC Column 43
3.3.2 Defining nodes in the software 45
3.3.3 Defining section of the column 45
3.3.4 Defining Mild Steel Bars in the software 46
3.3.5 Defining Thermal Load 46
3.3.6 Defining Output Files 47
3.4 Summary 47
CHAPTER 4 48
Results and Discussion 48
4.1 General 48
4.2 Selection of specifications for RC Column 48
4.3 Fire Scenario and Heat Transfer Rate 51
4.3.1 Fire Scenario used for the studies 51

4.3.2 Temperature used for Columns at different fibers 52
4.4 Data Obtained and Observations 53
4.4.1 Structural Response 53
4.4.2 Axial Deformation 53
4.4.2.1 Axial Deformation of HSCs Column 53
4.4.2.1 Axial Deformation of HSCh Column 54
4.4.3 Lateral Deformation 55
4.4.3.1 Lateral Deformation in HSCs Column 55
4.4.3.2 Lateral Deformation in HSCh Column 56
4.5 Validation of the Results 56
4.5.1 Material Properties 59
4.5.2 Confinement of Concrete 59
4.5.3 End Conditions 59
4.5.4 Heat Transfer Rate 59
4.6 Summary 59
CHAPTER 5 61
Conclusions and Recommendations 61
5.1 General 61
5.2 Key Findings 61
5.3 Recommendations for Future Research 62
5.4 Research Impact 63
REFERENCES 64
APPENDIX A 71
APPENDIX B 81
APPENDIX C 87

LIST OF FIGURES

Figure 2.1 - Thermal conductivity of Normal Strength Concrete 8
Figure 2.2 – Measured Thermal Conductivity of HSC (plain and fiber reinforce) 9
Figure 2.3 - Variation in specific heat of NSC as a function of temperature 10
Figure 2.4 – Measured Specific Heat as function of temperature for plain and fiber reinforced HSC 11
Figure 2.5 – Variation in linear thermal expansion of NSC as a function of temperature 12
Figure 2.6 – Measured thermal expansion as a function of temperature for plain and fiber reinforced HSC 13
Figure 2.7 – Variation in mass of concrete with different aggregates as a function of temperature 14
Figure 2.8 – Variation in mass of NSC and HSC as a function of temperature 14
Figure 2.9 – Measured mass loss as a function of temperature for plain and fiber reinforced HSC 15
Figure 2.10 – Variation in relative compressive strength as function of temperature for NSC 18
Figure 2.11 – Variation in relative compressive strength as function of temperature for HSC 19
Figure 2.12 – Measured compressive strength of HSC and fiber reinforced HSC as function of temperature 20
Figure 2.13 – Measured relative compressive strength of HSC and fiber reinforced HSC as function of temperature .....
Figure 2.14 – Variation in relative splitting tensile strength as function of temperature 24
Figure 2.15 – Measured splitting tensile strength of HSC and fiber reinforced HSC as function of temperature 25
Figure 2.16 – Measured relative splitting tensile strength of HSC and fiber reinforced HSC as function of temperature 26
Figure 2.17 – Variation in elastic modulus as a function of temperature 28
Figure 2.18 – Typical load deformation of NSC at various temperature 30
Figure 2.19 – Typical load deformation of HSC at various temperatures 31
Figure 2.20 – High temperatures stress-strain curves for HSC 32
Figure 4.1 – Column elevation and cross section showing design details 49
Figure 4.2 – Time temperature curve for fire scenario 52
Figure 4.4 - Measured Axial Deformation in HSCs Column as a function of fire exposure time 53
Figure 4.5 - Measured Axial Deformation in HSCh Column as a function of fire exposure time 54
Figure 4.5 – Measured lateral deformation in HSCs Column as a function of fire exposure time 55
Figure 4.5 – Measured lateral deformation as a function of fire exposure time 56
Figure 4.6 Comparison of results of HSCs Column 57

Figure 4.6 Comparison of results of HSCh Column 57
Figure 4.7 Comparison of results of Lateral Deformation of HSCs Column 58
Figure 4.7 Comparison of results of Lateral Deformation of HSCh Column 58
Figure A.2: Stress-strains and forces in columns 73
Figure A.3 - Load-moment interaction diagram for HSC-S column 77

LIST OF TABLES

Table 3.1 High temperature property relationship for thermal and mechanical properties of HSC41

Table 4.1 – Design Parameters used for the column 49

Table 4.2 – Mix Proportions used for concrete columns 50

Table A.1 - Design parameters used for the columns 71

Table A.2 - Calculated factored capacities of HSC-S and HSC-H columns 74

Table A.3 - Calculation of nominal load and moment for P-M diagram for HSC-S column 76

Table A.3 - Load and moment capacity calculated by moment magnification method. 78

CHAPTER 1

INTRODUCTION

1.1 General

The most popular artificial material on Earth is neither steel nor plastic but it's concrete. The main reasons are its excellent strength, durability, ease of fabrication and fire resistance properties (Dwaikat, 2009). Recent researches have resulted in high performance concrete (HPC) with improved qualities like high strength concrete (HSC) having enhanced compressive strength, fiber reinforced concrete (FRC), Fly Ash Concrete (FAC) and Self-consolidating concrete (SCC). Though the Normal Strength Concrete (NSC) is very much fire resistant but the fire resistance of these newly developed concrete is questionable. The problem becomes more aggravated when we do not have any physical nondestructive technique available for fire testing / fire performance evaluation of structures.

1.2 Problem Statement

Numerous finite element softwares are presently being used for computational modelling and analysis of existing structures which are subjected to extreme external static or dynamic loads like strong winds, snow or earthquakes. However, there are very few institutions around the world who have included structural response to fire in their syllabi (Jiang, Usmani and Welch, 2011). The main reason is the lack of cheap and easily available computer software to carry out such analyses and the complicated and tedious nature of modeling of a possible real fire scenario, heat transfer mechanism to structure and then the structural response.

OpenSees (Open System for Earthquake Engineering Simulation) is a software framework which is totally object-oriented and is being used to create finite element applications into it and then simulate the possible response of structural systems which are subjected to earthquake. The OpenSees developers group in School of Engineering, University of Edinburgh have successfully conducted the research to add modelling capability of structures-in-fire into the OpenSees framework by utilizing its well-designed software architecture (Jiang, Jiang, Kotsovinos, Zhang, Usmani, McKenna and Li, 2013). However, OpenSees modeling module lacks material properties of many concrete types such as High Performance Concrete, High Strength Concrete and Fiber Reinforced Concrete etc. Thus, there is a dire need to incorporate such material properties in existing OpenSees Software and make it a more versatile tool to simulate behavior of all types of concrete infrastructures.

1.3 Methodology

Professor Asif Usmani has studied that how one can extend finite-element software to include the possibility of modeling reinforced structures subjected to fire load. Another advantage of extending the existing finite-element codes, as opposed to creating fire-specific applications, is because to ability to perform multi-hazard type analysis, e.g., fire following earthquake (Jiang, Jiang, Kotsovinos, Zhang, Usmani, McKenna and Li, 2013). Due to object oriented design and open source nature of this software, OpenSees framework is the best choice for this purpose. Although the fire analysis module has been created for OpenSees Software, there is not much information

OpenSees, is well known for its computational efficiency, flexibility, extensibility and portability (McKenna, Scott and Fenves, 2009). One can conveniently introduce into OpenSees a new element, a new material model or even a new analysis procedure without the knowledge of every single piece of code in the framework (Jiang, Usmani and Welch, 2011). Keeping above in view, the OpenSees software has been chosen to be used for fire modelling of structures after introducing different types of HPC with and without fibers.

1.4 Objectives

The objectives of this study are as under:-

a. Study OpenSees software as a whole with special emphasis on its extension for fire analysis of reinforced concrete structures.

b. Incorporate additional varying types of HSC materials in the existing material library of OpenSees.

c. Evaluate fire performance evaluation of RC columns using newly incorporated HSC materials with fibers.

1.5 Scope and Limitation

In order to complete the research in limited available time, scope of work and limitations will be as under-

a. Only two types of materials i.e. HSCs and HSCh will be added to the existing material library of the software.

b. In order to validate the results with the available experimental data, the size and specifications of the column will be kept the same as the one used by Khaliq and Kodur 2012.

c. Horizontal displacement (Elongation or Contraction) and vertical displacements will be recorded and validated with the available experimental data.

1.6 Significance

Fire breakout in buildings has always remained a threat to the safety of human and material. This threat will definitely increase as larger number of people will be living and working in high rise buildings throughout the world (Buchanan, 2001). Presently fire testing of structures is seldom carried out in Pakistan due to its heavy cost. This computational fire testing capability will definitely help the authorities to conduct fire testing of existing structures and thereby prepare and upgrade their fire safety plans.

After introducing HPC materials in the framework of OpenSees, the fire safety engineers will be able to conduct structural analysis of almost all types of concrete structures. This concept of fire safety engineering is applicable to all situations where anyone can visualize fire as a potential threat. Although this research is mostly oriented with building structures, however the same principles will be equally applicable to the problems which are mostly associated with gas or oil installations or any other structures like highway bridges etc (Purkiss and Li, 2013).

1.6 Thesis Organization

Chapter 1 is a preliminary chapter about the significance and use of High Strength Concrete, its durability against fire, and the possibility of computer based fire analysis of structures made of it. It also discusses the objective and research significance of the study, and thesis overview.

Chapter 2 describes the detailed literature review of properties of concrete at high or elevated temperature, which includes thermal, mechanical and deformation properties.

Chapter 3 deals with analytical element modelling. It will describe the methods and procedures used to modify the OpenSees software by incorporation of new material into it.

Chapter 4 discusses the results obtained from the software analysis. It also describes the reasons for variation in results as that of the experimental data.

Chapter 5 summarizes the key findings, some major conclusions and recommendations for future research based on this study.

CHAPTER 2

LITERATURE REVIEW

2.1 General

In construction engineering, concrete has become a primary structural material because of its well-known advantages on other construction materials. These include economy, strength, ease of fabrication, durability, availability etcetra . Concrete also provide good fire resistance properties, but latest studies highlight that structural members made of improved concrete mixes known as high performance concrete like Self Consolidating Concrete, High Strength Concrete, Fly Ash Concrete and Fibre Reinforced Concrete are not likely to provide the same level of fire resistance as that of conventional concrete (Phan 1996; Bamonte and Gambarova, 2010; Kodur 2010; Tang and Lo, 2009).

Evaluating the behavior of a structural member which is exposed to fire, demands knowledge of high temperature properties of constituent materials of which the member is composed. The properties of concrete which are essential for fire resistance analysis can be described as thermal, mechanical, deformation and fire induced spalling. These properties change substantially within the temperature range of structural members associated with building fires and depend upon the composition and characteristics of the concrete.

In this chapter, some of the studies which discuss the properties of concrete on elevated temperatures have been reviewed.

2.2 Properties that effect Concrete at Elevated Temperature

Fire resistance of reinforced concrete (RC) is dependent upon the properties of its constituent materials which are concrete and steel. These properties include Thermal, mechanical, deformation and other properties which are material specific. The thermal properties describe the extent of transfer of heat to the structural member, mechanical properties reflect the level of loss of strength and deterioration of stiffness of the structural member, deformation properties describe strain and related extent of deformation in the member. Fire induced spalling also has a major role in performance of members under fire. The above mentioned properties largely depend upon the composition and characteristics

of both the constituent material i.e. concrete and steel. However, the temperature dependent variation in concrete properties is very much complex as that of the steel due to continuous variation of its constituents ingredients in different types of concrete mixes. Therefore, the main focus in this chapter will remain on the effect of temperature on the properties of concrete.

2.3 Thermal Properties of Concrete at Elevated Temperatures

2.3.1 General

The temperature distribution within the concrete structural member is dependent upon the thermal properties of concrete at high temperature. These thermal properties include thermal conductivity, thermal diffusivity, specific heat and mass loss.

2.3.2 Thermal Conductivity

The property of any material to conduct heat is known as Thermal conductivity. This is defined as ratio of flow of heat to temperature gradient and it represents the uniform flow of heat through concrete of unit thickness over a unit area which is subjected to a unit temperature difference between the two opposite sides.

At room temperature, the Thermal conductivity of concrete would remain in the range of 1.4 to 3.6 W/mK and it will vary with change of temperature. Figure 2.1 illustrate the test data compiled from different studies (Harda et al., 1972; Harmathy, 1970; Harmathy and Allen, 1973; Kodur and Sultan, 2003; Eurocode 2, 2004) .

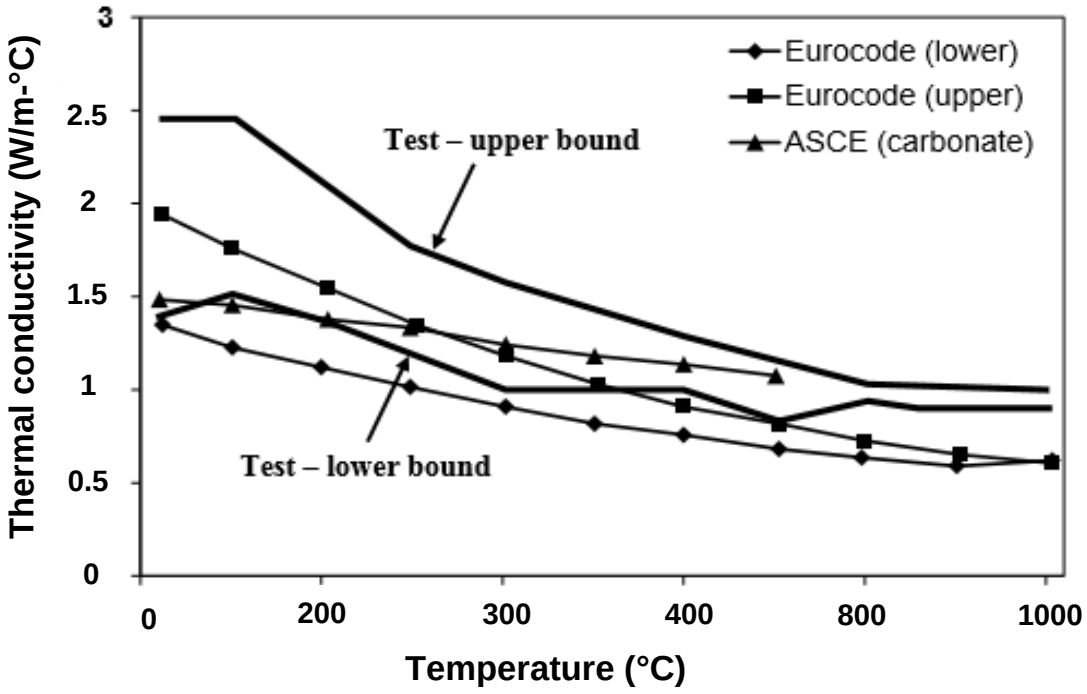

Figure 2.1 - Thermal conductivity of Normal Strength Concrete

There are variations in measured test data of thermal conductivity and that is mainly due to moisture content, type of aggregate, test conditions and measurement techniques that are used in the experiments. The graph represents that the overall thermal conductivity decreases gradually due to rise in temperature. The temperature based decrease is mostly dependent on properties of concrete mix like moisture content, permeability etc.

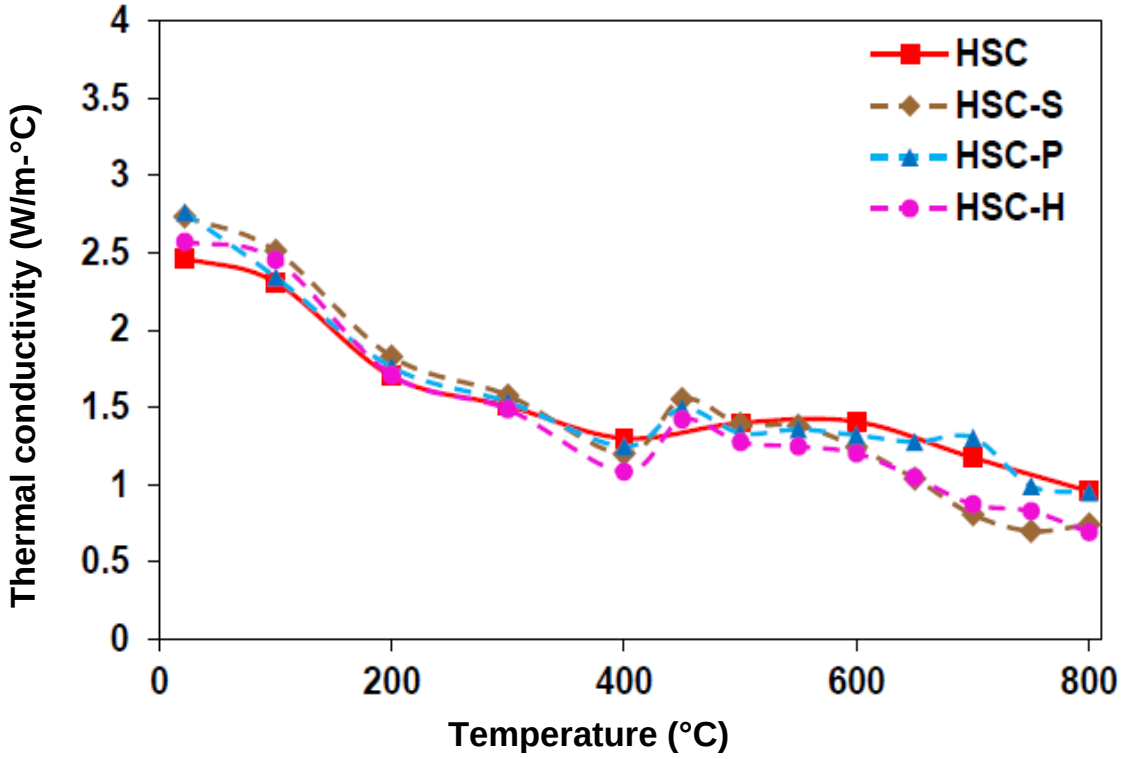

Figure 2.2 – Measured Thermal Conductivity of HSC (plain and fiber reinforce)

Thermal conductivity of HSC (Khaliq and Kodur, 2011) is between 2.4 and 3.3 W / mK at room temperature which is slightly higher than NSC within 600 C temperature range. From graph, it is visible the addition of any fiber like steel, polypropylene or hybrid does not significantly effect the thermal conductivity uptill 600°C. But when the temperature increases above 600°C, these fibers marginally influence the thermal conductivity. This slight influence is mostly due to the dehydration of the CSH, and also due to presence of steel fibers having higher thermal conductivity.

2.3.3 Specific Heat.

Specific heat is defined as the amount of heat per unit mass, required to change the temperature of a material by one degree and is expressed as thermal capacity that is product of specific heat and density. Moisture content, density and aggregate type have great influence on specific heat (Kodur and Sultan, 1998; Phan, 1996). At room temperature, specific heat of concrete varies in the range of 840 J/kg-K and 1800 J/kg-K.

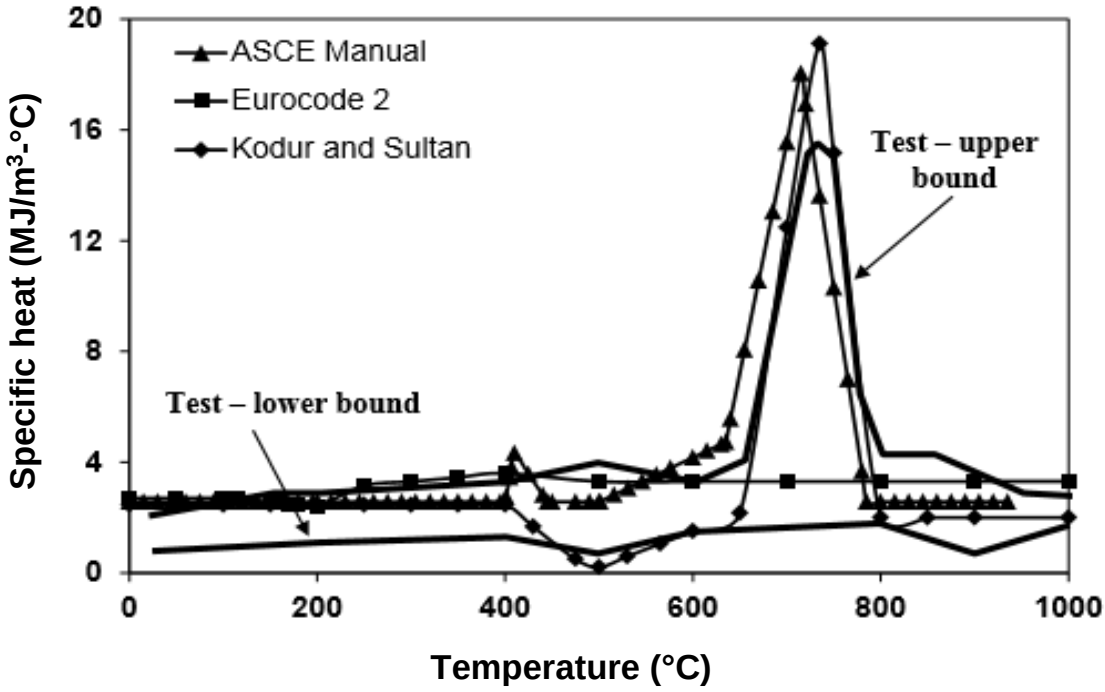

Figure 2.3 - Variation in the specific heat of NSC as a function of temperature

Figure 2.3 represents the variation of specific heat for normal strength concrete with temperature based on test data in various studies (Harmathy, 1970; Harmathy and Allen, 1973; Kodur and Sultan, 1998; Shin et al., 2002). At elevated temperature, specific heat is dependent on various physical and chemical transformation that take place due to temperature such as vaporization of free water at 100 C, the dissociation of Ca(OH)2 into H2O between 400-500 C and the quartz transformation of some aggregates at 600 C. Thus specific heat appears to be dependent on moisture content and it increases with increase in water cement ratio.

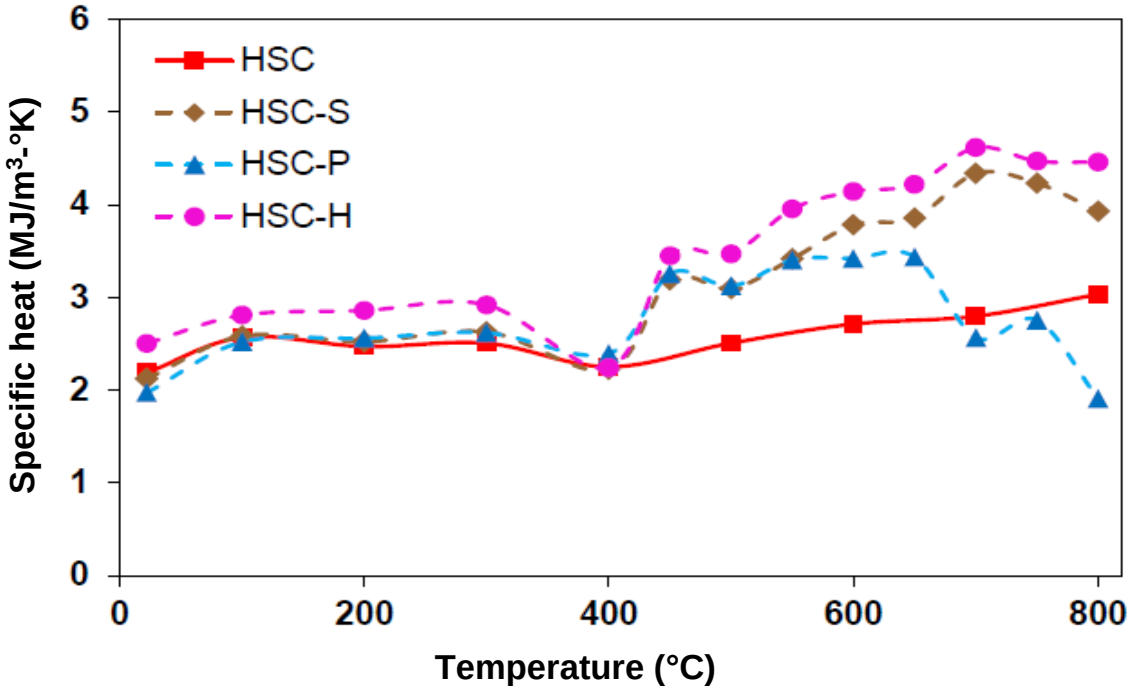

Figure 2.4 – Measured Specific Heat as function of temperature for HSC

The variation of specific heat HSC with temperature (Khaliq and Kodur, 2011) is illustrated in Figure 2.4. The specific heat for HSC normally remains constant till 400°C, then it increases up to about 650C and thereafter remain constant from 650-800 C. This is attributed to changing permeability characteristics of concrete. NSC has the specific heat closer to HSC between 600-800°C, porosity and dehydration resulting from loss of water at early temperatures is the cause of these decreasing values of NSC towards high temperature. Addition of fibers to HSC has marginal influence on the specific heat of concrete.

2.3.4 Thermal Expansion

Thermal expansion can be defined as the percentage change in length for per degree temperature rise of a given specimen. In concrete, it is generally influenced by type of cement, water content, type of aggregate, temperature and age (Lie, 1992). Thermal expansion of concrete is complicated by different factors such as change of volume due to change in moisture, by different chemical reactions (such as dehydration, change of composition), and by creep and micro-cracks which are the result of non-uniform thermal

stresses (Bažant and Kaplan, 1996). Thermal shrinkage can also result due to loss of water in heating, along with thermal expansion, and this may lead to overall volume change to be negative, i.e. shrinkage rather than expansion.

Mass is a property that enables concrete to absorb and store significant amounts of heat. Mass loss can affect the enthalpy and amount of latent heat which directly affects all the thermal properties of concrete. Higher mass in concrete acts as heat sink, by absorbing and holding heat for longer time. This delays the heat transfer through material in an RC member, thus mass loss influences thermal properties of the concrete as well as strength and stiffness properties of RC members. Mass loss of conventional NSC and HSC has been investigated earlier with most of the information pertaining to NSC.

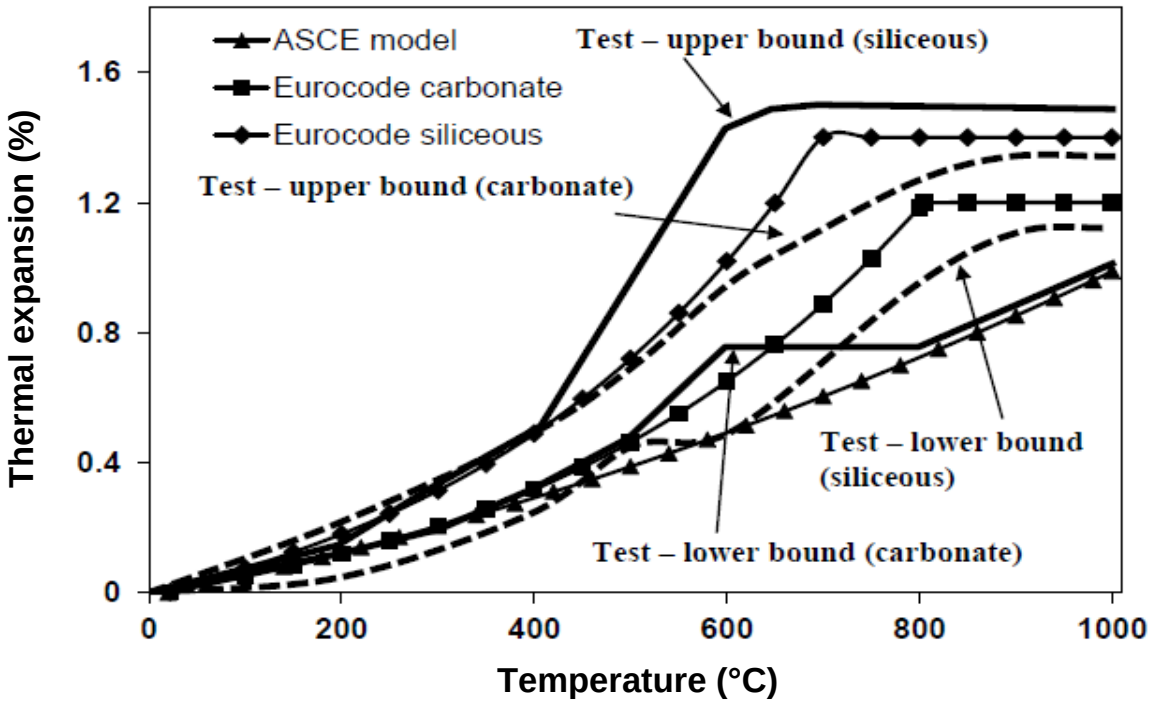

Figure 2.5 – Variation in linear thermal expansion of NSC as a function of temperature

Figure 2.5 represents the variation of thermal expansion in conventional concrete with temperature (ASCE, 1992; Eurocode 2, 2004). From figure, it is clear that thermal

expansion increases from zero to 1.3 % with change in temperature from room temperature to 700 C and later it remains constant till 1000 C.

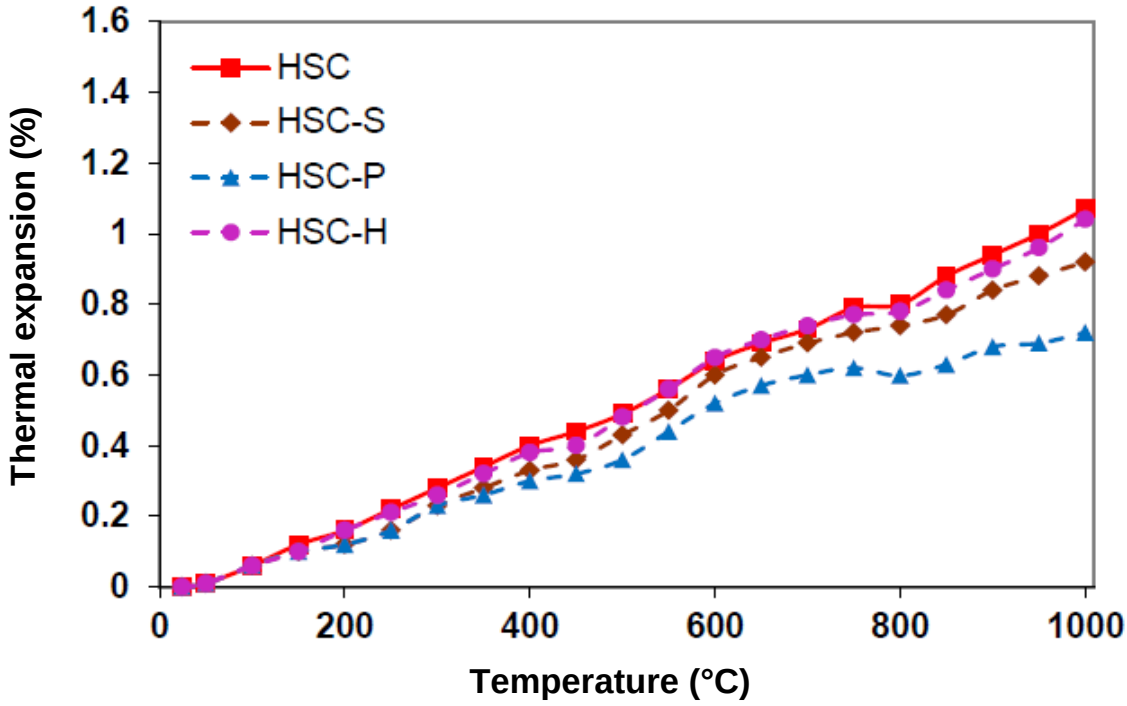

Figure 2.6 – Measured thermal expansion as a function of temperature for plain and fiber reinforced HSC

In HSC, the thermal expansion increases with increase in temperature. From 20-600°C, this increase is substantial which is the result of high thermal expansion due to presence of aggravate and cement paste in the concrete. From 600-800°C it reduces because ofloss of chemically bound water in hydrates which is now causing shrinkage. Again rise after 800°C is attributed to decarbonation of limestone based aggregates.

2.3.5 Mass Loss

Mass of concrete enables it to absorb and store significant amounts of heat. Thus, mass loss has direct effects on concrete properties at high temperatures. Figure 4 illustrates the changes occurring in the concrete mass as a function of temperature. It is also visible that there is a significant difference for mass loss in concretes made from two different types of aggregates. Thus at high temperature, mass loss of concrete is significantly influenced by aggregate type (Lie and Kodur, 1996; Kodur and Sultan, 1998).

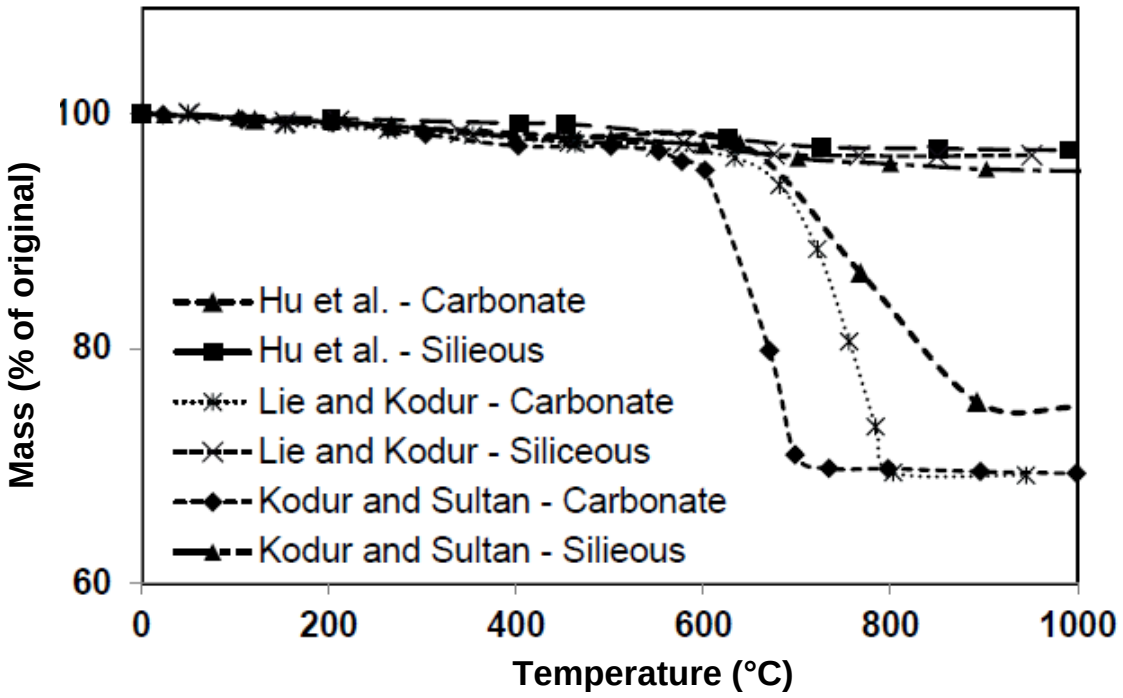

Figure 2.7 – The changes in concrete mass of different aggregates as a function of temperature

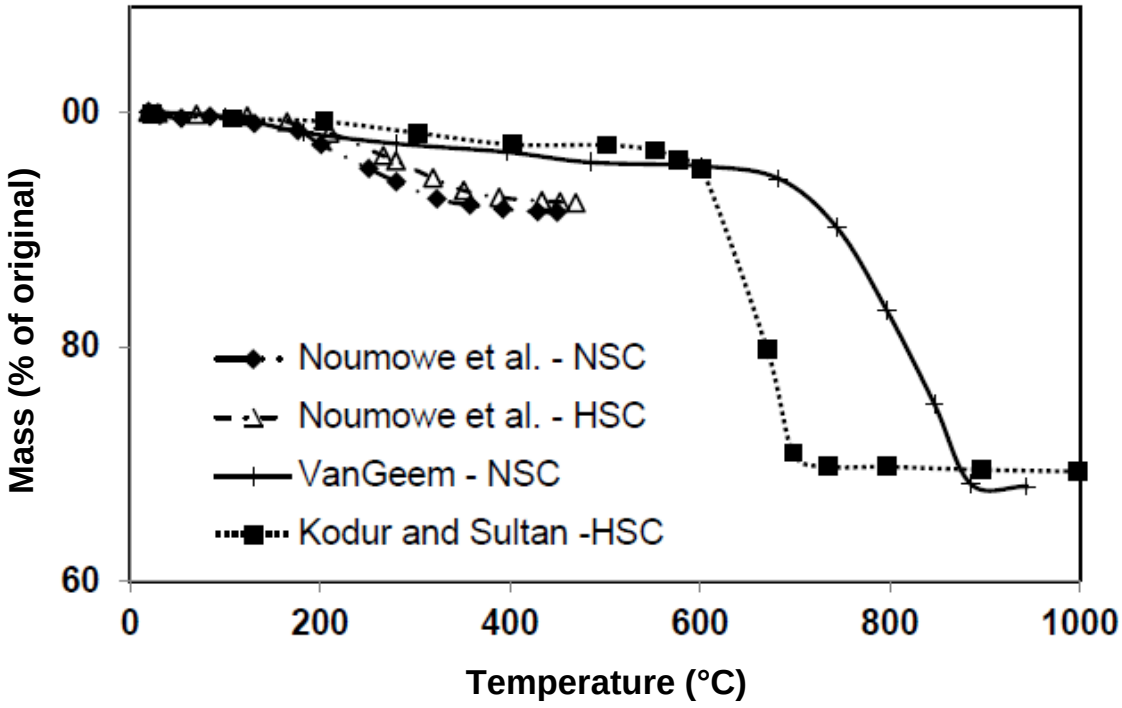

Figure 2.8 – Variation in mass of NSC and HSC as a function of temperature

Figure 2.8 illustrates the variation in mass of concrete as a function of temperature for concretes made with carbonate and siliceous aggregates. It can be seen that there is significant difference for mass loss in concretes made with two types of aggregates.

At high temperatures, the mass loss in concrete is much effected by the aggregate types. For carbonate and siliceous aggregate, this mass loss is quite low till 600°C. But after 600°C, carbonate aggregate concrete shows high percentage of mass loss as compared to siliceous aggregate concrete. This increased mass loss in carbonate aggregate concrete is actually the result of dissociation of dolomite at 700°C (Kodur and Harmathy, 2008).

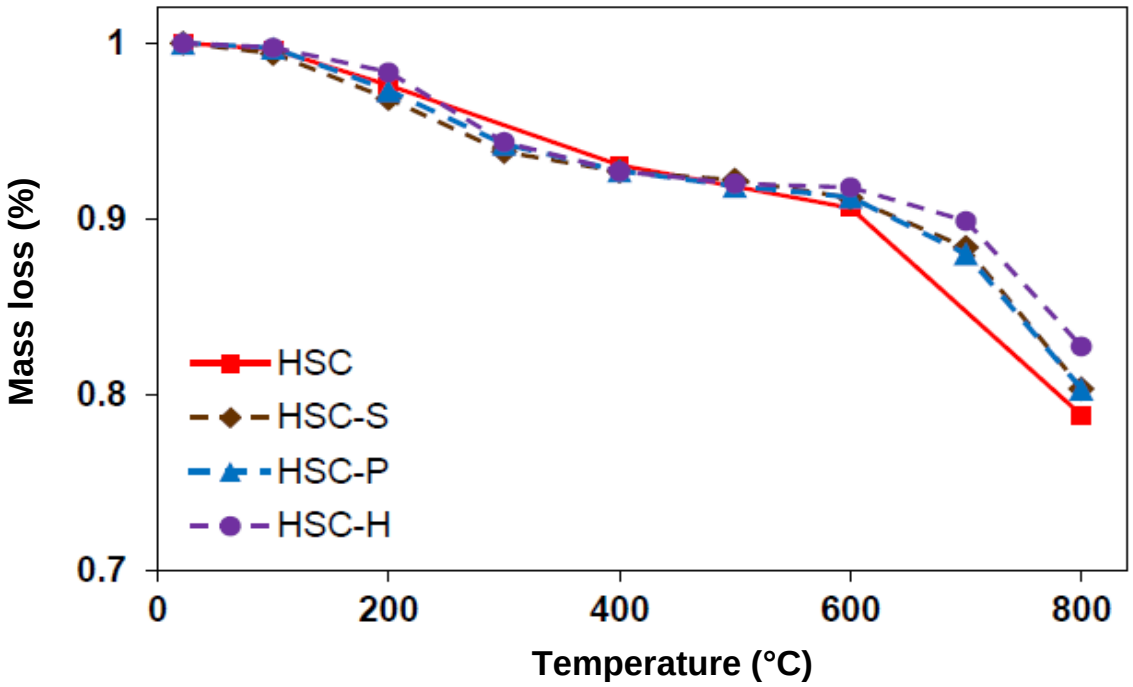

Figure 2.9 – Measured mass loss as a function of temperature for plain and fiber reinforced HSC

It can be seen that no significant mass loss occurs till 600°C. Higher mass loss takes place in HSC in 600-800°C, which can be attributed to the relatively easy dehydration in HSC which has comparatively less dense microstructure. It can be seen that there is no significant effect of fibers on mass loss of these HPC at elevated temperatures.

2.3.6 Summary

Thermal conductivity, specific heat, thermal expansion, and mass loss are important thermal properties which are desired for predicting the temperature profiles as well as spalling in concrete structures under fire exposure. As indicated by the review, there have been quite a few studies on NSC that show the influence of thermal properties on fire resistance of structural members.

Temperature has substantial effects on thermal properties of HSC. The thermal conductivity of HSC mostly decreases with rise in temperature. The thermal expansion also increases with change in temperature up to 800°C. Conversely, specific heat of HSC concrete types remains constant up to about 400°C, and then increases up to about 650°C before following a constant trend in 650-800°C range. Results show that HSC shows higher thermal conductivity and thermal expansion in the temperature range of 20-800°C.

2.4 Mechanical Properties of Concrete

2.4.1 General

Compressive strength, tensile strength, modulus of elasticity and stress strain response in compression are the main mechanical properties which are of interest in fire resistance of concrete.

2.4.2 Compressive Strength

In concrete, compressive strength is mostly dependent upon water cement ratio, aggregate-paste interface transition zone, curing conditions, type and size of aggregate, type of admixture types and type of stress (Mehta and Monteiro, 2006). Good amount of data is available on compressive strength of concrete at elevated temperatures for both NSC and HSC (Castillo and Durrani, 1990; Fu et al., 2005; Poon et al., 2001; Tang and Lo, 2009; Xu et al., 2001). Few of the notable studies presented here generate information on high temperature compressive strength of concrete.

Carette et al. (1982) did an important study on use of pozzolanas in NSC at elevated temperatures. They reported that addition of fly ash and slag in NSC did not improve the residual compressive strength of concrete after exposure to high temperatures. Even

change in water-cement ratio of NSC with these pozzolanas did not show any effect on high temperature mechanical properties behavior of concrete.

Lie and Kodur (1996) investigated high temperature strength properties of NSC with and without steel fibers. They reported that compressive strength steel fiber reinforced concrete degrades at a much higher rate with temperature than similar concrete without steel fibers. They also concluded that effect of aggregate type on the compressive strength is not significant.

Chan et al. (1999) investigated the residual compressive strength of both NSC and HSC after exposure to high temperatures. He identified three distinct temperature ranges having an effect on loss of compressive strength of concrete namely, 20-400°C, 400-800°C, and 800-1200°C. He reported that only small part of strength was lost in 20-400°C (1-10% for HSC and 15% for NSC), however severe loss occurred in 400-800°C range. This severe loss in 400-800°C range was attributed to deterioration of C-S-H gel and cementing ability due to dehydration in concrete. They suggested the temperature range of 400-800°C be regarded as critical strength-loss range for concrete. Above 800°C the residual strength was reported as only a small part of original strength.

Li et al. (2004) experimentally studied the residual mechanical properties of NSC and HSC at elevated temperatures. They investigated the influence of temperature, water content, specimen size, strength grade and temperature profiles on mechanical properties. Authors reported that the compressive strength of HSC drops with temperature after 200°C. The strength loss in HSC was higher (36.8%) in 20-400°C as compared to NSC (28.8%), and this higher loss was attributed to dense microstructure and impermeability of HSC. It was also reported that water content had minimum effect on high temperature strength loss of concrete. As for specimen size, it was concluded that compressive strength loss of larger concrete specimens was lower than that in smaller size specimens. Noumowé (2005) investigated the behavior of high temperature mechanical properties of plain HSC and polypropylene fiber reinforced HSC up to 200°C. He reported that the HSC containing polypropylene fibers has higher compressive strength loss as compared to plain HSC.

Sideris (2007) investigated the compressive strength characteristics of SCC exposed to elevated temperatures up to 700°C. For comparison, he also tested and compared the

results with conventional concretes. Residual strength properties were tested after exposure to 100, 200, 500, and 700°C. He reported that the residual strength loss trend of both SCC and conventional concretes was similar in 20-700°C. Both SCC and HSC suffered explosive spalling at temperatures beyond 380°C.

Kim et al. (2009) recently investigated the compressive strength characteristics of HSC exposed to elevated temperatures up to 700°C through stressed test method. During heating, the specimens were subjected to a pre-load of 25% of the ultimate compressive strength at room temperature, and then loaded to failure at target temperature. It was concluded by the researchers that with increase in strength of concrete, the loss of strength due to high temperature exposure also increase. It was also concluded from this research that HSC loses minimum strength in 100-400°C temperature but the rate of strength loss is significant beyond 400°C.

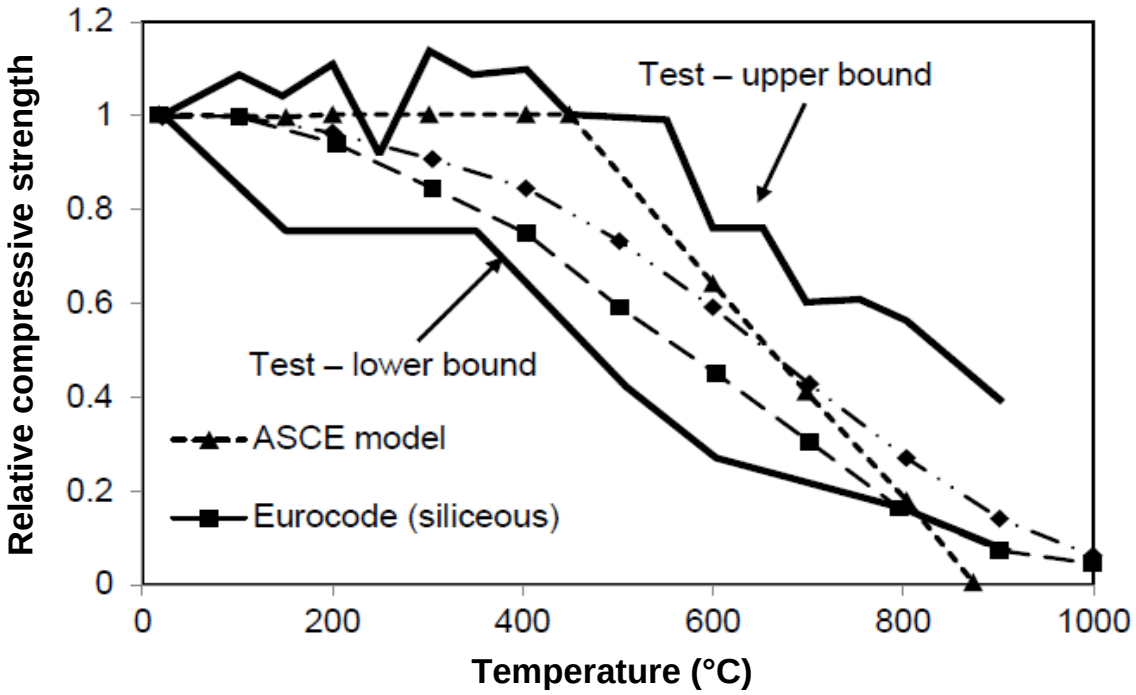

Figure 2.10 – Variation in relative compressive strength of NSC due to temperature

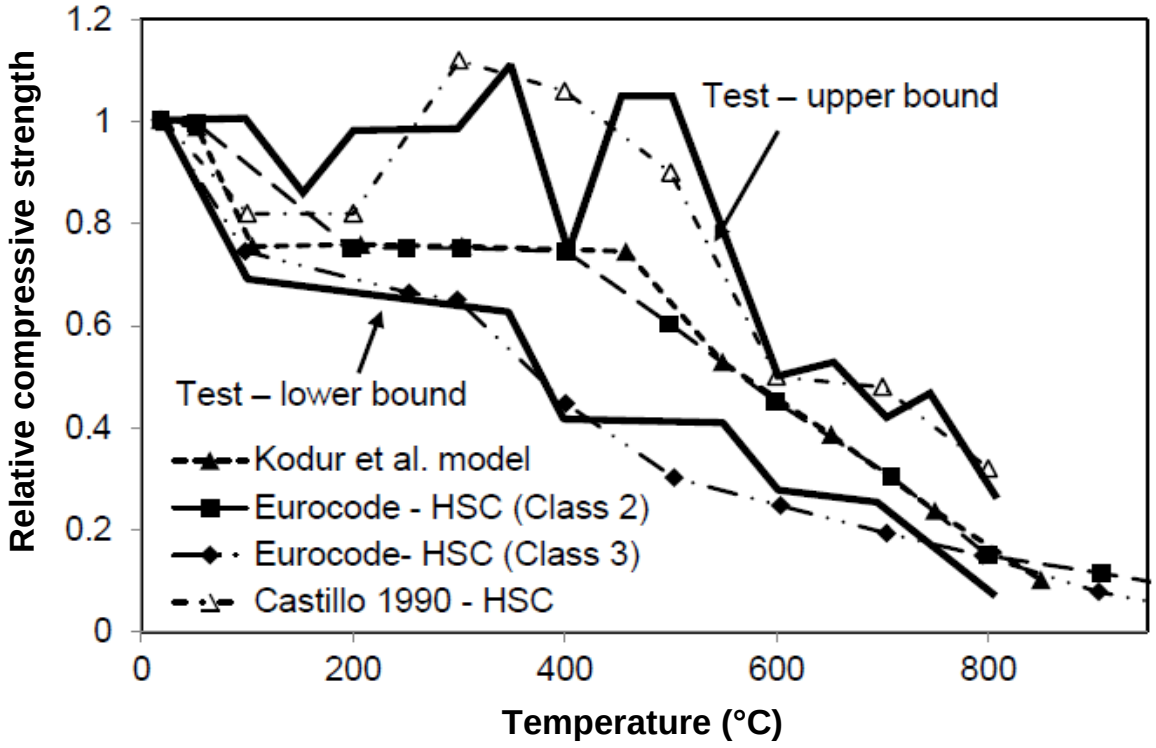

Figure 2.11 – Variation in relative compressive strength as function of temperature for HSC

Figure 2.10 and 2.11 illustrate the variation of compressive strength ratio of NSC and HSC concrete at raised temperatures respectively.

The compressive strength of NSC is marginally affected by temperatures up to 400°C. Due to high permeability of NSC, it allows easy diffusion of pore pressure. Therefore NSC is most suited for concrete infrastructure exposed to fire hazards. Use of different binders in HPC produce a superior and dense microstructure with less amount of calcium hydroxide which ensures a beneficial effect on compressive strength. Slag and silica fumes improves the compressive strength due to dense microstructure but this compact microstructure is highly impermeable and at high temperature becomes detrimental. It results in increasing pore pressure and development of microcracks which leads to spalling.

The review of compressive strength properties above shows that good amount of research has taken place for high temperature behavior of both NSC and HSC. However, it can be observed that the strength trends for both NSC and HSC are not consistent and there are significant variations in strength loss. Moreover, there is very limited data in literature on high temperature strength properties of new types of concrete such as SCC

and FAC. Therefore data on strength properties of new types of concretes as a function of temperature is needed for evaluating fire response of structural members made of HSC.

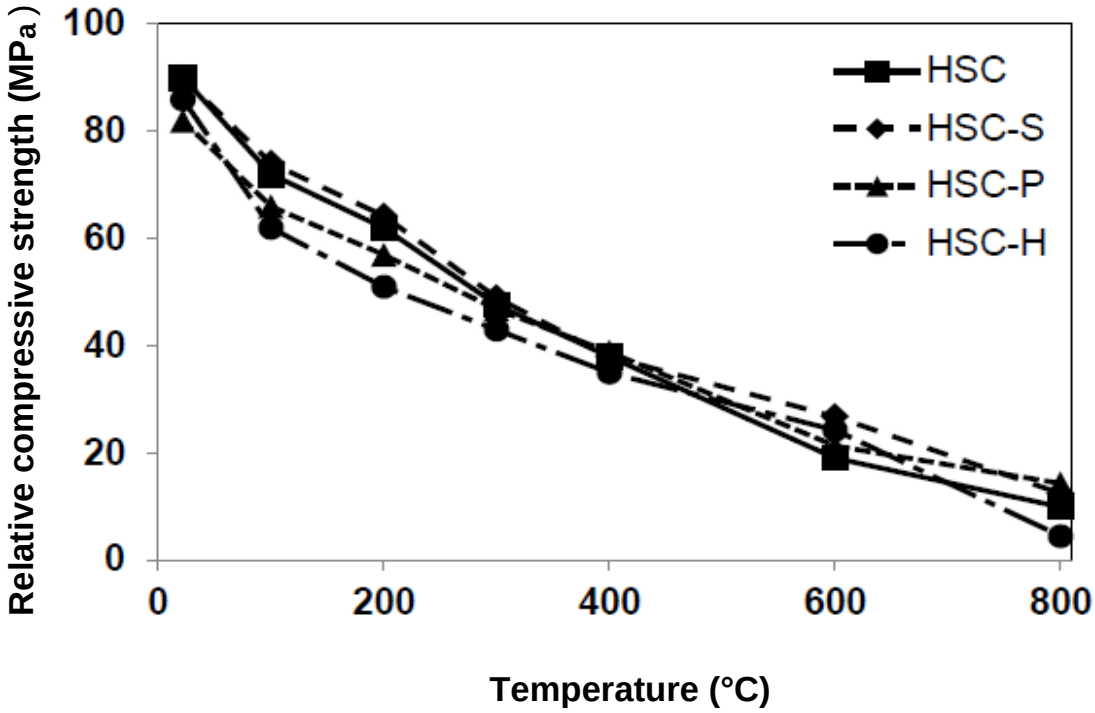

Figure 2.12 – Measured compressive strength of HSC and fiber reinforced HSC as function of temperature

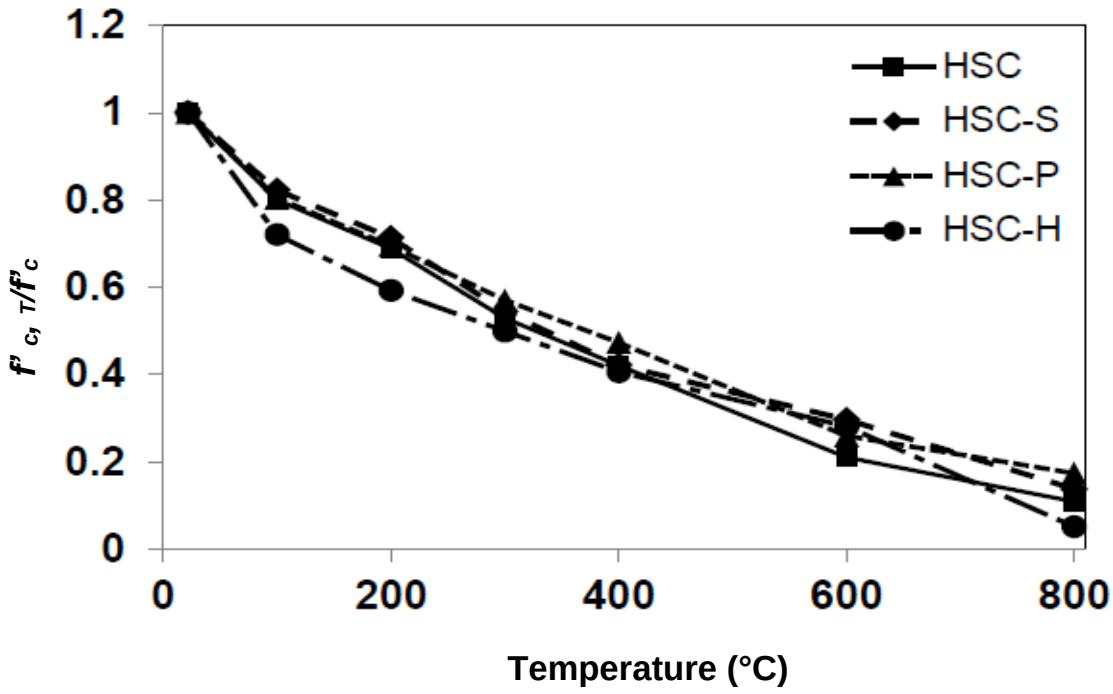

The compressive strength evaluated at each temperature is plotted as a function of temperature for HSC with and without fibers in Figure 4.16. In all types of concrete, physical and chemical changes at higher temperatures result in reduction of compressive strength. HSC (plain and with fibers) gradually lose strength with temperature in 20-800°C range in a similar trend. This loss is slightly higher in 20-400°C and can be attributed to dense microstructure of HSC that undergoes more thermal stresses from evaporation of moisture up to 400°C and does not let water vapors to escape easily. This effect has been established by Castillo and Durrani (Castillo and Durrani, 1990) that moisture in concrete has detrimental effect on high temperature compressive strength of HSC. It can be seen that fibers do not have much effect on high temperature compressive strength of HSC.

Beyond 400°C, all four HSCs exhibit similar trend of slower strength loss. This degradation in strength can be attributed to slow disintegration of microstructure due to loss of chemically bound water that is lost at a lower rate 400-800°C temperature range. This lower rate of loss of compressive strength between 600-800°C is also attributed to calcination of the limestone aggregate at high temperatures (Castillo and Durrani, 1990).

The ratio of recorded compressive strength $f'c,/f'c$ for HSC with and without fibers is shown in Figure 4.17. The strength loss is higher in 20-400°C range and lowers in 400-800°C range. This can be attributed to loss of moisture in concrete up to 400°C as explained above. Fibers do not have much pronounced effect on the compressive strength of HSC both at room temperature and at higher temperature.

2.4.3 Tensile Strength

Concrete has very less tensile strength as compare to its compressive strength. The reason is the ease with which the cracks can propagate under any tensile load (Mindess et all., 2003). Thus it is quite normal to neglect the tensile strength of concrete in strength calculations at room and elevated temperatures. But in case of fire, tensile strength of concrete may become crucial when fire induced spalling occurs in a SCC structural

member. Similarly the cracking in concrete is because of tensile stresses and the damage to structural member often generated by progression of microcracks (Mindess et al., 2003).

Tensile strength of concrete is dependent on compressive strength of concrete, water/cement ratio, aggregate-paste interface transition zone, presence of any flaws, and microstructure of concrete (Neville, 2004). A review of the literature indicates that there have been limited studies on high temperature tensile strength of concrete. It is also worth noting that all previous studies on high temperature tensile strength of concrete are based on residual strength tests that are applicable for concrete members cooled after fire exposure. This residual tensile strength property cannot represent the tensile strength behavior of hot concrete (during fire exposure) which is required for predicting spalling. Some of the notable studies presented here generate information on high temperature tensile strength behavior of concrete.

Carette et al. (1982) investigated the temperature effect on the tensile strength of NSC. He tested concrete cylinders in 75-600°C temperature range through residual strength technique. He reported 65-70% reduction in splitting tensile strength at 600°C. He concluded that both the water cement ratio and type of aggregate have quite significant effects on the splitting tensile strength of NSC.

Felicetti et al. (1996) investigated the residual tensile strength of two types of HSC from room temperature to 600°C by testing through direct tension method. They noticed reduction in tensile strength to zero at about 600°C. It was also observed in this study that concrete softens at high temperature and that temperature has a marked effect on its tensile strength.

Recently, Bahnood and Ghandehari (2009) reported residual splitting tensile strength of plain and polypropylene fiber reinforced HSC up to 600°C. The authors inferred that the decrease in splitting tensile strength is due to decomposition of hydrated cement products and thermal incompatibility between aggregates and cement paste. They also observed that there was no noticeable difference in the splitting tensile strength of polypropylene fiber reinforced HSC up to 600°C in comparison to plain HSC.

Li et al. (2004) conducted tests for residual splitting tensile strength of HSC in 200-1000°C temperature range. HSC batch mix contained 27 per cent fly ash as cement

replacement. Reduction in splitting tensile strength with temperature was attributed to thermal stresses induced in dense microstructure of HSC that resulted in micro and macro cracks.

Chen and Liu (2004) experimentally studied the residual splitting tensile strength of HSC and hybrid fiber reinforced concrete at various temperatures in 20-800°C ranges. The authors found that higher residual splitting tensile strength was obtained by hybrid fiber reinforced HSC. Steel fibers in concrete were observed to provide restriction against initiation and expansion of cracking, while polypropylene fibers provided micro-channels resulting in reduction of thermal stresses.

Anagnostopoulos et al. (2009) investigated the residual splitting tensile strength properties of SCC with different fillers at 20, 300, and 600°C temperatures respectively. Sharp loss in tensile strength was observed and was attributed to micro and macro cracks produced in specimens due to thermal incompatibility. SCC with limestone filler was reported to have displayed better performance at high temperature by preserving splitting tensile strength. In this study, explosive spalling was also reported in high strength SCC at 600°C temperature.

Eurocode (2004) fire provisions recommend accounting for tensile strength properties of concrete in fire resistance calculations. It treats both NSC and HSC alike for temperature dependent tensile strength of concrete by provision of a simple relationship for representation of tensile strength of concrete with temperature. On the other hand ACI 216.1 (2007) does not provide any guideline or relationship for tensile strength of concretes.

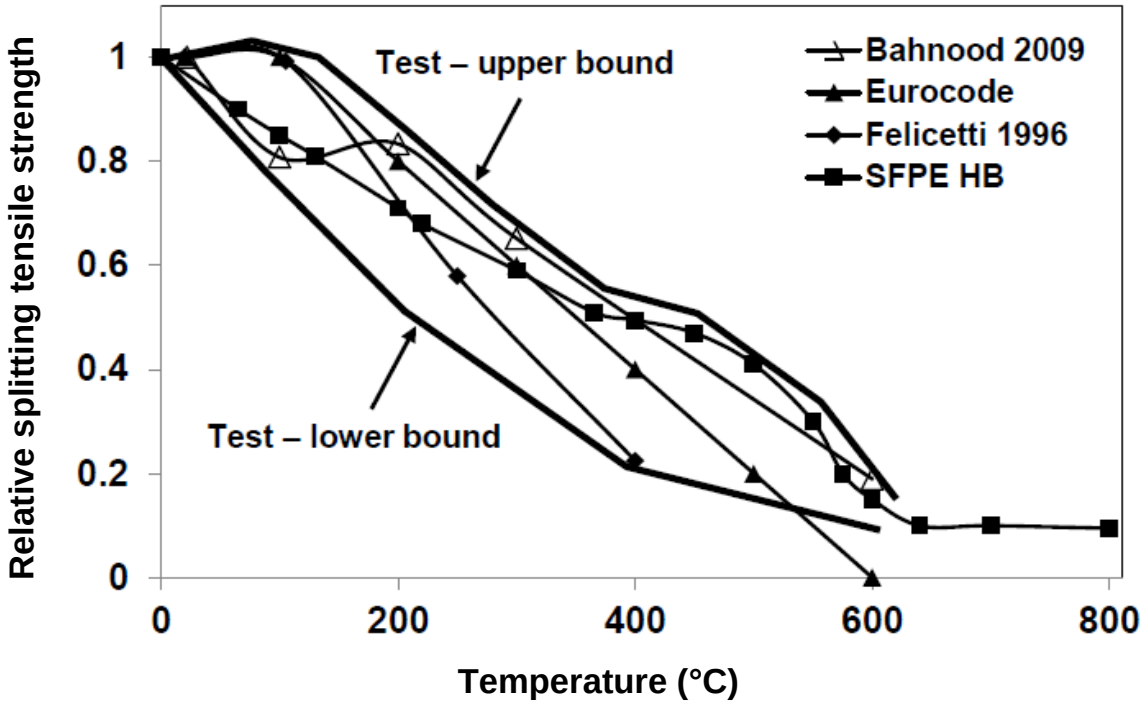

Figure 2.14 – Variation in relative splitting tensile strength as function of temperature

Figure 2.14 represents the variation in splitting tensile strength of NSC and HSC as a function of temperature found in previous studies and also recommended by Eurocode standard (Behnood and Ghandehari, 2009; Carette et al., 1982; Eurocode 2, 2004). The decrease in tensile strength of NSC with temperature is due to weak microstructure of NSC which allows initial micro cracks. Above 300 C, the tensile strength of NSC drops at a much faster rate which is attributed to pronounced thermal damage in the form of microcracking.

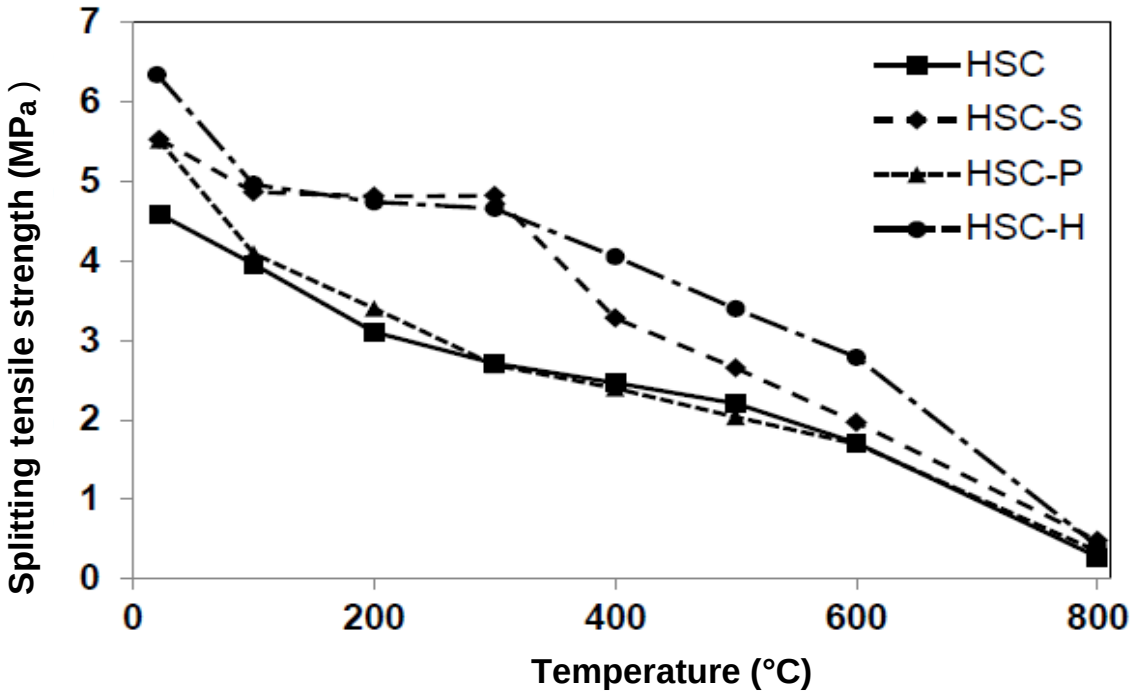

Figure 2.15 – Measured splitting tensile strength of HSC and fiber reinforced HSC as function of temperature

Figure 2.15 illustrates the splitting tensile strength as a function of temperature for HSC with fibers. Splitting tensile strength reduces with temperature in concrete up to 800°C. In both HSCs and HSCh, significant retention in splitting tensile strength is observed up to 300°C which can be effective in minimizing fire induced spalling. This retention in tensile strength can be credited to steel fibers in bridging cracks under tensile loading. Shah (1991) deduced that fibers substantially enhance room temperature tensile strength of concrete, as fibers suppress localization of microcracks into macrocracks and consequently tensile load capacity of concrete increases. In case of plain HSC and HSC-P the tensile strength loss is higher in 20-800°C temperature range compared to HSCs and HSCh.

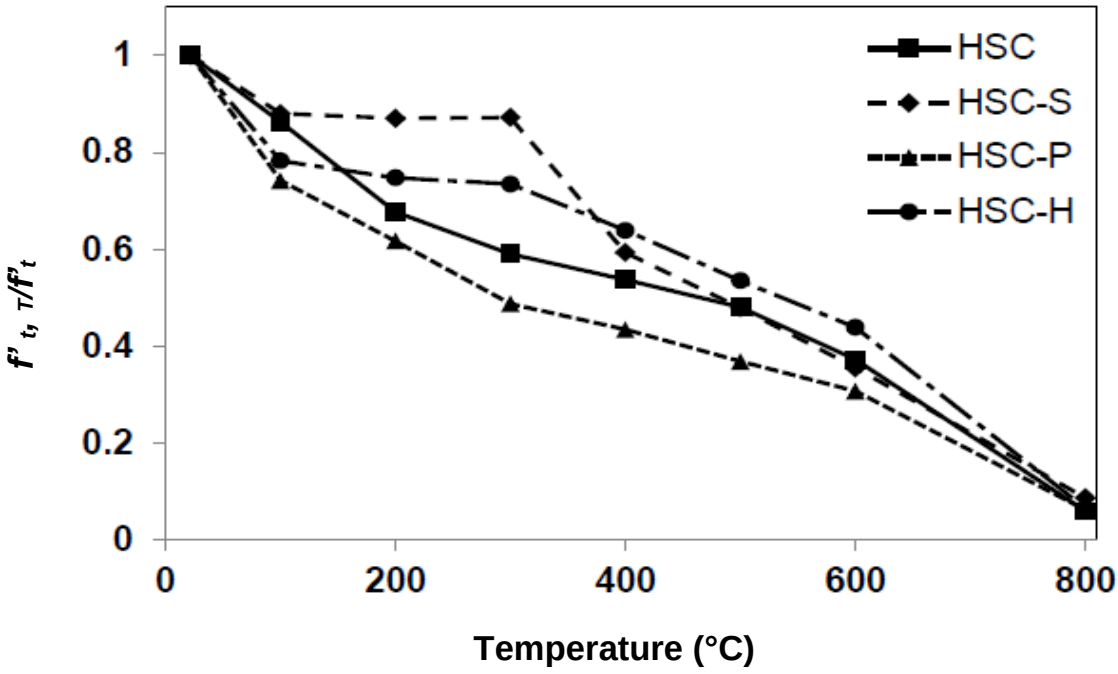

Figure 2.16 – Measured relative splitting tensile strength of HSC and fiber reinforced HSC as function of temperature

The ratio of recorded splitting tensile strength $f't,T/f't$ for HSC and fiber reinforced HSC (HSC-S, HSC-P, and HSC-H) is shown in Figure 4.25. The ratio of tensile strength loss is higher for HSC and HSC-P in 20-400°C where as it is least for HSC-S and HSC-H. This can be attributed to effectiveness of steel fibers which arrest crack initiation and propagation. Test data indicates that HSC and fiber reinforced HSC have about 35% to 45% of original tensile strength at 600°C which is quite significant and can be effective to mitigate spalling.

2.4.4 Modulus of Elasticity

Modulus of Elasticity of concrete decreases with increase in temperature. It is because of disintegration of hydrated cement products and breaking of bonds in the microstructure of cement paste. This reduction depends upon type of aggregate, moisture loss and high temperature creep.

Modulus of Elasticity of concrete also has an influence on fire response of concrete. As it degrades with rise in temperature, therefore it greatly influences the fire resistance of structural members. At high temperature, disintegration and breakage of bonds in microstructure results in reduction of elastic modulus. The degree of this reduction is dependent on loss of moisture, high temperature creep and type of aggregate (Bažant and Kaplan, 1996). Some of the prominent studies undertaken on high temperature elastic modulus are discussed below:

Castillo and Durrani (1990) experimentally studied the effect of temperature on elastic modulus of both NSC and HSC in 20-800°C temperature range. Modulus was measured using closed-loop servo-controlled hydraulic testing machine integrated with an electric furnace. The authors reported that both NSC and HSC have similar loss of modulus under elevated temperature. Slight loss was recorded up to 400°C and faster loss was observed between 400-600°C. The higher loss above 400°C was attributed to progressive dehydration and loss of bond between materials.

Bamonte and Gambarova (2010) tested HSC and SCC cylinders up to 90 MPa for elastic modulus at 20, 200, 400, and 600°C. They reported that the elastic modulus is much lower in hot state than residual which was attributed to thermal affects. It was also concluded that there is no difference in the elastic modulus of HSC and SCC.

Perrson (2004) did extensive experimental investigation on the elastic modulus of SCC at elevated temperatures and as residual property. Tested temperatures consisted of 20, 200, 400, 600 and 800°C. He observed a lower elastic modulus for SCC, as compared to HSC, throughout the temperature range in both hot state and as residual property.

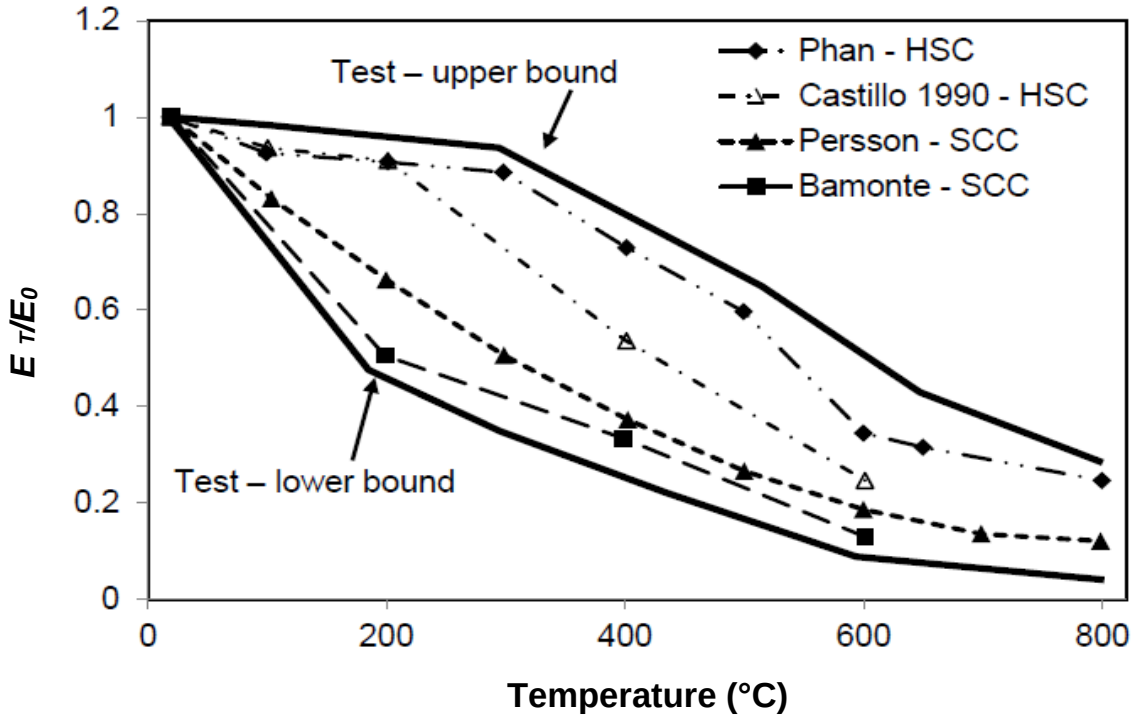

Figure 2.17 – Variation in elastic modulus as a function of temperature

Fig 2.17 represents the variation in the ratio of elastic modulus at target temperature to that of room temperature for HSC (Castillo and Durrani, 1990; Phan, 1996). The loss of modulus of elasticity in both the SCC and HSC is similar which is attribute to excessive thermal stresses and chemical and physical changes occurring in concrete microstructure.

2.4.5 Stress Strain Curves

For fire resistance analysis, the high temperature compressive stress strain behavior concrete is of paramount importance. Very limited information is available on stress strain curves of HSC subjected to high temperatures. These high temperature stress-strain curves are helpful to trace the structural response of RC structural members under fire conditions. The high temperature stress-strain response of concrete is dependent on factores such as aggregate – paste interface transition zone, curing conditions, aggregate type and size. The aggregate type has a significant effect on the ultimate strain attained in

HSC exposed to elevated temperatures, carbonate aggregate HSC attains higher peak strains as compared to siliceous aggregate HSC (Cheng et al, 2004).

Limited information is available on the compressive stress-strain curves of HSC exposed to high temperatures. The main reason for limited data is the complexity involved to generate high temperature stress-strain curves through stressed or unstressed test methods. However, researchers have carried out investigation on stress-strain curves of concrete under all three test conditions (stressed, unstressed and residual) to study the effect of elevated temperatures on stress-strain behavior. Some of the previous studies are discussed here to generate information on high temperature stress-strain response of concrete:

Castillo and Durrani (1990) studied the effect of transient high temperature on stress-strain response of HSC and NSC under both stressed and unstressed test conditions in 23-800°C range. It was found in this study that effect of temperature on stress-strain curves is same for HSC and NSC in entire temperature range. For both NSC and HSC the strain at peak stress did not significantly vary in 100-200°C range. There was a slight increase in strain at peak stress in 300-400°C range. However, there was a significant increase in strain at peak stress in 500-800°C range. At 800°C the recorded strain was measured to be four times to the strain at room temperature.

Furumura et al. (1995) tested cylinders to generate stress-strain curves for NSC and HSC, during heating and after heating. The test data indicated that the stress-strain curves for HSC are quite different from NSC. For HSC stress-strain curves showed brittle response below 500°C. However the stress-strain curves above 500°C showed more ductile response, and it was attributed to internal microcracks developed due to thermal stresses caused by contraction of cement paste, expansion of aggregates and thermal gradients. For both NSC and HSC the strains at maximum strength during heating and after heating increased rapidly with increasing temperature above 300-400°C temperature. It was concluded in this study that concrete strength has only a little effect on the strain at maximum strength.

Felicetti et al. (Felicetti et al., 1996) studied residual mechanical properties, including stress-strain curves, for HSC after heating to 105, 250, 400 and 500°C temperatures. It was

shown by stress-strain curves that there was significant decrease in the peak stress after exposure to high temperature. The peak stress decreased by 2.5% at 105°C, 25% at 250°C, 75% at 400°C, and 94% at 500°C. Above 500°C, residual strength was so small (10%) that HSC was considered to be unsuitable for bearing any loads.

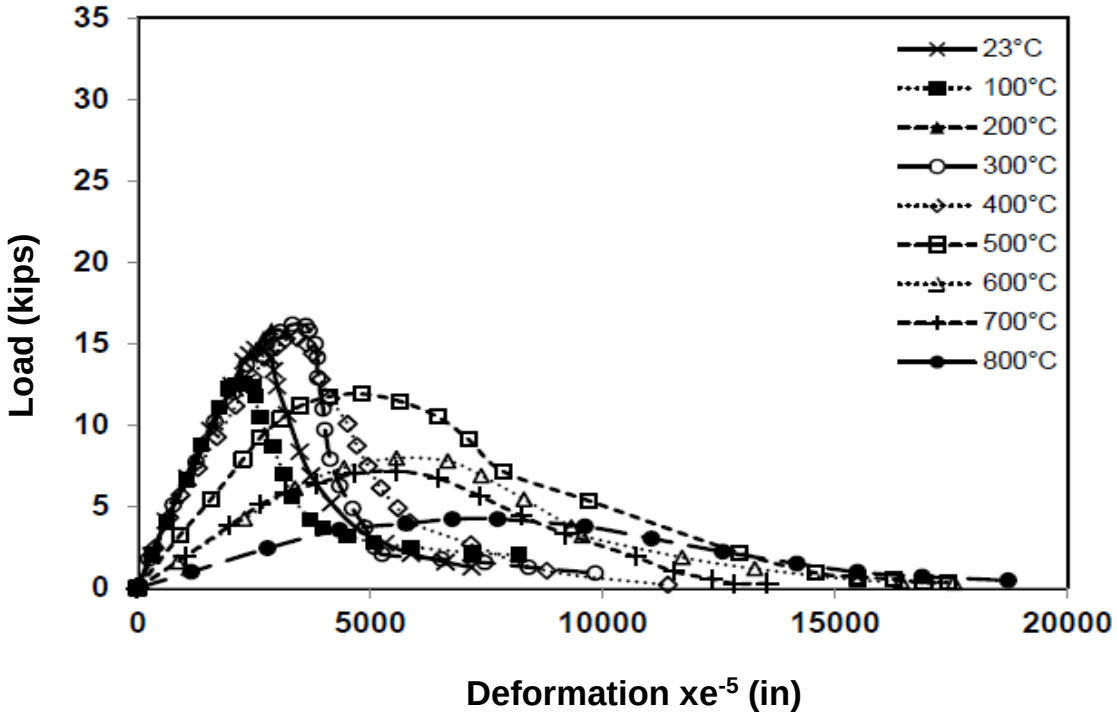

Figure 2.18 – Typical load deformation of NSC at various temperature

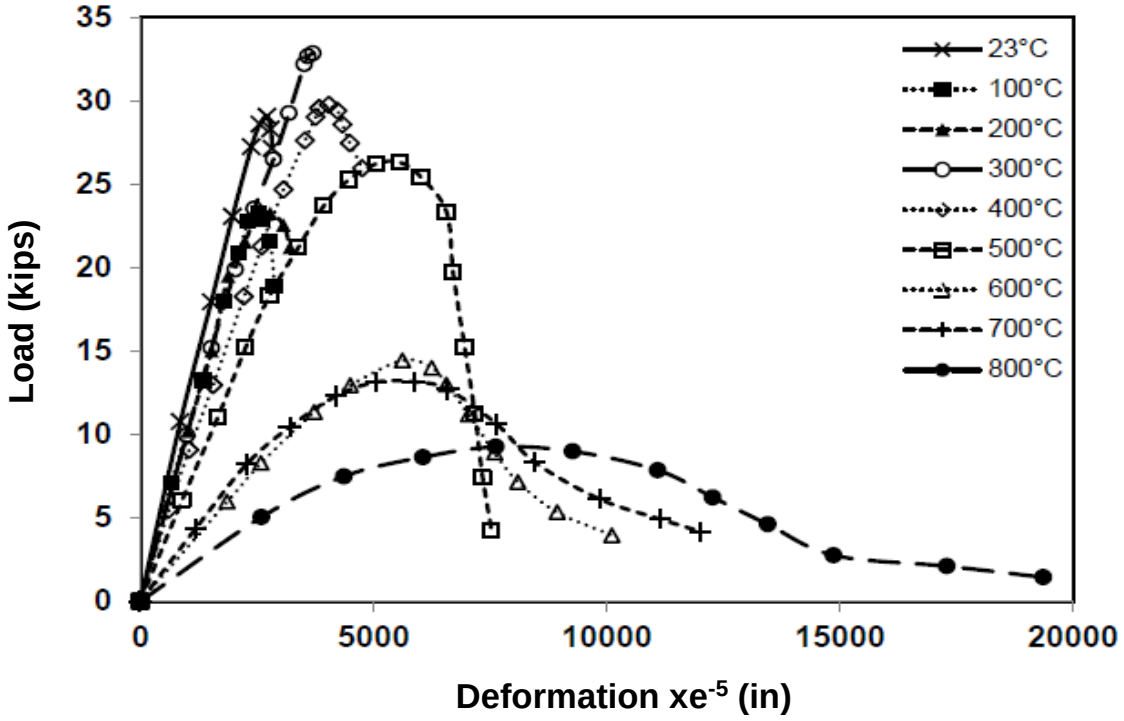

Figure 2.19 – Typical load deformation of HSC at various temperatures

Figure 2.18 and 2.19 illustrate the load-deformation response of NSC and HSC respectively (Castillo and Durrani, 1990). In general, it is known fact that HSC has got steeper and much linear stress-strain curves in comparison to NSC in 20-800°C. High temperature has significant effect on the stress-strain response of both NSC and HSC, as with the rise in temperature, the strain at peak stress starts to increase, especially above 500°C this increase is significant and the strain at peak stress can reach four times to strain at room temperature. HSC specimens exhibit brittle response as indicated by post peak behavior of stress-strain curves.

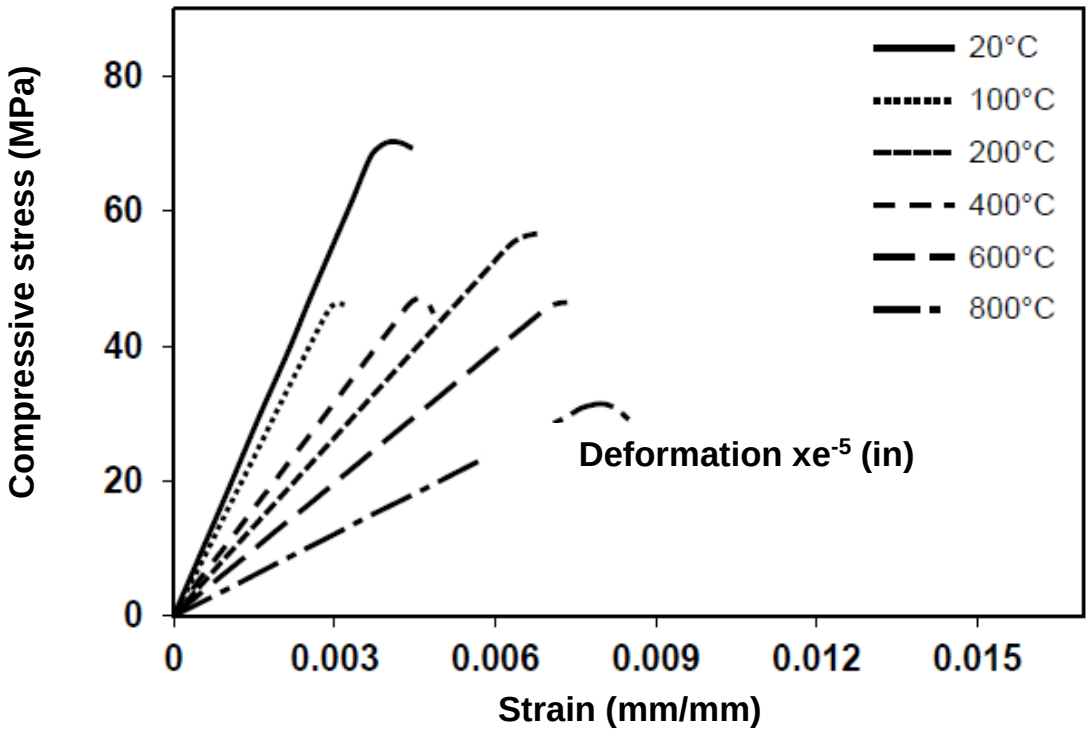

Figure 2.20 – High temperatures stress-strain curves for HSC

Stress-strain curves for SCC are plotted in Figures 2.20. At room temperature, HSC show linear-elastic response up to about 80% of peak stress. For HSC, the gradient of stress-strain curves decrease with temperature showing a drop in peak stress, and increase in peak strain. The plotted total strain is mainly composed of mechanical stain due to loading and thermal strain due to temperature. As the tested were done by unstressed test method (heating without applied load), therefore the creep and transient strains are not significant in the measured (total) strain. In all these concrete, development of micro and macro cracks due to high temperatures lead to rapid increase in peak strains.

CHAPTER 3

Analytical Element Modelling

3.1 General

The OpenSees software has emerged out of ‘Object oriented finite element programming: frameworks for analysis, algorithm and parallel computing” (1997), a Ph.D thesis written by by Frank McKenna at the University of California at Berkeley. Ever since its inception, a lot of modifications have been made to the framework, as a sign of incessant development however the original design has remained the same. Taking advantage of the software, a completely new material i.e. SCCs (Self consolidated Concrete with steel fibres) has been added to the existing library of OpenSees. When the software is updated or modified with additional materials then it can run the analysis of all the structures made up of those new construction materials. For this study, the construction element selected for analysis is a linear column. The modelling of linear column in OpenSees has also been discussed in this chapter.

3.2 Modification of Open Sees

OpenSees is an open source code and it enables the user and the developers to keep introducing the new sections, elements and materials into its existing library. In the study an effort has been made to introduce High Performance Concrete alongwith thermal properties into the existing material library of the software. In coming paragraphs, the detailed account of procedure will be described.

3.2.1 Existing material Library of Open Sees

In OpenSees, uniaxial Material Command is used to construct a Uniaxial Material object which represents uniaxial stress-strain (or force-deformation) relationships. The existing library of OpenSees has primarily two basic materials i.e. concrete and steel which are extensively used in concrete structures. Both the materials have their own peculiar properties which have been defined in their respective input files with help of different

commands. The different types of concrete material which are available in the software are as under

- **Concrete 01 Material (Zero Tensile Strength)**

This command is primarily utilized for construction of a uniaxial Kent-Scott-Park concrete material object with linear unloading/reloading stiffness.

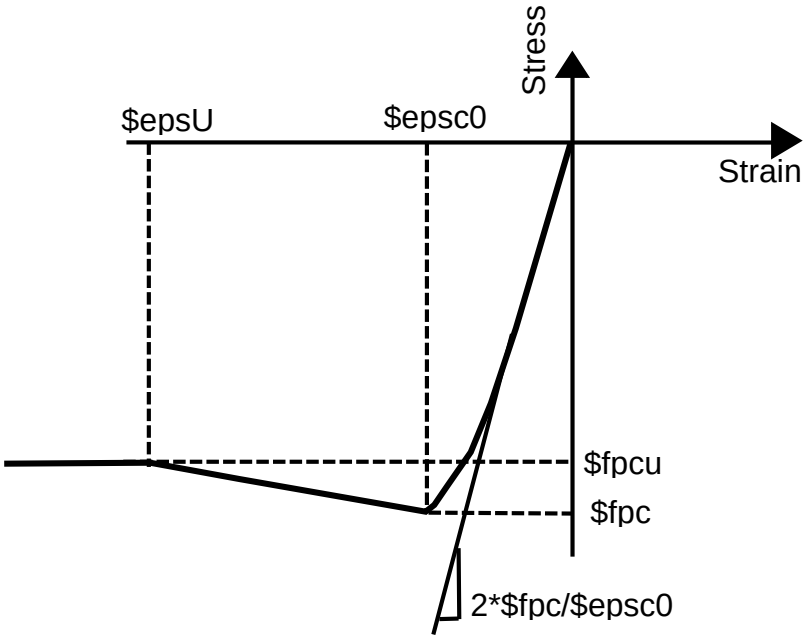

Where

$ matTag	tag integer for identification of the material
$fpc	28 days compressive strength
$epsc0	concrete strain at maximum strength
$fpcu	crushing strength of concrete
$epsU	Strain in concrete at crushing strength

- **Concrete 02 Material (Linear Tension Softening)**

Command utilized for construction of a uniaxial concrete material object with tensile strength and linear tension softening.

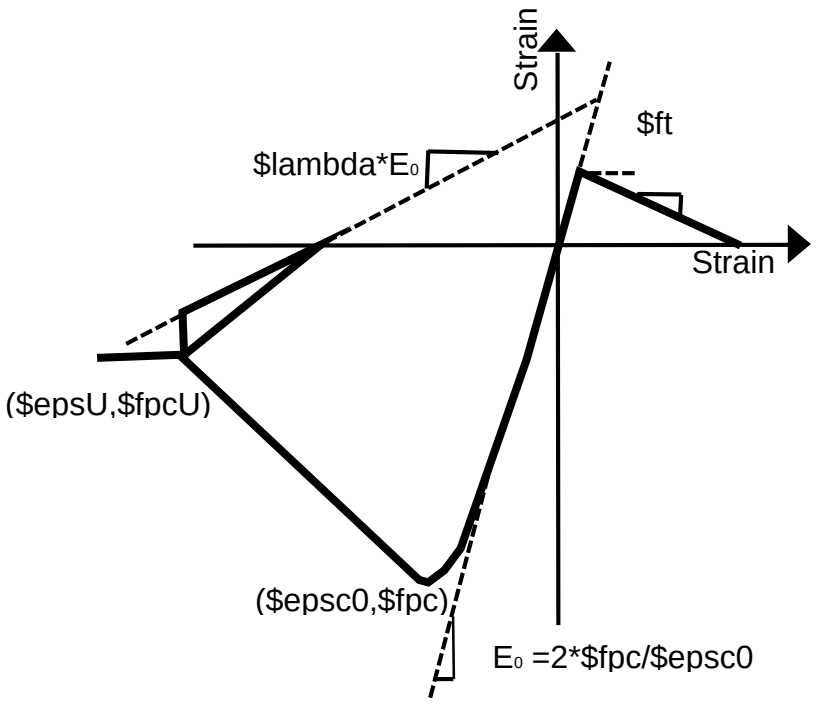

Where

$fpc	28 days compressive strength
$epsc0	concrete strain at maximum strength*
$fpcu	crushing strength of concrete*
$epsU	concrete strain at crushing strength*
$lambda	ratio between unloading slope at $epscu and initial slope
$ft	tensile strength
$Ets	tension softening stiffness

- **Concrete03 Material (Non Linear Tension Softening)**

Command utilized for construction of a uniaxial concrete material object with tensile strength and nonlinear tension softening.

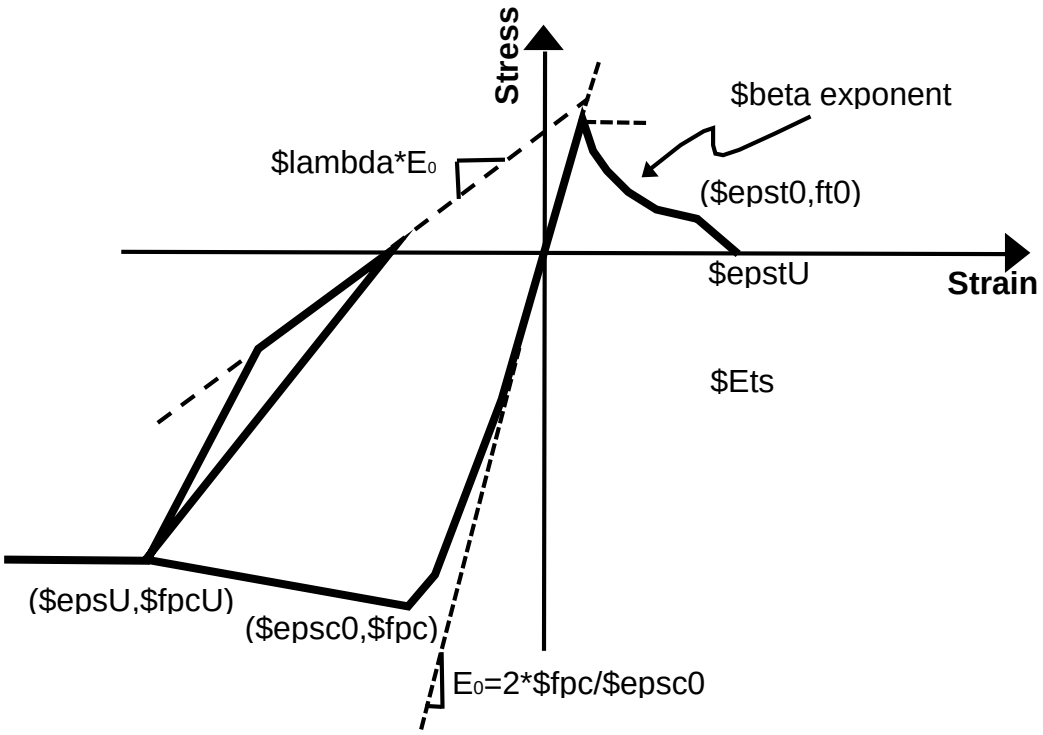

Where

$fpc	-	28 days Compressive Strength of Concrete
$epsc0	-	Strain of concrete at maximum strength*
$fpcu	-	Crushing strength of Concrete *
$epsU	-	Concrete strain at crushing strength*
$lambda	-	Ratio between unloading slope at $epscu and initial slope
$ft	-	Tensile strength
$Ets	-	Tension softening stiffness

- **Concrete 02 Thermal**

This class is derived by modification of the existing concrete material class "Concrete02" to include the temperature-dependent properties according to EN 1992-1-2 concrete with siliceous aggregates at elevated temperature. These properties include following: -

Compressive strength

Specific Heat

Tensile Strength

Thermal Elongation

The input file of Concrete02 Thermal is attached at Anx T.

3.2.2 Incorporating New Concrete Material in Open Sees

OpenSees material library is ever growing with induction of different materials by the developer. In this study, an effort has been made to introduce a new material Concrete02thermalSCC i.e. High Performance Concrete alongwith its material properties at elevated temperature. This will in term help to carry out the fire performance analysis of concrete structures constructed with HPC.

3.2.3 Relationship for Thermal Properties

The data prepared / generated from the measurements of thermal properties is then used to develop relationship of thermal properties for fiber reinforced concretes. The properties thus obtained are reflected in the form of empirical relationships over temperature range of 20-800°C for thermal conductivity, specific heat and mass loss, and in 20-1000°C for thermal expansion. These empirical relationships are based on linear regression. For the regression analysis, measured thermal properties were used as response parameter

with temperature as their predictor parameter. Three data points based on three measurements taken at a target temperature were used for regression analysis.

3.2.3.1 Relations for Thermal Conductivity

Data indicate that thermal conductivity is influenced mainly by the type of high strength concrete, moisture retention in concrete and temperature range. To capture this trend separate expressions are developed for thermal conductivity of HSC. For each concrete type, thermal conductivity relations are presented in two temperature ranges i.e. between 20-400°C and 400-800°C. These relations are presented in the following equations:-

$$k_t = 2.5 - 0.0033T \qquad 20℃ \leq T \leq 400℃$$

$$k_t = 2.3 - 0.002T \qquad 400℃ \leq T \leq 800℃$$

3.2.3.2 Relations for Specific Heat

Specific heat is mostly effected by concrete mix type and temperature range. The presence of steel and hybrid fibers is minimal throughout the range of temperature specified. However, polypropylene fibers have some influence on specific heat of HSC in 650-800°C temperature range. To capture this trend separate equations are proposed for polypropylene fiber reinforced HSC in 400-800°C temperature range. These relationships are presented as under :-

$$C_p = 2.4 + 0.0002T \qquad 20℃ \leq T \leq 400℃$$

$$C_p = 2.4 + 0.0006T \qquad 400℃ \leq T \leq 800℃$$

3.2.3.3 Relations for Thermal Expansion

The expression for thermal expansion of HSC is given below. Since thermal expansion of HSC has a direct correlation with temperature, a single equation is developed

over entire temperature range. As fibers have no pronounced effect on thermal expansion of HSC, same relations can be used for fiber reinforced HSCs and HSCh.

$\mathcal{E}_{th}$=−0.05+0.001T 20℃≤T≤1000℃

3.2.3.4 Relations for Mass Loss

Mass of HSC, SCC and FAC are presented in following equations. Since mass loss does not vary significantly throughout temperature range, a single equation is developed over entire temperature range for both concretes. Also fibers have no pronounced effect on mass loss of HSCs and HSCh.

$M/M_{\circ}$=1 20℃

$M/M_{\circ}$ =1.01 − 0.0002T 20℃≤T≤600℃

$M/M_{\circ}$ =1.25 − 0.00055T 600℃≤T≤800℃

3.2.4 Relationships for Mechanical Properties

3.2.4.1 General

Khaliq and Kodur conducted experiments and the data generated from the mechanical property measurements is further utilized to develop mechanical property relationships for SCC. These properties are expressed in the form of empirical relationships over temperature range of 20-800°C for compressive strength, splitting tensile strength and elastic modulus. These empirical relationships were arrived at based on linear regression

3.2.4.2 Relations for Compressive Strength

The variation of compressive strength ($f'c,T$), tensile strength ($f't,T$) and elastic modulus (Et) with temperature can be related through a coefficient βt representing ratio of respective strength at target temperature to that at room temperature ($f'c$, $f't\ and\ E$0) given by following equations. The strength reduction coefficient ratio (βt) for compressive strength is given as βt,,compressive=f′c,Tf′c .

βt,compressive=1.0	20℃
βt,compressive=1−0.0016T	100℃≤T<400℃
βt,compressive=0.74−0.0008T	400℃≤T≤800℃

3.2.4.3 Relations for Splitting Tensile Strength

The strength reduction coefficient ratio (βt) for splitting tensile strength is given as: βt tensile=f′t,Tf′t.

HSC-S

βt,,tensile=1	20℃
βt,tensile=0.9	100℃≤T<300℃
βt,,tensile=1.42−0.0018T	300℃≤T≤800℃

HSC-H

βt,,tensile=1	20℃
βt,,tensile=0.78	100℃≤T≤300℃

βt,,tensile=1.28−0.0016T 400℃≤T≤800℃

3.2.4.4 Relations for Elastic Modulus

The strength reduction coefficient ratio (βt) for elastic modulus is given as βT,modulus=ETE0

βT,modulus=1 20℃

βT,modulus=0.84−0.001T 100℃≤T≤800℃

3.2.4.5 Summary of Thermal properties of HSC at elevated temperature

The summary of thermal properties of HSC at high temperature can be shown as under :-

Property	Relation
Thermal conductivity $(W/m\text{-}^{\circ}C)$	$k_{t=}$ { 3.12-0.0045T 20°C≤T≤400°C ; 3-0.0025T 400°C≤T≤800°C }
Specific heat $(MJ/m^3\text{-}^{\circ}C)$	$C_{p=}$ { 2.4+0.001T 20°C≤T≤400°C ; 0.6-0.006T 400°C≤T≤800°C }
Specific heat $(MJ/m^3\text{-}^{\circ}C)$	$C_{p=}$ { 2.4+0.001T 20°C≤T≤400°C ; 0.6-0.006T 400°C≤Tb650°C ; 10.6-0.01T 650°C≤T≤800°C }
Thermal expans	$\varepsilon_{th=}$ { 0 20°C ; -0.1+0.0015T 20°CbT≤800°C }
Compressive str	$\beta_{r,\ compression=}$ { 1.0 20°C ; 0.99-0.002T 100°C≤Tb200°C ; 0.73-0.0005T 200°C≤T≤800°C }
Splitting tensile	$\beta_{r,\ tensile=}$ { 1.0 20°C ; 0.99-0.001T 100°C≤T≤800°C }
Splitting tensile	$\beta_{r,\ tensile=}$ { 1.0 20°C ; 1.1-0.001T 100°C≤Tb800°C }
Elastic modulus	$\beta_{r,\ modulus=}$ { 1.0 20°C ; 0.84-0.001T 100°C≤T≤800°C }
Elastic modulus	$\beta_{r,\ modulus=}$ { 1.0 20°C ; 1.1-0.002T 100°C≤Tb200°C ; 0.88-0.008T 200°C≤Tb800°C }

Table 3.1 High temperature property relationship for thermal and mechanical properties of HSC

3.2.5 Input file of Concrete02thermalHCC

The input file of new material Concrete02thermalHCC is derived by modification of Concrete02thermal. The new material contains all the results of the tests conducted by Dr Wasim Khaliq. The detailed commands alongwith description is at Appendix C.

3.2.6 Adding new material Code in OpenSees

Externally written codes (C / C++ / Fortran) can be added to OpenSees interpreters using dynamic link libraries (*.dll) on windows machine. The newly prepared material was further incorporated in the existing library of the OpenSees. For this purpose source code of the software was downloaded and modified. Now the modified OpenSees software is capable of conducting thermal analysis of structures compose of HPC materials.

3.2.7 Testing the New Material Code

The modified OpenSees software was further tested. A new tcl file made up of new material code was run and out put was checked which was found correct. This shows that the new material has successfully been added to the software.

3.3 Modelling of RCC Columns in OpenSees

The source codes of OpenSees have been written in the Object oriented language, C++. The source codes for OpenSees were developed using Microsoft Visual Studio 2005.

In order to carryout modelling in OpenSees, the user have to create an input file of C++. The input file is just a script which carries a series of commands that instruct the interpreter what to do. These commands either create objects or invoke methods (procedures) on those objects. In OpenSees there are 3 types of objects the user will have to create:

- **Modeling**: In modeling, one will have to create a Model Builder object which is used to define the type of model. Different commands are available for

building the model. Element, Node, Load Pattern and Constraint objects etc are the commands to define the model.

- **Analysis**: After defining the model, the next step is to create the Analysis object for analyzing the model. In this software, an Analysis object is composed of several component objects, whereas the component objects consist of Solution Algorithm, Integrator, Constraint Handler, DOF Numberer, SystemOfEqn, Solver, and ConvergenceTest. This method of analysis provides flexibility for conduct of analysis.
- **Output Specification**: After defining the model and analysis, the user must specify what is to be monitored during the analysis. OpenSees by default will producde no output. The outputs specified could for example be the displacement history at a node or internal stress state at some material point in an element element. The user typically creates Recorder objects to store what the user wants to examine, though the user can also use the tcl puts command.

3.3.1 Writing Input File of OpenSees for RCC Column

The Element command s used to construct an element and add it to the Domain. For reinforced concrete column, Elastic Beam Column Element will be used. And in order to conduct thermal analysis, a derived command i.e. Beam Column Element Thermal is used in this study. The detail code at Annexx T. The RCC column is taken as nonlinear model having 11 nodes. The diagram of the RCC along with dimensions is as under: -

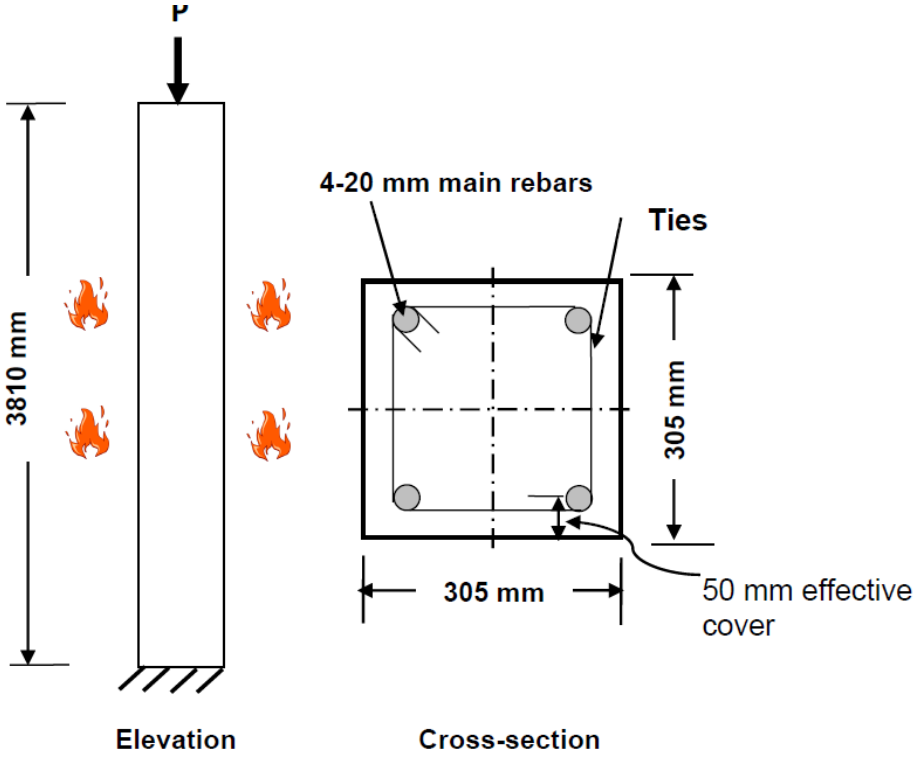
P
3810 mm
4-20 mm main rebars
Ties
305 mm
305 mm
50 mm effective cover
Elevation
Cross-section

3.3.2 Defining nodes in the software

The length of entire column i.e. 3.3 m or 3300 mm is taken as one element and in the code, it is defined by 11 nodes as under:-

node 1 0 0;

node 2 0 330;

node 3 0 660;

node 4 0 990;

node 5 0 1320;

node 6 0 1650;

node 7 0 1980;

node 8 0 2310;

node 9 0 2640;

node 10 0 2970;

node 11 0 3300;

3.3.3 Defining section of the column

The section properties of the columns are defined by fiber sectionthermal as under:-

fiber 88.8125 0 5151.25 2;

fiber 63.4375 0 5151.25 2;

fiber 38.0625 0 5151.25 2;

fiber 12.6875 0 5151.25 2;

fiber -12.6875 0 5151.25 2;

fiber -38.0625 0 5151.25 2;

fiber -63.4375 0 5151.25 2;

fiber -88.8125 0 5151.25 2;

3.3.4 Defining Mild Steel Bars in the software

Layer command is used to define the reinforcement of the column.

layer straight 1 2 284 -51.5 51.5 51.5 51.5 # upper layer

layer straight 1 2 284 -51.5 -51.5 51.5 -51.5 # lower layer

3.3.5 Defining Thermal Load

The temperature is applied in terms of thermal load and the FireLoadPattern command is used for this purpose. This command is used to create a load pattern which Co-works with TimeSeries definition, and Generates a vector of load factors. And in FireLoadPattern, An Interface is provided to define a set of "Beam2dThermalAction"s.

pattern Fire $ Pattern Tag $Path $Path $Path $Path $Path $Path $Path $Path $Path { eleLoad -ele $eleTag -type -beamThermal $T1 $Y1 $T2 $Y2 < $T3 $Y3... $T9 $Y9> ... eleLoad -ele $eleTag -type -beamThermal $T1 $Y1 $T2 $Y2 < $T3 $Y3... $T9 $Y9> }

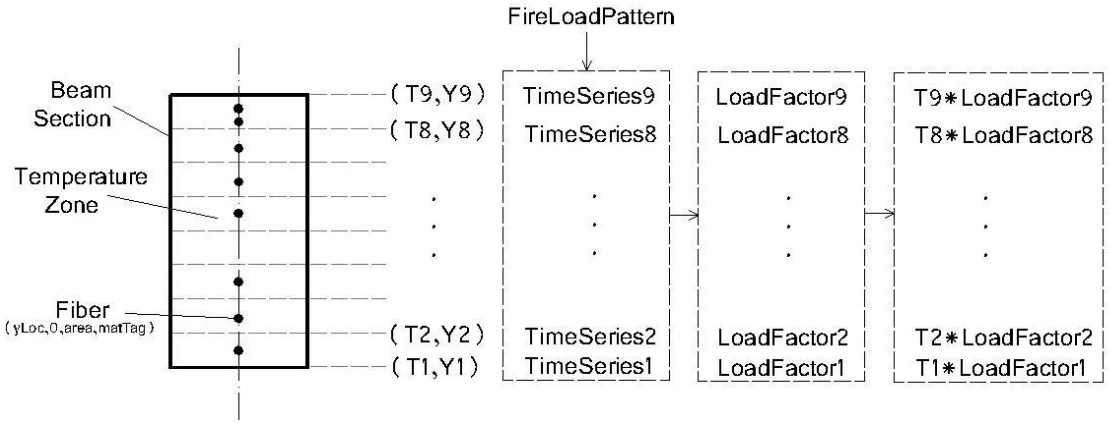

Set T1 640; set T2 275; set T3 222; set T4 275; set T5 640;

set Y1 -101.5; set Y2 -50.75; set Y3 0; set Y4 50.75; set Y5 101.5;

3.3.6 Defining Output Files

Output files in OpenSees are defined as txt files. The command used for taking output from this software is known as recorder. In this particular case, displacements of nodes in both two dimensions have been taken out and recorded.

```
Recorder    Node -file node61mycol.out -time -node 6 -dof 1 disp;

Recorder    Node -file node62mycol.out -time -node 6 -dof 2 disp;
```

3.4 Summary

OpenSees is a versatile open source software. It provides ample opportunities to the user and developer to conduct analysis as per their requirements. It also enables everyone to add additional section, elements and materials into it existing setup and conduct analysis. During the conduct of study an entirely new material i.e. High performance concrete has been added to already existing materials of the software which has been successfully done and required results are being recorded.

CHAPTER 4

Results and Discussion

4.1 General

After incorporation of HSC into the existing material library of OpensSees and software and modelling of column in the software, the fire performance analysis of was carried out. The dimension and cross section of column has been kept the same as that used by Dr Khaliq in his experimental studies. The experimental data was of great help, not only to get the actual fire scenario and heat transfer rate but also remained useful for validation of numerical studies.

4.2 Selection of specifications for RC Column

The RC columns with geometric details is shown in Figure 4.1 is selected with varying parameters. The column specifications were kept the same as that used by Khaliq and Kodur in the experimental studies. In the experimental studies, the dimensions of columns were mainly dictated by fire test furnace in which those columns were to be tested. The cross sections of the columns used are as under:-

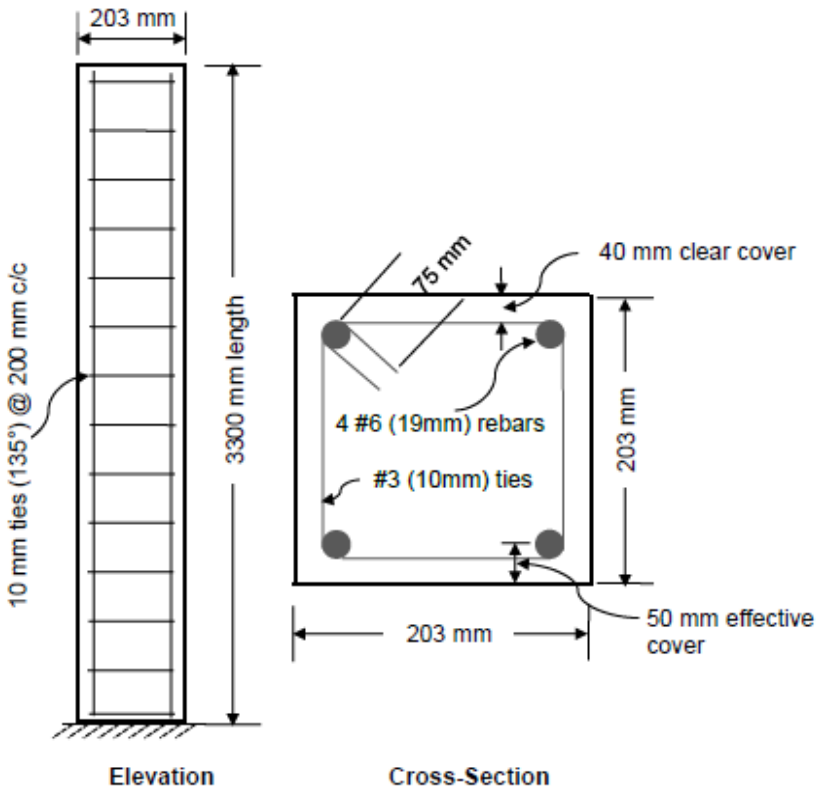

Figure 4.1 – Column elevation and cross section showing design details

Design parameter	**Notation**	**Value**
Gross area (Cross-section = 203x203 mm)	Ag	41209 mm
Steel yield strength	f_y	420 MPa
Steel area (4 # 6 bars)	A_{st}	4 x 285 = 1140 mm^2
Length of column	1	3300mm
Concrete cover to main rebar's for minimum 2 hours fire resistance	-	50 mm (AC1216.1 2.5.3)
Column end conditions	-	Pin-pin

Table 4.1 – Design Parameters used for the column

The mix proportions used in the preparation of the columns for the experimental studies is also attached as under:

Component	HSC-S	HSC-H
Cement (Type I), kg/m^3	513	513
Fine Aggregate, kg/m^3	684	684
Course Aggregate (max size 10mm), kg/m^3	1078	1078
Silica fume, kg/m^3	43	43
Fly ash- Class C (25% replacement of cement) kg/m^3	-	-
Slag – Grade 120, kg/m^3	-	-
Water, kg/m^3	130	130
Water cement ratio (w/c)	0.25	0.25
Retarding admixture – Type D, kg/m^3	-	-
High range water reducer/Superplasticizer – Type F, kg/m^3	15	15
Shump, mm	100	90
Polypropylene fiber, kg/m^3 (0.22% by volume)	-	2
Steel fibers, kg/m^3 (0.54% by volume)	42	42
Unit weight of concrete, kg/m^3	2490	2490
Compressive strength (MPa)		
7 days	66	68
28 days	67	68
90 days	72	75
Test day	77	80

Table 4.2 – Mix Proportions used for concrete columns

The test parameters used are

Column designation	Fire exposure (ASTM E119 – decay)	Total test time (minutes)	Concrete strength (MPa)		Column strength (kN)	Load ratio (%)	Applied load (kN)	Relative humidity (%)	Failure times (minutes)	Extent of spalling	Residual strength kN (% of ultimate load capacity)
			28 days	Test day							
HSC-S	**SF – decay @11º C/min**	270	72	77	1612	60	967	91.25	No Failure (270)	Nil	839 (52%)
HSC-H	**SF – decay @11º C/min**	270	75	80	1665	60	999	89.65	No Failure (270)	Nil	741 (44.5%)

Table 4.3 – Miscellaneous parameters used for the tests

4.3 **Fire Scenario and Heat Transfer Rate**

The heat transfer rate was taken from the experimental data of the tests conducted by Dr Wasim Khaliq. The results are

4.3.1 Fire Scenario used for the studies

The ASTM E119 fire was used in the experimental studies. The time temperature curve of the furnace is shown in fig…

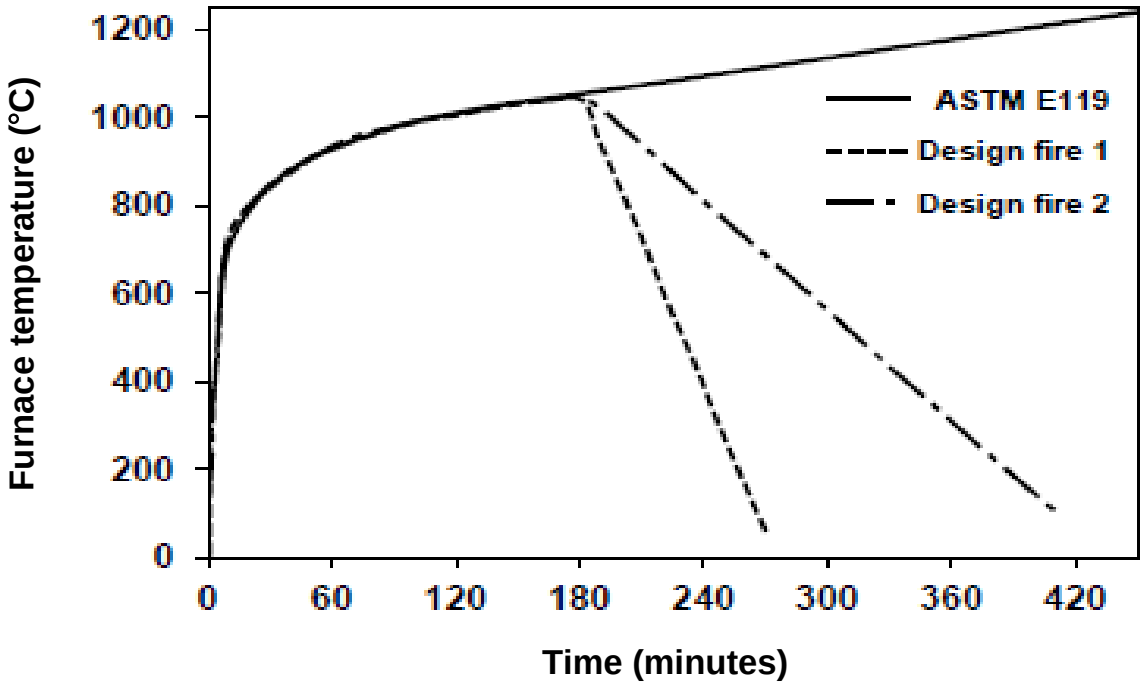

Figure 4.2 – Time temperature curve for fire scenario

4.3.2 Temperature used for Columns at different fibers

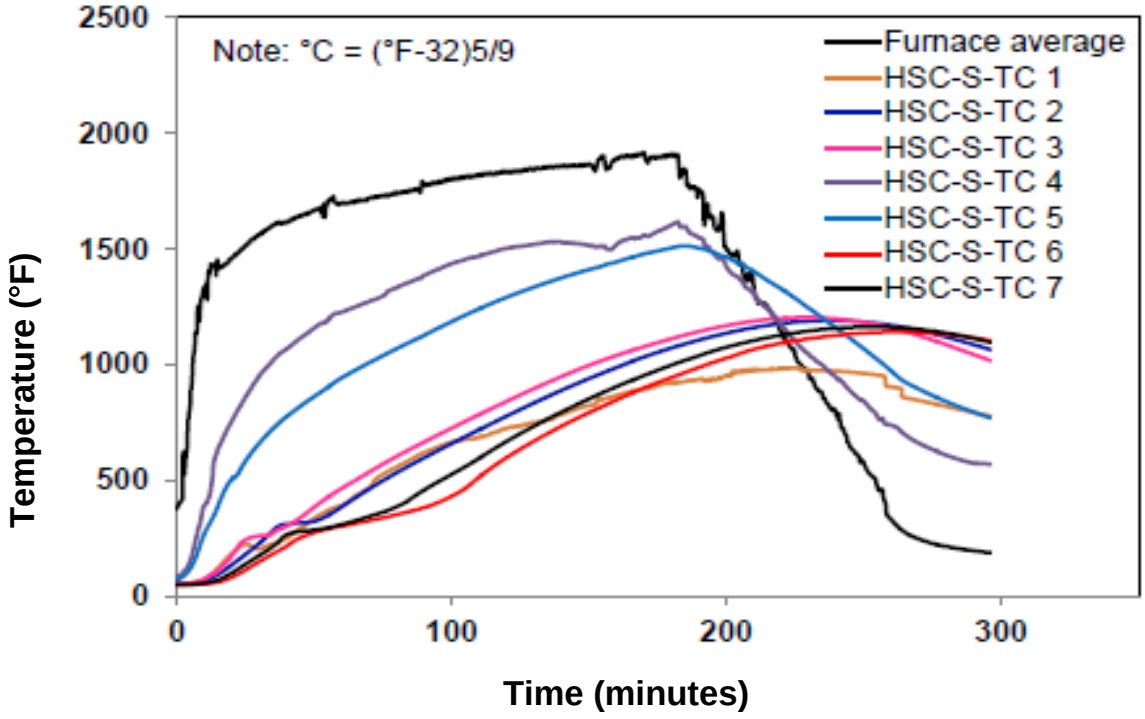

Figure 4.3 – Measured rebars and concrete temperature for HSC-S Column

4.4 Data Obtained and Observations

The test data of column temperature, axial deformations, lateral deformation and loading were recorded.

4.4.1 Structural Response

Structural response of the column is generally assessed by measuring axial and lateral deformation in column. Both axial and lateral deformations were calculated from the software and presented here for analysis.

4.4.2 Axial Deformation

The structural response of the columns is evaluated by comparing measured axial deformations as a function of fire exposure time.

4.4.2.1 Axial Deformation of HSCs Column

The axial deformation measured in HSCs column is shown in Figure 4.4.

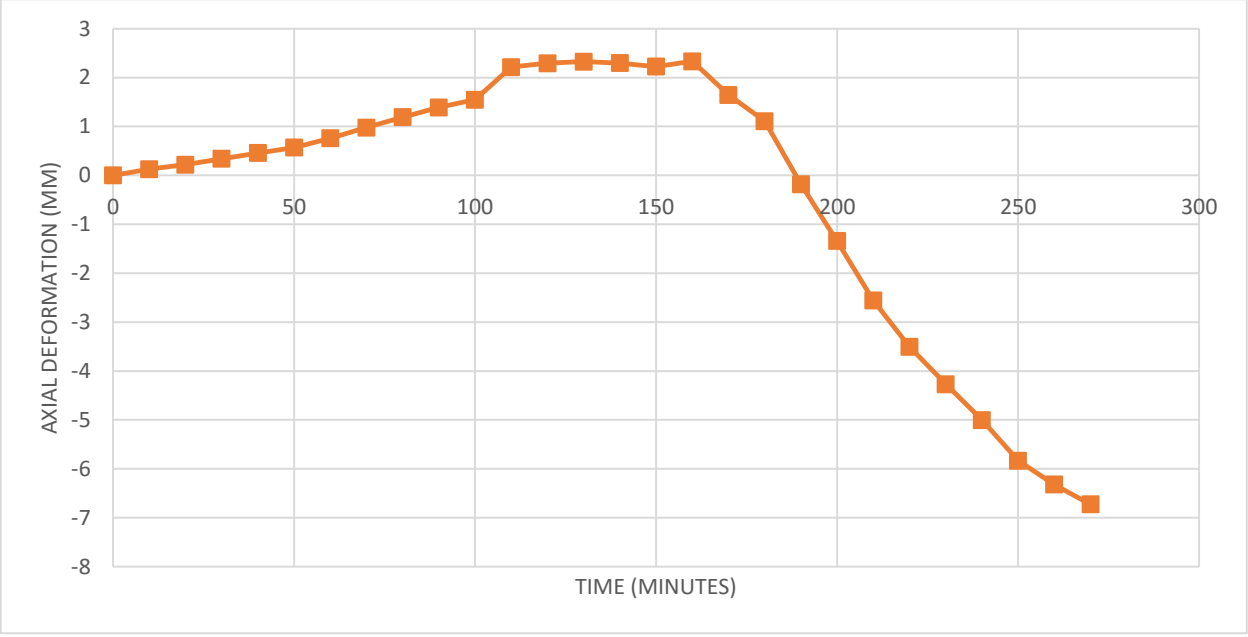

Figure 4.4 - Measured Axial Deformation in HSCs Column as a function of fire exposure time

It has been noticed that initially the column expands till 160 minutes. The maximum expansion measured is 2.32 mm. After that the contraction phase starts.

4.4.2.1 Axial Deformation of HSCh Column

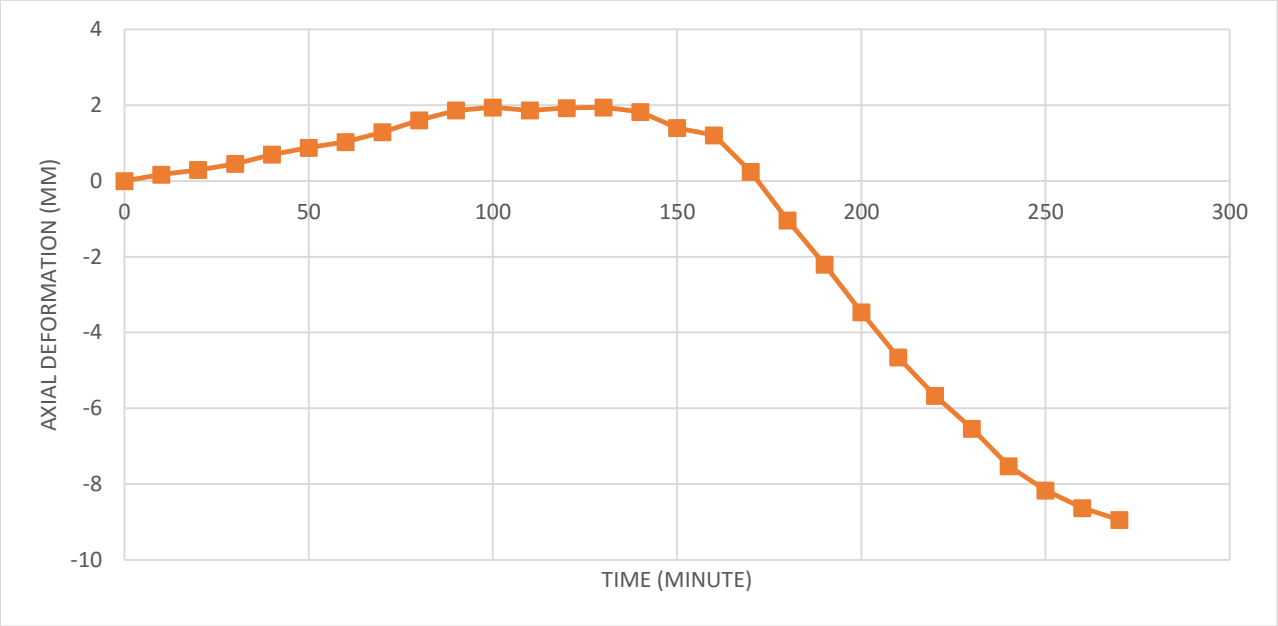

Figure 4.5 - Measured Axial Deformation in HSCh Column as a function of fire exposure time

The maximum expansion in HSCh column is 1.94 mm which is little less than the expansion measured in HSCs column.

A RCC column, when exposed to fire, expands initially due to thermal expansion occurring both in steel rebars and in concrete. With increasing fire exposure time, temperatures in rabar rise and the steel yields at about 600 C, a temperature which is critical for steel as it loses 50% of its yield strength (Lie, 1992). After steel yields, concrete core in the column progressively carries higher percentage of applied load. With increasing temperatures, strength and stiffness properties also deteriorate in concrete (Kodur and McGrath, 2003) leading to increased load induced mechanical strains which in turn results in contraction of the columns. With increasing fire exposure time, the strength of the concrete also decreases due to deteriorating properties of concrete, and ultimately, when the column can no longer support the load, failure of column occurs.

4.4.3 Lateral Deformation

The lateral deformation measured at mid-height is plotted as a function of fire exposure time.

4.4.3.1 Lateral Deformation in HSCs Column

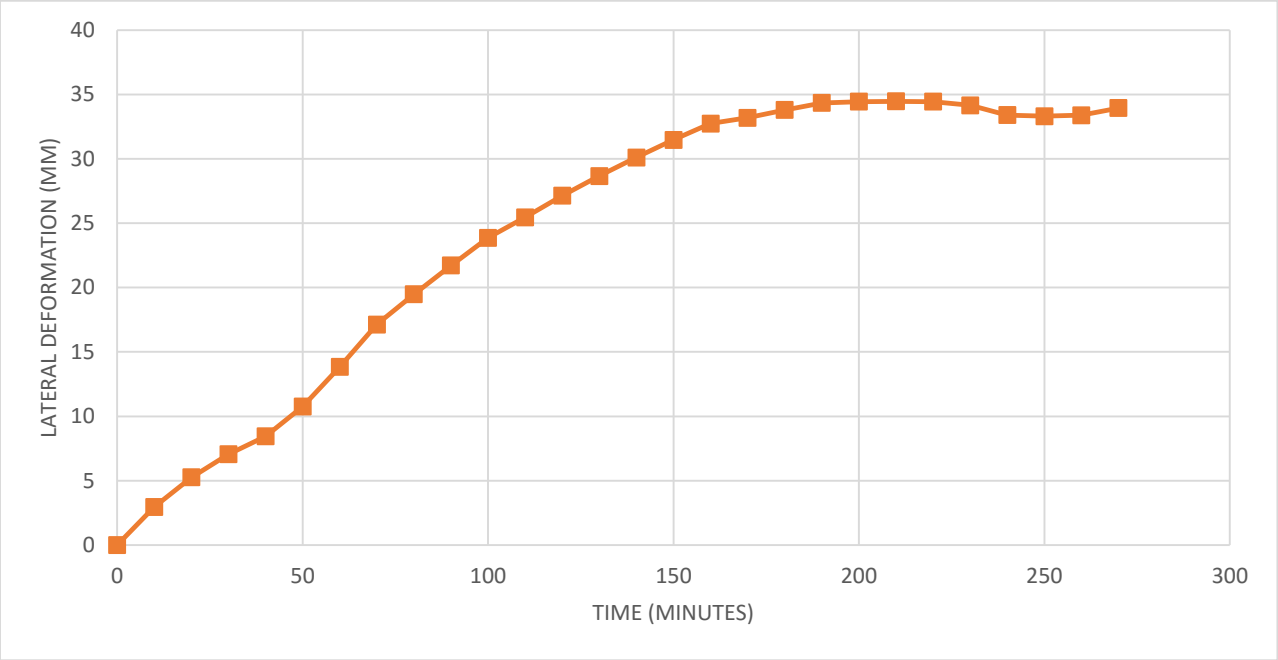

Figure 4.5 – Measured lateral deformation in HSCs Column as a function of fire exposure time

The maximum lateral deformation measured is 34.46 mm in HSCs Column.

4.4.3.2 Lateral Deformation in HSCh Column

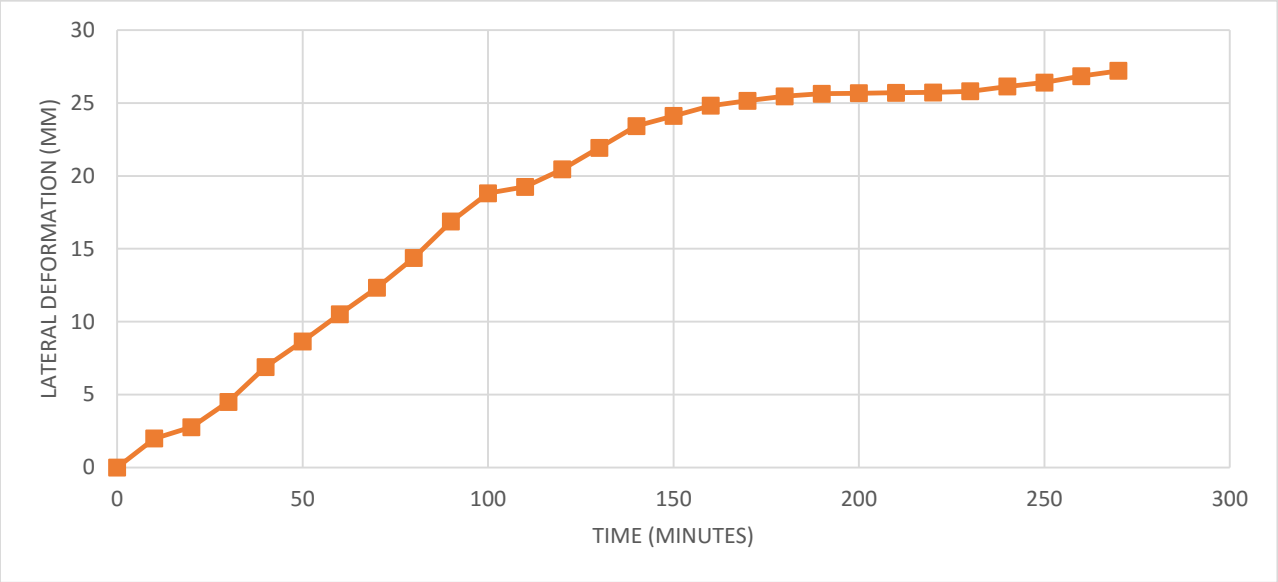

Figure 4.5 – Measured lateral deformation as a function of fire exposure time

Both the columns had similar end (restraint) conditions i.e. completely fixed. These columns exhibited lateral deformation in the expansion phase (in the initial stages of fire) and the deformation reached 25 mm at 100 minutes in to fire exposure. However, in HSCs column, the lateral deformation significantly increased to 34,44 mm, at the time of failure, when the column moved in to contraction phase. The excessive lateral deformation in first column is due to presence of steel fibers whereas the second column showed more ductility due to presence of polypropylene fibers.

4.5 Validation of the Results

The validation of the analysis results is carried out with following two available research papers:-

a. Performance Characterization of High Performance Concrete under fire condition by Wasim Khaliq, 2012
b. Fire Performance of High Strength Concrete Structural Members by V.K.R. Kodur, 1999

The specifications of the structural elements i.e. column and all the material properties were kept the same as that of the experimental studies conducted by Wasim Khaliq 2012. The experimental results of the study are placed at Annex A.

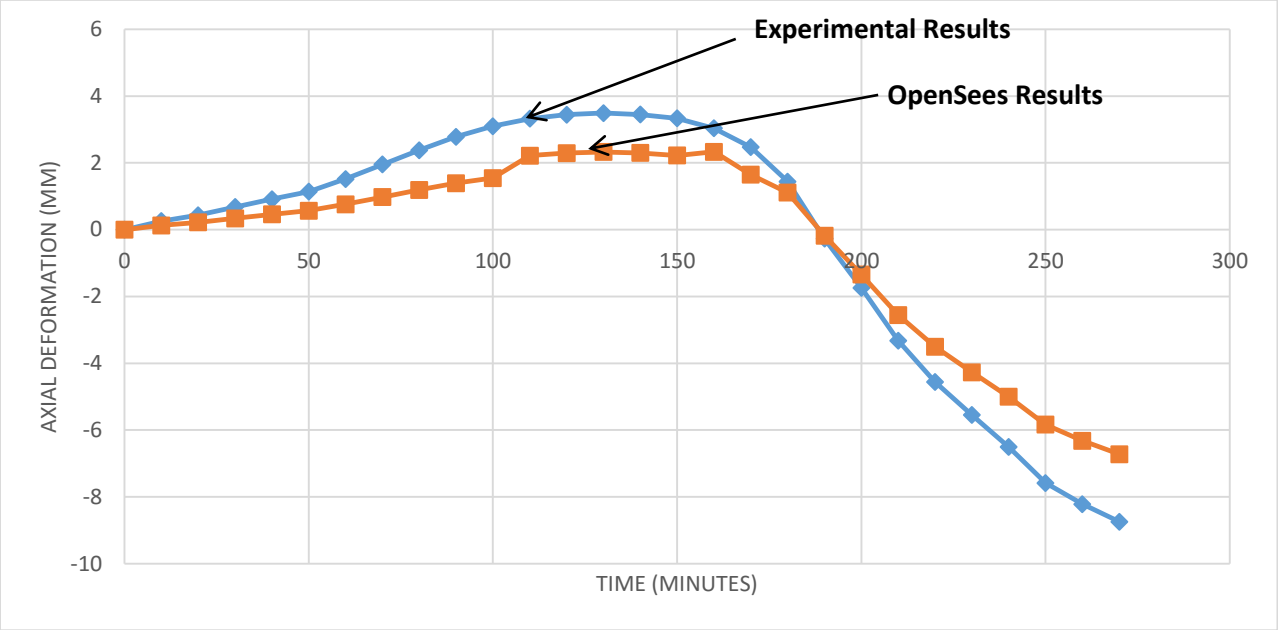

Figure 4.6 Comparison of results of HSCs Column

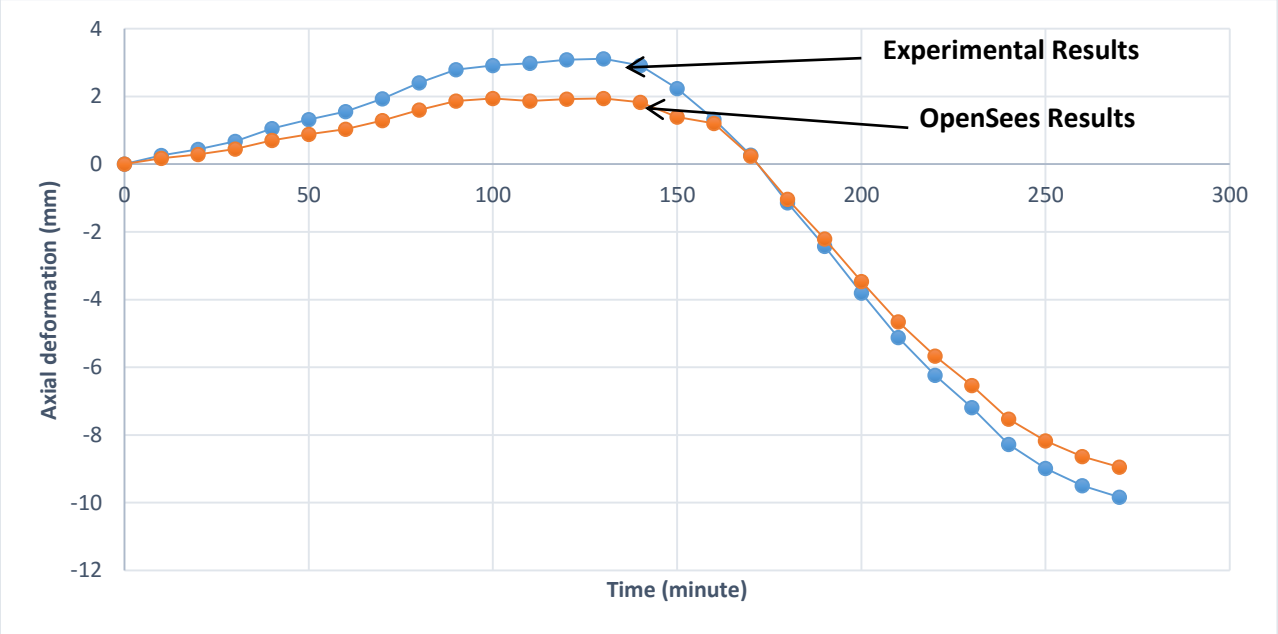

Figure 4.6 Comparison of results of HSCh Column

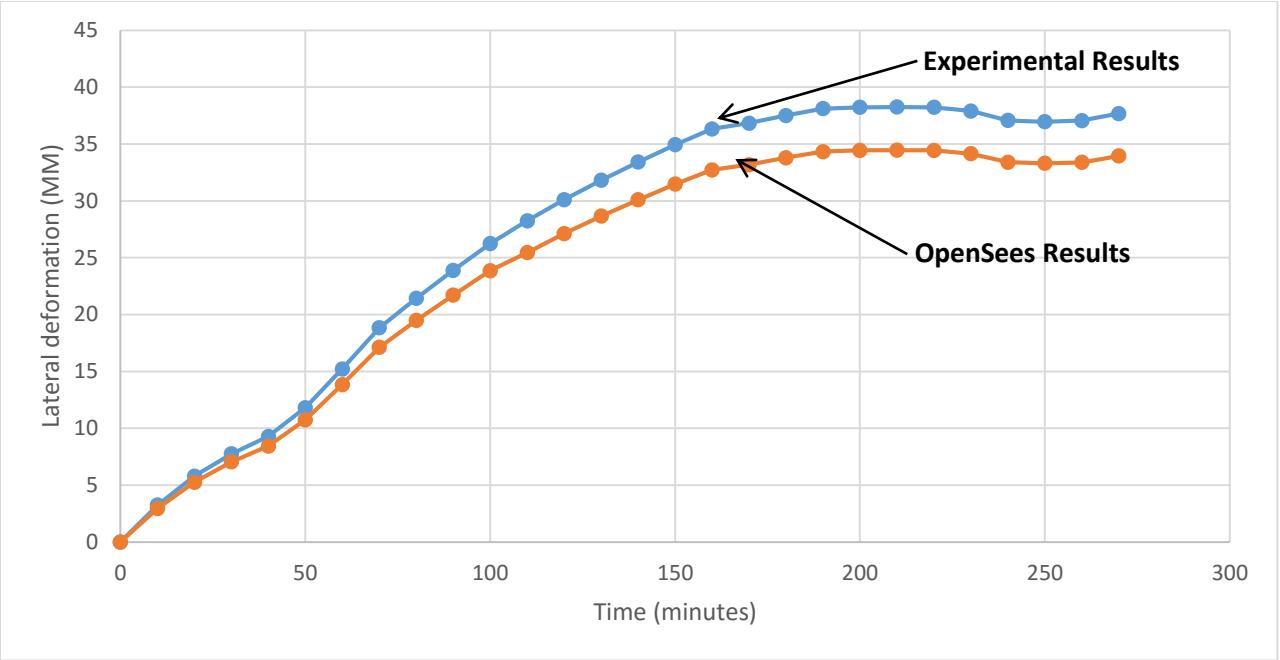

Figure 4.7 Comparison of results of Lateral Deformation of HSCs Column

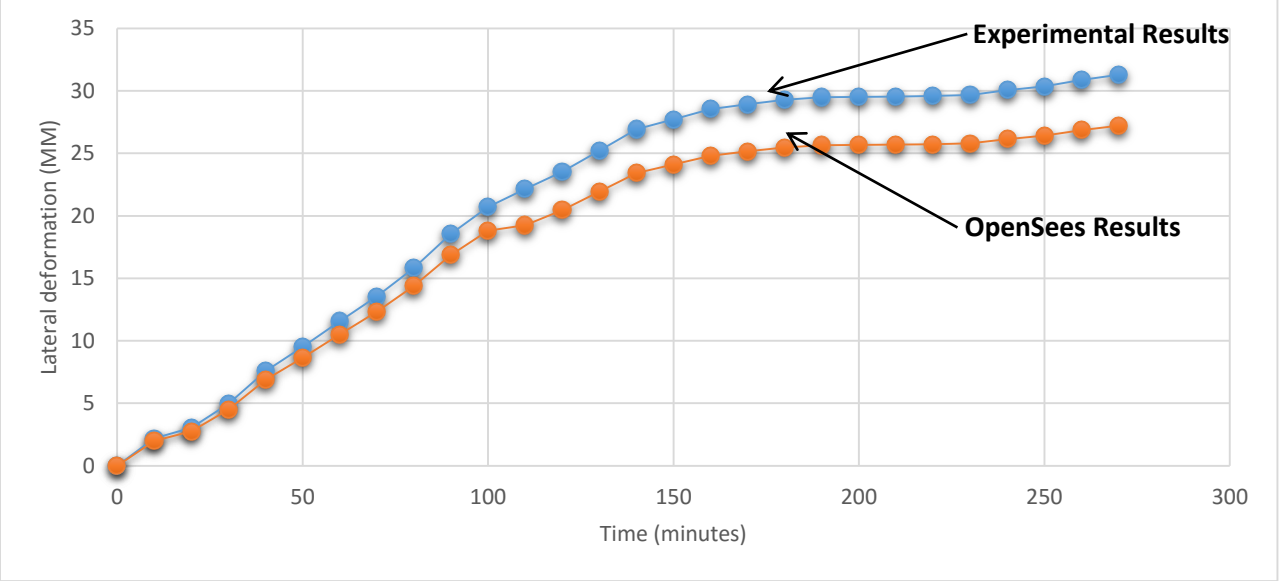

Figure 4.7 Comparison of results of Lateral Deformation of HSCh Column

Thus, the results obtained from software were validated by that of the experimental data obtained. The results obtained from software were found quite similar to that obtained from experiments. However, the difference or changes observed were due to the reasons as explained below.

4.5.1 Material Properties

In software, the material i.e. concrete and steel properties are constant whereas in experiments, the properties of concrete depends upon a lot of factors which includes type of cement, type of aggregate, mix proportion, water cement ratio etc. Thus the experimental results will always show some deviation from the data obtained from softwares.

4.5.2 Confinement of Concrete

In OpenSees software, the confinement of concrete is expressed in terms of increased compressive strength of concrete. Whereas in actual experiments, the confinement of concrete in columns changes with tie configuration etc.

4.5.3 End Conditions

In software, the end conditions i.e. support types is either fixed or free, whereas in actual conditions it is never completely free or fixed. This also play a role in obtaining slightly different values of displacements recorded at different nodes.

4.5.4 Heat Transfer Rate

In software heat transfer rate is defined on selected nodes whereas in actual experiment, there is continuous changes occurring in temperatures of different fibres.

4.6 Summary

Fire response of reinforced concrete structures is influenced by a number of factors, most of these factors are interdependent and make it complex to carry out fire resistance predictions. Factors such as high temperature material properties of a specific HSC and effect of fibers significantly influence the fire performance of RC Columns and study need to be undertaken to quantify them. As additional subroutines based on empirical relations for high temperature material properties of HPC (plain and with fibers) and tie configuration are added to the numerical model, the usefulness of model is established by undertaking parametric studies to account for the influence of these factors.

There are several factors that influence the fire response of RC columns. These factors have been well studied through qualitative parametric studies and reported in

previously (Ali et al., 2001; Kodur, 2003; Raut, 2011) and the important factors that have been quantified consist of:

- Fire scenario,
- Size (cross-section) of column,
- Concrete cover thickness,
- Aggregate type,
- Load ratio,
- Reinforcement ratio,
- Load eccentricity (uniaxial and biaxial),
- Column face exposure
- Concrete strength (permeability) based on NSC and HSC,

However, as indicated in state-of-the-art review in Chapter 2, some of the critical factors that influence the fire response of HPC columns have not been studied yet. These factors consist of:

- Material Properties of New types of HSC
  - Thermal properties consisting of thermal conductivity, specific heat, thermal expansion and mass loss
  - Mechanical properties consisting of compressive strength, splitting tensile strength, elastic modulus and stress-strain response
- Use of fibers
- Concrete strength (permeability) based on HSC

CHAPTER 5

Conclusions and Recommendations

5.1 General

This research study has endeavored to compile data on elevated temperature material properties of normal strength concrete as well as fiber reinforced high strength concretes alongwith fire / thermal analysis of high strength concrete columns using OpenSees software and its validation with the experimental data as conducted by Khaliq and Kodur 2011. Material properties consist of thermal properties namely thermal conductivity, specific heat, thermal expansion, and mass loss and mechanical properties namely compressive strength, splitting tensile strength, elastic modulus, and stress-strain curves. Whereas, fire resistance tests also provided useful data for validation of the model for RC columns made of HSC that included cross-sectional temperatures, vertical and horizontal deflections on fire response.

5.2 Key Findings

Based on the information presented in this study, some of the key findings/ conclusions are as under:

- A very limited information and compiled data is available on high temperature material properties of various emerging types of concrete like self-consolidating concrete etc.
- Data generated from high temperature thermal property tests of HSC indicates that:
    - Temperature has significant influence on thermal conductivity and specific heat of HSC and it decreases with temperature similar to conventional NSC. Specific heat of HSC remains almost constant up to about 400°C, and then increases up to about 650°C before following a constant trend in 650-800°C range.
    - Thermal expansion of HSC increases with temperature up to 800°C and this increase is higher compared to NSC.

- No significant mass loss occurs in HSC up to 600°C, and moderate mass loss occurs in 600-800°C.

- The mechanical properties namely compressive strength, tensile strength and elastic modulus significantly degrade with temperature for HSC.
- Conduct of analysis through OpenSees software indicates that:
  - OpenSees is an object oriented, software framework primarily used for structural analysis of earthquake engineering simulation.
  - The software platform can successfully be utilized for fire analysis of structures.
  - OpenSees is an open source software which affords incorporation of new materials, sections and framework into its existing libraries.
  - The high temperature properties of High Strength concretes as measured through experiments can be incorporated in the source code of OpenSees.
  - Incorporation of new material will modify the existing software which then enables to run analysis of structures made up of new types of construction materials.
    - OpenSees Fire module can ***reliably simulate the fire behavior of RC structures***
    - The module produced ***85-90 % accurate results as that of the available experimental data*** when used for HSC structures after incorporating HSC materials into the existing framework
    - Presence of fibers in the mixes improves tensile strength and ductility, thus ***significantly enhance their fire resistance***

5.3 Recommendations

This study has introduced the new software i.e. OpenSees for modelling of fire for RC structures. After conduct of analysis and doing validating with the aval date, following recommendation are proffered:-

- OpenSees, a non destructive testing tool, should extensively be used for **fire analysis of existing structures**
- Future studies should endeavor to ***incorporate all types of HPC*** into existing framework and make it a versatile tool for analysis of structures under fire

5.4 Research Impact

The information that is developed as part of this research will have significant impact on use of HSC in fire safety applications. HSC have excellent strength and durability characteristics, but are much more susceptible to fire induced spalling and thus have lower fire resistance. This aspect can now be analysed by carryout out nondestructive testing of the structures by using modified OpenSees software.

REFERENCES

ACI-216.1 (2007). "Code requirements for determining fire resistance of concrete and masonry construction assemblies." American Concrete Institute, Farmington Hills, MI.

ACI-318 (2008). "Building Code Requirements for Reinforced Concrete and Commentary." American Concrete Institute, Farmington Hills, MI.

ACI 216.1 (2007). "Code requirements for determining fire resistance of concrete and masonry construction assemblies." *ACI 216.1-07 / TMS-0216-07*, American Concrete Institute, Farmington Hills, MI, 1-32.

ACI 318-08 (2008). "Building Code Requirements for Reinforced Concrete and Commentary." American Concrete Institute, Farmington Hills, MI.

Ali, F. (2002). "Is high strength concrete more susceptible to explosive spalling than normal strength concrete in fire?" *Fire and Materials*, 26, 127–130.

Ali, F., and Nadjai, A. (2008). "Fire resistance of concrete columns containing polypropylene & steel fibers." *ACI Special Publication, SP-255-9, American Concrete Institute, Farmington Hills, MI*, 255(9), 199-216.

Ali, F., Nadjai, A., Silcock, G., and Abu-Tair, A. (2004). "Outcomes of a major research on fire resistance of concrete columns." *Fire Safety J*, 39(6), 433-445.

ASCE (1992). "Structural fire protection." ASCE Committee on Fire Protection, Structural Division, American Society of Civil Engineers, New York.

ASTM C39 (2009). "Standard Test Method for Compressive Strength of Cylindrical Concrete Specimens." ASTM International, West Conshohocken, PA.

ASTM C78 (2009). "Standard Test Method for Flexural Strength of Concrete." ASTM International, West Conshohocken, PA.

ASTM C496 (2011). "Standard Test Method for Splitting Tensile Strength of Cylindrical Concrete Specimens." ASTM International, West Conshohocken, PA.

ASTM C496 (2004). "Standard Test Method for Splitting Tensile Strength of Cylindrical Concrete Specimens." ASTM International, West Conshohocken, PA.

ASTM C1113 (2009). "Standard Test Method for Thermal Conductivity of Refractories by Hot Wire (Platinum Resistance Thermometer Technique)." ASTM International, West Conshohocken, PA.

ASTM C1269 (2011). "Standard Test Method for Determining Specific Heat Capacity by Differential Scanning Calorimetry." ASTM International, West Conshohocken, PA. 29 8

ASTM C1583 (2004). "Standard Test Method for Tensile Strength of Concrete Surfaces and the Bond Strength or Tensile Strength of Concrete Repair and Overlay Materials by Direct Tension (Pull-off Method)." ASTM International, West Conshohocken, PA.

ASTM E119-08b (2008). "Standard test methods for fire tests of building construction and materials." ASTM International, West Conshohocken, PA.

ASTM E831 (2006). "Standard Test Method for Linear Thermal Expansion of Solid Materials by Thermomechanical Analysis." ASTM International, West Conshohocken, PA.

ASTM E1530 (2011). "Standard Test Method for Evaluating the Resistance to Thermal Transmission of Materials by the Guarded Heat Flow Meter Technique." ASTM International, West Conshohocken, PA.

ASTM E1868 (2010). "Standard Test Method for Loss-On-Drying by Thermogravimetry." ASTM International, West Conshohocken, PA.

ASTM Standard E119 (2007). "Standard test methods for fire tests of building construction and materials." ASTM International, West Conshohocken, PA.

Behnood, A., and Ghandehari, M. (2009). "Comparison of compressive and splitting tensile strength of high-strength concrete with and without polypropylene fibers heated to high temperatures." *Fire Safety J*, 44(8), 1015-1022.

Bilodeau, A., Kodur, V. R., and Hoff, G. C. (2004). "Optimization of the type and amount of polypropylene fibers for preventing the spalling of lightweight concrete subjected to hydrocarbon fire." *Cement and Concrete Composites*, 26(2), 163-174.

Bilodeau, A., Kodur, V. R., and Hoff, G. C. (2004). "Optimization of the type and amount of polypropylene fibers for preventing the spalling of lightweight concrete subjected to hydrocarbon fire." *Cement and Concrete Research*, 26, 163-174.

Blaine, R. L., and Hahn, B. K. (1998). "Obtaining kinetic parameters by modulated thermogravimetry." *J Therm Anal Calorim*, 54(2), 695-704.

Boel, V., Audenaert, K., and Schutter, G. D. (2008). "Gas Permeability and Capillary Porosity of Self-compacting Concrete." *Journal of Materials and Structures*, 41(7), 1283-1290.

Buchanan, A. H. (2002). *Structural Design for Fire Safety*, John Wiley and Sons Ltd, Chichester, England.

Campbell, T. I., and Kodur, V. (1990). "Deformation controlled nonlinear analysis of prestressed cocnrete continuous beams." *PCI Journal*, PCI, 42-55. 29 9 Carette, G. G., Painter, K. E., and Malhotra, V. M. (1982). "Sustained high temperature effect on concretes made with normal portland cement, normal portland cement and slag, or normal portland cement and fly ash." *Concrete International*, 4(7), 41-51.

Castillo, C., and Durrani, A. J. (1990). "Effect of transient high temperature on high strength concrete." *Aci Mater J*, 87(1), 47-53.

Chan, Y. N., Peng, G. F., and Anson, M. (1999). "Residual strength and pore structure of high-strength concrete and normal strength concrete after exposure to high temperatures." *Cement and Concrete Composites*, 21(1), 23-27.

Chan, Y. N., Peng, G. F., and Anson, M. (1999). "Residual strength and pore structure of high-strength concrete and normal strength concrete after exposure to high temperatures." *Cement and Concrete Composites*, 21(1), 23-27.

Chen, B., and Liu, J. (2004). "Residual strength of hybrid-fiber-reinforced high-strength concrete after exposure to high temperatures." *Cement Concrete Res*, 34, 1065-1069.

Cheng, F. P., Kodur, V. K. R., and Wang, T. C. (2004). "Stress-strain curves for high strength concrete at elevated temperatures." *National Research Council of Canada, Report # NRCC-46973*, 1-30.

Cook, R. D., Malkus, D. S., Plesha, M. E., and Witt, R. J. (2007). *Concepts and applications of finite element*, John Wiley & Sons, Inc., NY, USA.

Dias, W. P. S., Khoury, G. A., and Sullivan, P. J. E. (1990). "Mechanical properties of hardened cement paste exposed to temperaures up to 700°C." *ACI Mateials Journal*, 87(2), 160-166.

Dwaikat, M. B. (2009). "Flexural response of reinforced concrete beams exposed to fire." Doctoral Thesis, Michigan State University, East Lansing, Michigan, USA.

Dwaikat, M. B., and Kodur, V. K. R. (2009). "Hydrothermal model for predicting fire induced spalling in concrete structural systems." *Fire Safety J*, 44(3), 425-434.

Flynn, D. R. (1999). "Response of high performance concrete to fire conditions: review of thermal property data and measurement techniques." National Institute of Standards and Technology, Millwood, US. 30 0 Fu, Y. F., Wong, Y. L., Poon, C. S., and Tang, C. A. (2005). "Stress-strain behavior of high-strength concrete at elevated temperatures." *Magazine of Concrete Research*, 57(9), 535-544.

Fu, Y. F., Wong, Y. L., Poon, C. S., and Tang, C. A. (2005). "Stress-strain behaviour of high-strength concrete at elevated temperatures." *Mag Concrete Res*, 57(9), 535-544.

Fu, Y. F., Wong, Y. L., Poon, C. S., Tang, C. A., and Lin, P. (2004). "Experimental study of micro/macro crack development and stress-strain relations of cement-based composite materials at elevated temperatures." *Cement Concrete Res*, 34(5), 789-797.

Furumura, F., Abe, T., and Shinohara, Y. (1995). "Mechanical properties of high strength concrete at high temperatures." *High performance concrete; material properties and design; prodeedings of the Fourth Weimar Workshop on High Performance Concrete; Material Properties*, 237-254.

Ganguli, S., Roy, A. K., and Anderson, D. P. (2008). "Improved thermal conductivity for chemically functionalized exfoliated graphite/epoxy composites." *Carbon* 46(5), 806-817.

Harada, T., Takeda, J., Yamane, S., and Furumura, F. (1972). "Strength, elasticity and thermal properties of concrete subjected to elevated temperatures." *International Seminar on Concrete for Nuclear Reactor, ACI Special Publication, SP34-21*, 34(1), 377-406.

Harmathy, T. Z. (1967). "A comprehensive creep model." *Journal of Basic Engineering*, 89(3), 496-502.

Harmathy, T. Z. (1971). "Moisture and heat transport with particular reference to concrete." *National Council of Canada, NRCC 12143*.

Harmathy, T. Z. (1993). *Fire safety design and concrete*, John Wiley & Sons Inc., New York, NY.

Harmathy, T. Z. (1970). "Thermal properties of concrete at elevated temperatures." *ASTM Journal of Materials*, 5(1), 47-74.

Harmathy, T. Z., and Allen, L. W. (1973). "Thermal properties of selected masonry unit concretes." *ACI Journal, Proceedings*, 70(2), 132-142.

Hertz, K. D. (2003). "Limits of spalling of fire-exposed concrete." *Fire Safety J*, 38(2), 103-116.

Hu, X. F., Lie, T. T., Polomark, G. M., and MacLaurin, J. W. (1993). "Thermal properties of building materials at elevated temepratures." *Internal Report - 643 , Institute for Research in Construction, Natrional Research Council Canada*, 1-54.

Huang, C. L. (1979). "Multi-phase moisture transfer in porous media subject to temperature gradient." *International Journal of Heat and Mass Transfer*, 22, 1295-1307.

ISO/DIS22007-2:2008 (2008). "Determination of thermal conductivity and thermal diffusivity, Part 2: Transient plane heat source (hot disc) method." ISO, Geneva, Switzerland.

Kalifa, P., Chéné, G., and Gallé, C. (2001). "High-temperature behavior of HPC with polypropylene fibers from spalling to microstructure." *Cement Concrete Res*, 31(10), 1487-1499.

Khaliq, W., and Kodur, V. (2012). "High temperature mechanical properties of high strength fly ash concrete with and without fibers." *Aci Mater J*, Submitted.
Khoury, G. A. (1992). "Compressive strength of concrete at high temperatures: a reassessment." *Mag Concrete Res*, 44(161), 291-309. 30 1 Khoury, G. A. (2008). "Concrete spalling assessment methodologies and polypropylene fibre toxicity analysis in tunnel fires." *Structural concrete*, 9(1), 11-18.
Khoury, G. A., Grainger, B. N., and Sullivan, P. J. E. (1985). "Strain of concrete during fire heating to 600 °C." *Mag Concrete Res*, 37(133), 195-215.
Kim, G. Y., Kim, Y. S., and Lee, T. G. (2009). "Mechanical properties of high-strength concrete subjected to high temperature by stressed test." *Transactions of Nonferrous Metals Society of China*, 19, 128-133.
Kodur, V., and Khaliq, W. (2011). "Effect of temperature on thermal properties of different types of high strength concrete." *Journal of Materials in Civil Engineering, ASCE*, 23(6), 793-801.
Kodur, V., and Raut, N. (2010). "Performance of concrete structures under fire hazard: emerging trends." *ICI Journal*, April - June 2010, 7-18.
Kodur, V. K. R. (2003). "Fiber Reinforcement for Minimizing Spalling in High Strength Concrete Structural Members Exposed to Fire." *ACI, Special Publication, Innovations in Fibre-Reinforced Concrete for Value*, 216-14, 221-236.
Kodur, V. K. R., and Fike, R. (2009). "Guidelines for improving the standard fire resistance test specifications." *Journal of ASTM International (JAI)*, 6(7), 16.
Kodur, V. R. (2000). "Spalling in high strength concrete exposed to fire - concerns, causes, critical parameters, and cures." *Proc., Proceedings of the ASCE Structures Congress*, 1-9.
Kodur, V. R. (2003). "Fire resistance design guidelines for high strength concrete columns." *National Research Council of Canada, Institute for research in Construction*, Internal Report No. 46116, 1-11.
Kodur, V. R. (1999). "Fire performance of high strength concrete structural members." *Construction Technology update No. 31*, Institute for Research in Construction, Canada.
Kodur, V. R. (1999). "Fiber reinforced concrete for enhancing structural fire resistance of columns." *American Concrete Institute*, SP 182-12(12), 215-234.
Kodur, V. R. (2003). "Fire resistance design guidelines for high strength concrete columns." National Research Council, Canada, 1-11.
Kodur, V. R., Dwaikat, M., and Raut, N. (2009). "Macroscopic FE model for tracing the fire response of reinforced concrete." *Eng Struct*, 31(6), 2368-2379.
Kodur, V. R., Dwaikat, M. M. S., and Dwaikat, M. B. (2008). "High temperature properties of concrete for fire resistance modeling of structures." *Aci Mater J*, 105(5), 517-527.
Kodur, V. R., and Harmathy, T. Z. (2008). "Properties of building materials." *SFPE Handbook of Fire Protection Engineering*, P. J. DiNenno, ed., National Fire Protection Association, Quincy, MA, 1-167-161-195.
Kodur, V. R., and McGrath, R. (2003). "Fire endurance of high strength concrete columns." *Fire Technol*, 39(1), 73–87.
Kodur, V. R., and McGrath, R. (2006). "Effect of silica fume and lateral confinement on fire endurance of high strength concrete columns." *Can. J. Civ. Eng.*, 33, 93-102.
Kodur, V. R., and McGrath, R. (2003). "Fire endurance of high strength concrete columns." *NRCC-45141,* , National Research Council Canada, Ottawa, Canada, 1-13.

Kodur, V. R., and Sultan, M. A. (1998). "Structural behaviour of high strength concrete columns exposed to fire." *Proc., Proceedings, Int. Symposium on High Performance and Reactive Powder Concrete*, 217–232.
Kodur, V. R., and Sultan, M. A. (1998). "Thermal propeties of high strength concrete at elevated temperatures." *American Concrete Institute, Special Publication*, SP-179, 467-480. 30 2
Kodur, V. R., and Sultan, M. A. (2003). "Effect of temperature on thermal properties of high-strength concrete." *Journal of Materials in Civil Engineering*, 15(2), 101-107.
Kodur, V. R., Wang, T. C., Cheng, F. P., and Sultan, M. A. (2002). "A model for evaluating the fire resistance of high performance concrete columns." National Research Council Canada, Canada, 1-10.
Lie, T. T. (1992). "Structural fire protection." ASCE Committee on Fire Protection, Structural Division, American Society of Civil Engineers, New York, NY, 225-229.
Lie, T. T., and Irwin, R. J. (1993). "Method to calculate the fire resistance of reinforced concrete columns with rectangular cross section." *Aci Struct J*, 90(1), 52-60.
Lie, T. T., and Kodur, V. R. (1996). "Thermal and mechanical properties of steel-fibre-reinforced concrete at elevated temperatures." *Canadian Journal of Civil Engineering*, 23(2), 511-517.
Lie, T. T., and Woolerton, J. L. (1988). "Fire resistance of reinforced concrete columns - test results." National Research Council Canada, Ottawa, Canada.
Lie, T. T., and Woolerton, J. L. (1988). "Fire Resistance of Reinforced Concrete Columns - Test Results." *National Research Council Canada, Report 569*.
Mehta, P. K., and Monteiro, P. J. M. (2006). *Concrete: Microstructure, Properties, and Materials*, The McGraw-Hill Companies, Inc., New York, USA.
Mindess, S., Young, J. F., and Darwin, D. (2003). *Concrete*, Pearson Education, Inc., New Jersey, USA.
Nasser, K. W., and Marzouk, H. M. (1979). "Properties of mass concrete containing fly ash at high temperatures." *ACI Journal*, 76(4), 537-550.
Neville, A. M. (2004). *Properties of Concrete*, Pearson Education Limited, Essex, England.
Noumowé, A., Siddique, R., and Debicki, G. (2009). "Permeability of high-performance concrete subjected to elevated temperature (600°C)." *Constr Build Mater*, 23 (5), 1855-1861.
Pantazopoulou, S. J. (1998). "Detailing for reinforcement stability in RC members." *Journal of Structural Engineering, ASCE*, 124(6), 623-632.
Persson, B. (2004). "Fire resistance of self-compacting concrete, SCC." *Mater Struct*, 37(9), 575-584.
Phan, L. T. (1996). "Fire performance of high-strength concrete: A report of the state-of-the-art." National Institute of Standards and Technology, Gaithersburg, Md, USA. 30 3 Phan, L. T. (2007). "Spalling and mechanical properties of high strength concrete at high temperature." *Concrete under Severe Conditions: Environment & Loading, CONSEC' 07 Tours*, CONSEC committee, France.
Poon, C. S., Azhar, S., Anson, M., and Wong, Y. L. (2001). "Comparison of the strength and durability performance of normal- and high-strength pozzolanic concretes at elevated temperatures." *Cement Concrete Res*, 31(9), 1291-1300.
Popovics, S. (1998). *Strength and related properties of concrete, a quantitative approach*, John Wiley and Sons Publisher, New York.

Purkiss, J. A. (2007). *Fire safety engineering design of structures*, Butterworth-Heinemann - Elsevier, Oxoford, UK.

Raut, N. (2011). "Response of high strength concrete columns under fire-induced biaxial bending ", Doctoral Thesis, Michigan State University, East Lansing, MI, USA.

Raut, N., and Kodur, V. K. R. (2011). "Response of high strength concrete columns under design fire exposure." *Journal of Structural Engineering, ASCE*, 137(1), 69-79.

Richart, F. E., Brandtzaeg, A., and Brown, R. L. (1929). "A study of the failure of concrete under combined compressive stresses." Engineering Experimental Station, Univ. of Illinois, Urbana IL.

RILEM TC 129-MHT (2000). "Test methods for mechanical properties of concrete at high temperatures, Part 4 - Tensile strength for service and accident conditions." *Mater Struct*, 33, 219-223.

Rossi, P. (1994). "Steel fiber reinforced concrete (SRC): An example of French research." *Aci Mater J*, 91(3), 273-279.

Sahota, M. S., and Pagni, P. G. (1979). "Heat and mass transfer in porous media subjecte to fire." *International Journal of Heat and Mass Transfer*(1069-1081), 22.

Schneider, U. (1988). "Concrete at high temperatures - A general review." *Fire Safety J*, 13, 55-68.

SFPE (2008). *Handbook of Fire Protection Engineering*, Society of Fire Protection Engineers and National Fire Protection Association.

Shah, S. P. (1991). "Do fibers increase the tensile strength of cement-based matrixes?" *Aci Mater J*, 88(6), 595-602.

Shin, K. Y., Kim, S., Kim, J., Chung, M., and Jung, P. (2002). "Thermo-physical properties and transient heat transfer of concrete at elevated temperatures." *Nucl Eng Des*, 212(1-3), 233-241. 30 4

Tang, W. C., and Lo, T. Y. (2009). "Mechanical and fracture properties of normal- and high-strength concretes with fly ash after exposure to high temperatures." *Mag Concrete Res*, 61(5), 323-330.

VanGeem, M. G., Gajda, J. W., and Dombrowski, K. (1997). "Thermal properties of commercially available high-strength concretes." *Cement, Concrete, and Aggregates*, 19(1), 38-53.

Wackerly, D. D., Mandenhall III, W., and Scheaffer, R. L. (2008). *Mathematical statistics with applications*, Thomson Higher Education, Belmont, CA, USA.

Xiao, J., and König, G. (2004). "Study on concrete at high temperature in China—an overview." *Fire Safety J*, 39(1), 89-103.

APPENDIXES

APPENDIX A

DESIGN OF COLUMN SPECIMENS

A.1 Column Capacity Calculations

This appendix summarizes the design calculations using ACI 318 (2008) and ACI 216.1 (2007) provisions for HSC-S, and HSC-H columns. Dimensions for design of columns are mainly dictated by fire test furnace in with these columns were to be tested. Table A.1 gives the dimensions and properties of the steel used in calculations.

Table A.1 - Design parameters used for the columns

Design parameter	Notation	Value
Gross area (Cross-section = 203x203 mm)	A_g	41209 mm^2
Steel yield strength	f_y	420 MPa
Steel area (4 # 6 bars)	A_{st}	4 - 285 = 1140 mm^2
Length of column	l	3300 mm
Concrete cover to main rebars for minimum 2 hours fire resistance	-	50 mm (**ACI 216.1 2.5.3)**
Column end conditions	-	Pin-pin

Note: Maximum usable strain at extreme concrete compressive fiber shall be assumed equal to 0.003. (**ACI 10.2.3)**

Notations:

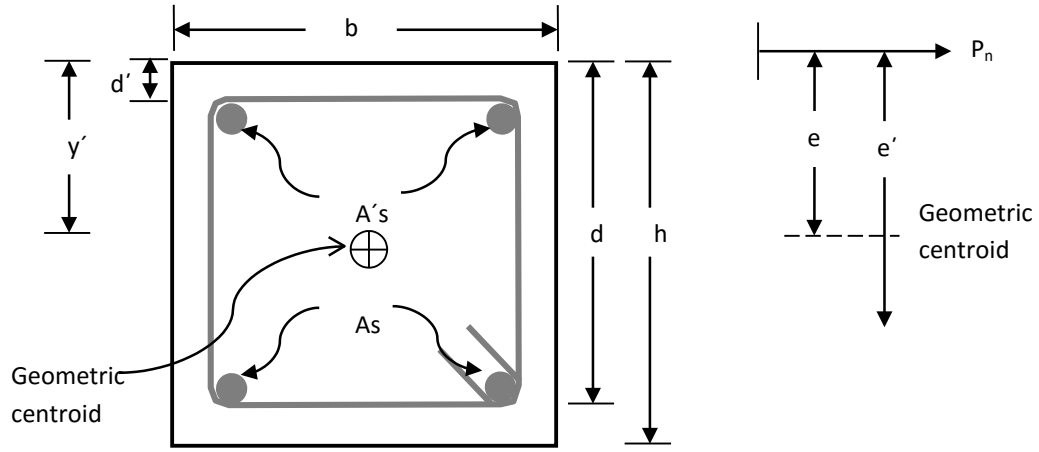

c = distance to neutral axis

$\bar{Y}$ = distance to geometric centroid

ε_s = steel strain in tension side

ε'_s = steel strain in compression side

e = eccentricity of load to geometric centroid

e' = eccentricity of load to tension steel

d' = effective cover of compression steel

Figure A.1 - Notations used in calculations

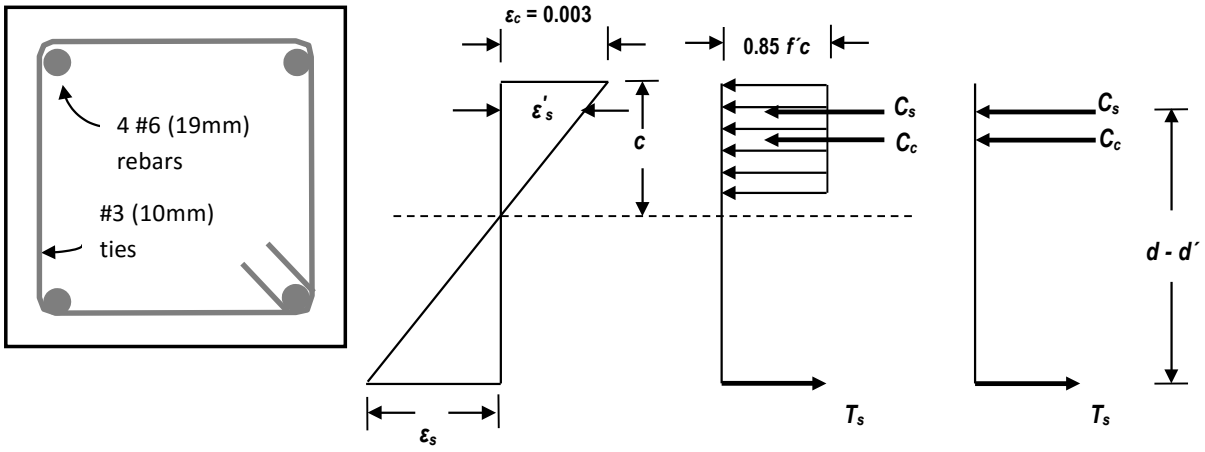

Strains

$$\varepsilon_s = 0.003\,\frac{d-c}{c}$$

$$\varepsilon'_s = 0.003\,\frac{c-d'}{c}$$

Stresses

$$f_s = E_s\varepsilon_s \le f_y$$

$$f'_s = E_s\varepsilon'_s \le f_y$$

Internal forces

$$C_c = 0.85 f'_c\, ba$$

$$C_s = A'_s\, f'_s$$

Figure A.2: Stress-strains and forces in columns

A.2 P-M interaction Diagram for HSC-S and HSC-H column

Design parameters for HSC-S and HSC-H are same as given in table B.1.

Table A.2 - Calculated factored capacities of HSC-S and HSC-H columns

HAC-S		
	Compressive strength (f'_c)	77 MPa
	Ultimate load (P_u)	1612 kN
	Ultimate moment (M_u)	50.84 kN.m
HAC-H		
	Compressive strength (f'_c)	80 MPa
	Ultimate load (P_u)	1665 kN
	Ultimate moment (M_u)	53.45 kN.m

Point 1 - (depth of neutral axis > d)

c = infinity

$Pn = 0.8(A_{net} - 0.85\, f'_c + Ast\, fy)$

= 0.8 - (40069 - 0.85 - 77+1140 - 420)/1000 = 2481.05 kN

φPn = 0.65 - = 1612 kN

Mn = 0

Point 2 - (depth of neutral axis at d)

at c = d = 153 mm

$f's = Es \times 's = 200000 \qquad \frac{0.003(c - d')}{c} \leq fy$

$f's = Es \times \varepsilon's = 200000 \quad \frac{0.003(153-50)}{153} = 403\ MPa < 420\ MPa$

$Cs = A's \times f's = 570 \times \frac{403}{1000} = 230\ kN$

$fs = Es \times \varepsilon = 200000\ (0.003(d-c))/c$

$fs = Es \times \varepsilon = 200000\ (0.003(d-c))/c = 0$

$Ts = 0$

$Cc = 0.85 \times f'c \times \beta \times a \times b = 0.85 \times 77 \times 203 \times 0.85 \times \frac{153}{1000} = 1727.89\ kN$

$= C + Cs - Ts = 1727.89 + 230 - 0 = 1958.13\ kN$

φPn = 0.65 - 1958.13 = 1272.78 kN

$Mn = Cc(\bar{Y} - a/2) + Cs(\bar{Y} - d') + Ts(d - \bar{Y})$

Mn = 74.88 kN.m

φMn = 0.65 - 74.88 = 48.67 kN.m **(ACI 9.3.2)**

Point 3 - (depth of neutral axis < d)

at c = d = 122.4 mm

$f's = Es \times \varepsilon's = 200000\ \frac{0.003}{c}\bar{Y}\ (c-d)$, **(ACI 10.2.4)**

$f's = Es \times \varepsilon's = 200000 \quad \frac{0.003(122.4-50)}{122.4} = 354.90 < 420\ MPa$

$Cs = A's \times \ 's = 570 \times \frac{354.90}{1000} = 202.29\ kN$ **(ACI 10.2.4)**

$fs = Es \times \ = 200000\ (0.003(d - c))/c$

$fs = Es \times \ = 200000\ \frac{0.003(153-122.4)}{122.4} = 354.93$ MPa < 420 MPa

$1000Cc = 0.85 \times f'c \ \times \beta \times c \times b = 0.85 \times$

$Ts = As \times \ = 570 \times \frac{354.93}{} = 85.5\ kN$

$77 \times 0.85 \times 122.4 \times 203/1000 = 1382.31\ kN$

$= C + Cs - Ts = 1382.31 + 202.29 - 85.5 = 1499.11\ kN$ **(ACI 10.3.6)**

φPn = 0.65 - 1499.11 = 974.41 kN **(ACI 9.3.2)**

$= Cc\ (\bar{Y}\ a/2)\ Cs\ (\bar{Y} - d') + Ts\ (d - \bar{Y}\ )$

Mn = 83.22 kN.m

$\varphi\ Mn$ = 0.65 - 83.22 = 54.10 kN.m **(ACI 9.3.2)**

Obtain more points for P-M diagram as given in Table B.6

Table A.3 - Calculation of nominal load and moment for P-M diagram for HSC-S column

Point #	c	Pn	φPn	Mn	φMn
1	infinity	2481.05	1612.68	0.00	0.00
2	153.00	1958.13	1272.78	74.88	48.67
3	122.40	1499.11	974.42	83.22	54.09
4	91.80	964.46	626.90	84.54	54.95
5	61.20	514.34	334.32	67.73	44.02
6	30.60	-110.65	-71.92	31.74	20.63
7	0.01	-478.69	-311.15	0.01	0.01

From all these points we get the P-M diagram

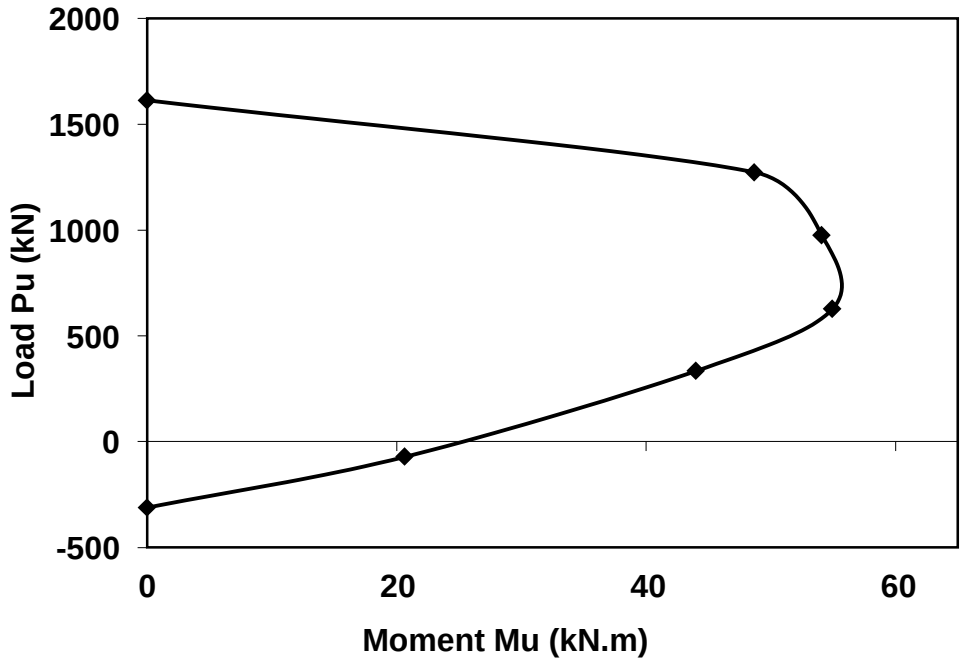

Figure A.3 - Load-moment interaction diagram for HSC-S column

Calculate buckling load – concentrically loaded slender column

$E_{FAC} = 3.32\sqrt{f'c} + 6895(w_c/2320)^{1.5}$

$E_{FAC} = 3.32\sqrt{107/1000} + 6895(2530/2320)^{1.5} = 37142.88$ MPa

$I_g = \frac{bd^3}{12} = 141515140.1\ mm^4$

Flexural rigidity = EI

(ACI 10.15)

$EI = \frac{0.4EcI}{1+\beta_d}$

$EI_{FAC} = \frac{0.4 \times 37142.88 \times 141515140.0}{(1+0.5)1000} = 1.40e$ MPa

Euler buckling Load P_c **(ACI 10.13)**

$P_c = \frac{\pi^2 EI}{(\ )^2}$

$P_{c\ HSC-S} = 1232.7\ kN$

Calculate the load and moment capacity of the column, the moment calculated by moment magnification factor will be checked against P-M diagram.

$$\delta_{ns} = Cm/(1 - \frac{Pu}{0.75Pc})$$

Table A.3 - Load and moment capacity calculated by moment magnification method.

Mu (kN.m)	Pu (kN)	δ_{ns}	e (mm)
0.00	0	1	0
5.64	222.4	1.2	25.4
14.11	444.8	1.5	33.02
28.22	667.2	2	43.18
56.45	889.6	3	63.5
65.86	934.08	3.3	71.12
68.00	942.976	3.4	73.66

Superimposing the calculated Pu and Mu against P-M diagram of the column gives the capacity of the column.

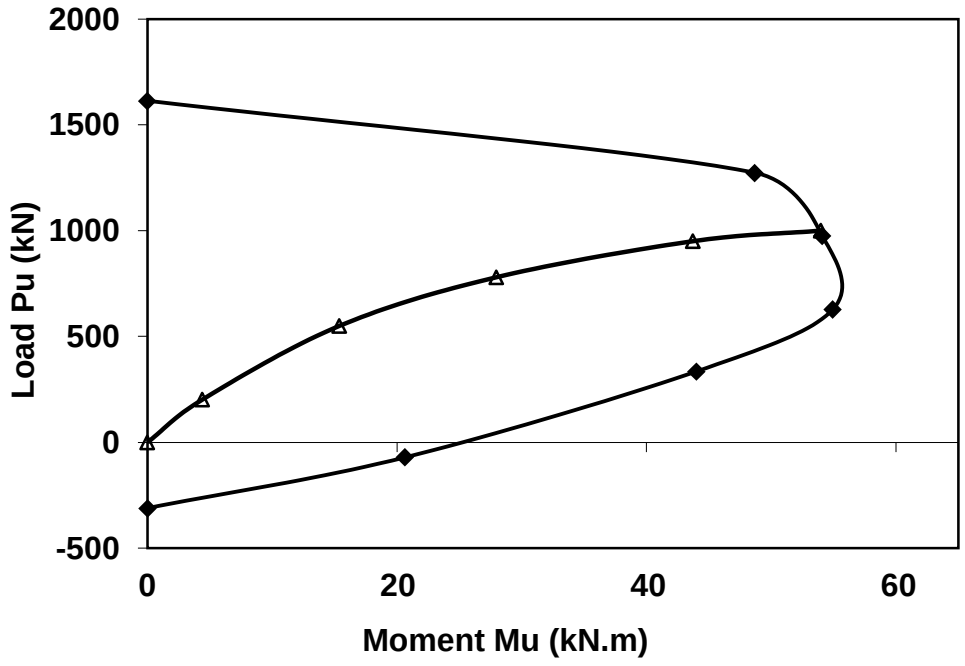

Figure A.4 - Calculation of P_u from load-moment interaction diagram for HSC-S column

APPENDIX B

REINFORCED CONCRETE COLUMN – OPENSEES FILE

```
##########################################################################
##########################################################################

# STRUCTURAL FIRE PERFORMANCE OF HPC COLUMN WITH AND WITHOUT
FIBRES USING OPENSEES SOFTWARE #

#                    MSc Thesis Structural Engg 2013                    #

#                     Written by: Saif ur Rehman                        #

#     October 2016, NICE / SCEE, National University of Science and Technology,
Islamabad   #

##########################################################################
##########################################################################

# Length of the Column = total 10 elements for  Total Length 3810 mm

# Axial Load;

# 8 fibers for both the slab and steel beam section;

# Material class Steel01Thermal is used for steel and Concrete02Thermal for concrete;

# unit i.e. mm, KN, MPa

# SET UP ----------------------------------------------------------------------------

wipe;

model BasicBuilder -ndm 2 -ndf 3;

#source DisplayPlane.tcl

#source DisplayModel2D.tcl

# define NODAL COORDINATES FOR THE COL
```

```
node 1 0 0;
node 2 0 330;
node 3 0 660;
node 4 0 990;
node 5 0 1320;
node 6 0 1650;
node 7 0 1980;
node 8 0 2310;
node 9 0 2640;
node 10 0 2970;
node 11 0 3300;
fix 1     0 0 0;
fix 11  1 1 1;
uniaxialMaterial Steel01Thermal 1 420 2.1e5 0.01;
set fpc -80
set epsc0 -0.003
set fpcu [expr $fpc*0.05];
set epsU -0.02
set lambda 0.1
set ft 0.0
set Ets [expr $ft/0.002];
uniaxialMaterial Concrete02ThermalSCCp 2 $fpc $epsc0 $fpcu $epsU $lambda $ft $Ets
#
```

```
# Concrete section 3810 mm x 3810 mm
# Cover 50 mm
# 20 mm bar two up and two down
section fiberSecThermal 2   {
    #slab section
        fiber  88.8125 0 5151.25 2;
        fiber  63.4375 0 5151.25 2;
        fiber  38.0625 0 5151.25 2;
        fiber  12.6875 0 5151.25 2;
        fiber -12.6875 0 5151.25 2;
        fiber -38.0625 0 5151.25 2;
        fiber -63.4375 0 5151.25 2;
        fiber -88.8125 0 5151.25 2;
        layer straight 1 2 284 -51.5 51.5 51.5 51.5          # upper layer
        layer straight 1 2 284 -51.5 -51.5 51.5 -51.5        # lower layer
        }
geomTransf Corotational 1;
element dispBeamColumnThermal 1 1 2 5 2 1;
element dispBeamColumnThermal 2 2 3 5 2 1;
element dispBeamColumnThermal 3 3 4 5 2 1;
element dispBeamColumnThermal 4 4 5 5 2 1;
```

```
element dispBeamColumnThermal 5 5 6 5 2 1;
element dispBeamColumnThermal 6 6 7 5 2 1;
element dispBeamColumnThermal 7 7 8 5 2 1;
element dispBeamColumnThermal 8 8 9 5 2 1;
element dispBeamColumnThermal 9 9 10 5 2 1;
element dispBeamColumnThermal 10 10 11 5 2 1;
recorder Node -file node61mycol.out -time -node 6 -dof 1 disp;
recorder Node -file node62mycol.out -time -node 6 -dof 2 disp;
#  Define Gravity Load
set P 967.0;
# Create a plain load pattern with a Linear Timeseries
pattern Plain 1 "Linear" {
        load  1  0  [expr -$P] 0
}
constraints Plain;
numberer Plain;
system BandGeneral;
test NormUnbalance 1.0e-2 12;
algorithm Newton;
integrator LoadControl 1;
analysis Static;
analyze 1;
loadConst -time 0.0
```

```
# Define DISPLAY ----------------------------------------------------------

##set  xPixels 1000;# height of graphical window in pixels

##set  yPixels 490;  # height of graphical window in pixels

##set  xLoc1 10;      # horizontal location of graphical window (0=upper left-most corner)

##set  yLoc1 10;      # vertical location of graphical window (0=upper left-most corner)

##set ViewScale 0.0000002;         # scaling factor for viewing deformed shape, it depends on the dimensions of the model

##DisplayModel2D DeformedShape $ViewScale $xLoc1 $yLoc1 $xPixels $yPixels 0

#define thermal load

# apply thermal load, temperature is linearly distributed through section

# bottom and top temp of steel beam is 1000 and 600;

# bottom and top temp of slab is 600 and 0;

# Time 100

set T1 640; set T2 275; set T3 222; set T4 275; set T5 640;

set Y1 -101.5; set Y2 -50.75; set Y3 0; set Y4 50.75; set Y5 101.5;

pattern Plain 2 Linear        {

for {set level 1} {$level <=10} {incr level 1} {

set eleID $level

eleLoad -ele $eleID -type -beamThermal $T1 $Y1 $T2 $Y3 $T3 $Y3 $T4 $Y4 $T5 $Y5;

}

}
```

```
test NormUnbalance 1.0e-2 100;

algorithm Newton;

integrator LoadControl 0.01;

analysis Static;

analyze 100;

loadConst -time 0.0
```

APPENDIX C

NEW MATERIAL CLASS – CONCRETE02THERMALHSC

```
// This code is the modification of Concrete02Thermal and is named as Concrete02ThermalHSC, the interface of it is the same with concrete02.
#include <stdlib.h>
#include <Concrete02ThermalSCC.h>
#include <OPS_Globals.h>
#include <float.h>
#include <Channel.h>
#include <Information.h>
#include <elementAPI.h>
#include <OPS_Globals.h>
void *
OPS_NewConcrete02ThermalSCC()
{  // Pointer to a uniaxial material that will be returned
  UniaxialMaterial *theMaterial = 0;
  int    iData[1];
  double dData[7];
  int numData = 1;
  if (OPS_GetIntInput(&numData, iData) != 0) {
    opserr << "WARNING invalid uniaxialMaterial Concrete02ThermalSCC tag" << endln;
    return 0;  }
  numData = OPS_GetNumRemainingInputArgs();
  if (numData != 7) {
    opserr << "Invalid #args, want: uniaxialMaterial Concrete02ThermalSCC " << iData[0] << "fpc? epsc0? fpcu? epscu? rat? ft? Ets?\n";
    return 0;  }
  if (OPS_GetDoubleInput(&numData, dData) != 0) {
    opserr << "Invalid #args, want: uniaxialMaterial Concrete02ThermalSCC " << iData[0] << "fpc? epsc0? fpcu? epscu? rat? ft? Ets?\n";
    return 0;  }
  // Parsing was successful, allocate the material
  theMaterial = new Concrete02ThermalSCC(iData[0], dData[0], dData[1], dData[2], dData[3], dData[4], dData[5], dData[6]);
```

```
  if (theMaterial == 0) {
    opserr << "WARNING could not create uniaxialMaterial of type Concrete02ThermalSCC Material\n";
    return 0;  }
  return theMaterial;}
Concrete02ThermalSCC::Concrete02ThermalSCC(int tag, double _fc, double _epsc0, double _fcu,
                                           double _epscu, double _rat, double _ft, double _Ets):
  UniaxialMaterial(tag, MAT_TAG_Concrete02ThermalSCC),
  //fc(_fc), epsc0(_epsc0), fcu(_fcu), epscu(_epscu), rat(_rat), ft(_ft), Ets(_Ets)
  fcT(_fc), epsc0T(_epsc0), fcuT(_fcu), epscuT(_epscu), rat(_rat), ftT(_ft), EtsT(_Ets) //JZ
{//JZ 07/10 ////////////////////////////////////////////////////////////////start
  fc = fcT;
  epsc0 = epsc0T;
  fcu = fcuT;      epscu = epscuT;
  ft = ftT;      Ets = EtsT;
//JZ 07/10 ////////////////////////////////////////////////////////////////end
 ecminP = 0.0;
  deptP = 0.0;
  eP = 2.0*fc/epsc0;
  //eP = 1.5*fc/epsc0; //for the euro code, the 2.0 should be changed into 1.5
  epsP = 0.0;
  sigP = 0.0;
  eps = 0.0;
  sig = 0.0;
  e = 2.0*fc/epsc0;
  //e = 1.5*fc/epsc0;//for the euro code, the 2.0 should be changed into 1.5
  //if epsc0 is not 0.0025, then epsc0 = strainRatio*0.0025
  strainRatio = epsc0/0.0025;
  ThermalElongation = 0; //initialize
  cooling=0; //PK add
  TempP = 0.0; //Pk add previous temp}
Concrete02ThermalSCC::Concrete02ThermalSCC(void):
```

```
 UniaxialMaterial(0, MAT_TAG_Concrete02ThermalSCC)
Concrete02ThermalSCC::~Concrete02ThermalSCC(void)
{  // Does nothing}
UniaxialMaterial*
Concrete02ThermalSCC::getCopy(void)
{    Concrete02ThermalSCC *theCopy = new Concrete02ThermalSCC(this->getTag(), fc, epsc0, fcu, epscu, rat, ft, Ets);
   return theCopy;}
double
Concrete02ThermalSCC::getInitialTangent(void)
{  return 2.0*fc/epsc0;}
int
Concrete02ThermalSCC::setTrialStrain(double trialStrain, double FiberTemperature, double strainRate)
{  double      ec0 = fc * 2. / epsc0;//?
  // double     ec0 = fc * 1.5 / epsc0; //JZ. 27/07/10 ??
    // retrieve concrete hitory variables
    ecmin = ecminP;
  dept = deptP;
   // calculate current strain
    eps = trialStrain;
  double deps = eps - epsP;
    // if the current strain is less than the smallest previous strain
  // call the monotonic envelope in compression and reset minimum strain
    if (eps < ecmin) {
    this->Compr_Envlp(eps, sig, e);
    ecmin = eps;  else {;
       // else, if the current strain is between the minimum strain and ept
    // (which corresponds to zero stress) the material is in the unloading-
    // reloading branch and the stress remains between sigmin and sigmax
        // calculate strain-stress coordinates of point R that determines
    // the reloading slope according to Fig.2.11 in EERC Report
    // (corresponding equations are 2.31 and 2.32
    // the strain of point R is epsR and the stress is sigmR
```

```
    double epsr = (fcu - rat * ec0 * epscu) / (ec0 * (1.0 - rat));
double sigmr = ec0 * epsr;
    // calculate the previous minimum stress sigmm from the minimum
// previous strain ecmin and the monotonic envelope in compression
    double sigmm;
double dumy;
this->Compr_Envlp(ecmin, sigmm, dumy);
    // calculate current reloading slope Er (Eq. 2.35 in EERC Report)
// calculate the intersection of the current reloading slope Er
// with the zero stress axis (variable ept) (Eq. 2.36 in EERC Report)
    double er = (sigmm - sigmr) / (ecmin - epsr);
double ept = ecmin - sigmm / er;
    if (eps <= ept) {
  double sigmin = sigmm + er * (eps - ecmin);
  double sigmax = er * .5f * (eps - ept);
  sig = sigP + ec0 * deps;
  e = ec0;
  if (sig <= sigmin) {
      sig = sigmin;
      e = er;      }
  if (sig >= sigmax) {
      sig = sigmax;
      e = 0.5 * er;      }      } else {
  // else, if the current strain is between ept and epn
  // (which corresponds to maximum remaining tensile strength)
  // the response corresponds to the reloading branch in tension
  // Since it is not saved, calculate the maximum remaining tensile
  // strength sicn (Eq. 2.43 in EERC Report)
       // calculate first the strain at the peak of the tensile stress-strain
  // relation epn (Eq. 2.42 in EERC Report)
       double epn = ept + dept;
  double sicn;
  if (eps <= epn) {
      this->Tens_Envlp(dept, sicn, e);
```

```
        if (dept != 0.0) {
          e = sicn / dept;       } else {
          e = ec0;       }
        sig = e * (eps - ept);         } else {
        // else, if the current strain is larger than epn the response
        // corresponds to the tensile envelope curve shifted by ept
                double epstmp = eps - ept;
        this->Tens_Envlp(epstmp, sig, e);
        dept = eps - ept;    }    }  }
   return 0;}
double
Concrete02ThermalSCC::getStrain(void)
{  return eps;}
double
Concrete02ThermalSCC::getStress(void)
{  return sig;}
double
Concrete02ThermalSCC::getTangent(void)
{  return e;}
double
Concrete02ThermalSCC::getThermalElongation(void) //***JZ
{  return ThermalElongation;}
double
Concrete02ThermalSCC::getElongTangent(double TempT, double& ET, double&
Elong, double TempTmax) //PK add to include max temp
{  //material properties with temperature
  Temp = TempT;  //make up the 20 degree which is minus in the class of
thermalfield
  Tempmax = TempTmax; //PK add max temp for cooling
  // The datas are from EN 1992 part 1-2-1
  // Tensile strength at elevated temperature
        //if (Temp >= 1080) {
  //        opserr << "temperature " << " " << Temp <<endln;  //}
  if (Temp <= 100) {
```

```
            ft = ftT;  }
  else if (Temp <= 800) {
            ft = (0.99 - (0.001*Temp))*ftT;
            Ets = (1.0 - 1.0*(Temp -80)/500)*fcT * 1.5 / epsc0T;
            //Ets = (1.0 - 1.0*(Temp -80)/500)*EtsT;  }
  else {  ft = 1.0e-3;
            Ets = 1.0e-3;
            //ft = 0;
            //Ets = 0;  }
  // compression strength, at elevated temperature
  //   strain at compression strength, at elevated temperature
  //   ultimate (crushing) strain, at elevated temperature
  if (Temp <= 0) {
            fc = fcT;
            epsc0 = -0.0025;
            fcu = fcuT;
            epscu = -0.02;
            //Ets = EtsT;  jz what is there the statement?  }
  else if (Temp <= 100) {
            fc = fcT;
            epsc0 = -(0.0025 + (0.004-0.0025)*(Temp - 0)/(80 - 0));
            fcu = fcuT;
            epscu = -(0.0200 + (0.0225-0.0200)*(Temp - 0)/(80 - 0));  }
  else if (Temp <= 200) {
     fc = fcT*(0.99 - (0.002*Temp));
            epsc0 = -(0.0040 + (0.0055-0.0040)*(Temp - 80)/100);
     fcu = fcuT*(1 - (Temp - 80)*0.05/100);
            epscu = -(0.0225 + (0.0225-0.0200)*(Temp - 80)/100);  }
//  //else if (Temp <= 280) {
//    //  fc = fcT*(0.95 - (Temp - 180)*0.1/100);
//          //epsc0 = -(0.0055 + (0.0070-0.0055)*(Temp - 180)/100);
//          fcu = fcuT*(0.95 - (Temp - 180)*0.1/100);
//          epscu = -(0.0250 + 0.0025*(Temp - 180)/100); //  }
//  //else if (Temp <= 380) {
```

```
//      fc = fcT*(0.85 - (Temp - 280)*0.1/100);
//          epsc0 = -(0.0070 + (0.0100-0.0070)*(Temp - 280)/100);
//          fcu = fcuT*(0.85 - (Temp - 280)*0.1/100);
//          epscu = -(0.0275 + 0.0025*(Temp - 280)/100);
//  }
//  else if (Temp <= 480) {
//      fc = fcT*(0.75 - (Temp - 380)*0.15/100);
//          epsc0 = -(0.0100 + (0.0150-0.0100)*(Temp - 380)/100);
//          fcu = fcuT*(0.75 - (Temp - 380)*0.15/100);
//          epscu = -(0.03 + 0.0025*(Temp - 380)/100);
//  }
//  else if (Temp <= 580) {
//      fc = fcT*(0.60 - (Temp - 480)*0.15/100);
//          epsc0 = -(0.0150 + (0.0250-0.0150)*(Temp - 480)/100);
//          fcu = fcuT*(0.60 - (Temp - 480)*0.15/100);
//          epscu = -(0.0325 + 0.0025*(Temp - 480)/100);    //  }
//  else if (Temp <= 680) {
//      fc = fcT*(0.45 - (Temp - 580)*0.15/100);
//          epsc0 = -0.0250;
//          fcu = fcuT*(0.45 - (Temp - 580)*0.15/100);
//          epscu = -(0.035 + 0.0025*(Temp - 580)/100);    //  }
//  else if (Temp <= 780) {
//      fc = fcT*(0.30 - (Temp - 680)*0.15/100);
//          epsc0 = -0.0250;
//          fcu = fcuT*(0.30 - (Temp - 680)*0.15/100);
//          epscu = -(0.0375 + 0.0025*(Temp - 680)/100);     //  }
   else if (Temp <= 800) {
      fc = fcT*(0.73 - (0.0005*Temp));
          epsc0 = -0.0250;
          fcu = fcuT*(0.15 - (Temp - 780)*0.07/100);
          epscu = -(0.04 + 0.0025*(Temp - 780)/100);  }
//  else if (Temp <= 980) {
//      fc = fcT*(0.08 - (Temp - 880)*0.04/100);
//          epsc0 = -0.0250;
```

```
//          fcu = fcuT*(0.08 - (Temp - 880)*0.04/100);
//          epscu = -(0.0425 + 0.0025*(Temp - 880)/100);
//  }
//  else if (Temp <= 1080) {
//      fc = fcT*(0.04 - (Temp - 980)*0.03/100);
//          epsc0 = -0.0250;
//          fcu = fcuT*(0.04 - (Temp - 980)*0.03/100);
//          epscu = -(0.045 + 0.0025*(Temp - 980)/100);  //  }
  else  {      opserr << "the temperature is invalid\n";   }
//jz assign a miner to the valuables
          // epsc0 = epsc0T*strainRatio;
          // epscu = epscuT*strainRatio;
  // caculation of thermal elongation
           if (Temp <= 1) {
                   ThermalElongation = (Temp - 0) * 9.213e-6;      }
  else if (Temp <= 680) {
     ThermalElongation     =     -1.8e-4     +     9e-6     *(Temp+20)     +     2.3e-11
*(Temp+20)*(Temp+20)*(Temp+20);  }
  else if (Temp <= 1180) {
     ThermalElongation = 14.009e-3;  //Modified by Liming,2013  }
  else {            opserr << "the temperature is invalid\n";  }
  ET = 1.5*fc/epsc0;
  Elong = ThermalElongation;
  //For cooling to exist T must go to Tmax and then decrease
//if cooling the factor becomes 1
 //if (Temp = Tempmax) {
    //cooling=1;   // }
///PK COOLING PART FOR DESCENDING BRANCH OF A FIRE////
  // If temperature is less that previous committed temp then we have cooling taking
place
  if (Temp < TempP) {
 //opserr << "cooling " << Temp << " " << TempP << endln;
  double kappa;
  double fcmax; //compr strength at max temp
```

```
  double fcumax; //ultimate compr strength at max temp
  double fcamb; //compr strength at cooled ambient temp
  double fcuamb; //ultimate compr strength at cooled ambient temp
  double epsc0max; //strain at compression strength for the max temp
  double epscumax; //ultimate strain at ultimate compression strength for the max temp
  if (TempP == Tempmax) {
    //opserr << "cooling,T,TP,Tmax " << Temp << " " << TempP << " " << Tempmax <<endln;  }
  // PK Determine residual compressive strength of concrete heated to the max temp and then having cooled down to ambient
  // This will be the same for all the timesteps during the cooling phase
  // PK 1st step is to determine Kc,Tempmax according to table in 3.2.2 (EN1994-1-2:2005)
  if (Tempmax < 0) {
    opserr << "max temperature cannot be less than zero " << " " << Tempmax <<endln;
  else if (Tempmax <= 80) {
    kappa = 1;
    fcmax = fcT;
    fcumax = fcuT;  }
  else if (Tempmax <= 180) {
    kappa = 1 - (Tempmax - 80)*0.05/100;
    fcmax = fcT*(1 - (Tempmax - 80)*0.05/100);
    fcumax = fcuT*(1 - (Tempmax - 80)*0.05/100);  }
  else if (Tempmax <= 280) {
    kappa = 0.95 - (Tempmax - 180)*0.1/100;
    fcmax = fcT*(0.95 - (Tempmax - 180)*0.1/100);
    fcumax = fcuT*(0.95 - (Tempmax - 180)*0.1/100);  }
  else if (Tempmax <= 380) {
    kappa = 0.85 - (Tempmax - 280)*0.1/100;
    fcmax = fcT*(0.85 - (Tempmax - 280)*0.1/100);
    fcumax = fcuT*(0.85 - (Tempmax - 280)*0.1/100);  }
  else if (Tempmax <= 480) {
    kappa = 0.75 - (Tempmax - 380)*0.15/100;
```

```
  fcmax = fcT*(0.75 - (Tempmax - 380)*0.15/100);
  fcumax = fcuT*(0.75 - (Tempmax - 380)*0.15/100);  }
 else if (Tempmax <= 580) {
  kappa = 0.60 - (Tempmax - 480)*0.15/100;
  fcmax = fcT*(0.60 - (Tempmax - 480)*0.15/100);
  fcumax = fcuT*(0.60 - (Tempmax - 480)*0.15/100);  }
 else if (Tempmax <= 680) {
  kappa = 0.45 - (Tempmax - 580)*0.15/100;
  fcmax = fcT*(0.45 - (Tempmax - 580)*0.15/100);
  fcumax = fcuT*(0.45 - (Tempmax - 580)*0.15/100);  }
 else if (Tempmax <= 780) {
  kappa = 0.30 - (Tempmax - 680)*0.15/100;
  fcmax = fcT*(0.30 - (Tempmax - 680)*0.15/100);
  fcumax = fcuT*(0.30 - (Tempmax - 680)*0.15/100);  }
 else if (Tempmax <= 880) {
  kappa = 0.15 - (Tempmax - 780)*0.07/100;
  fcmax = fcT*(0.15 - (Tempmax - 780)*0.07/100);
  fcumax = fcuT*(0.15 - (Tempmax - 780)*0.07/100);  }
 else if (Tempmax <= 980) {
  kappa = 0.08 - (Tempmax - 880)*0.04/100;
  fcmax = fcT*(0.08 - (Tempmax - 880)*0.04/100);
  fcumax = fcuT*(0.08 - (Tempmax - 880)*0.04/100);  }
 else if (Tempmax <= 1080) {
  kappa = 0.04 - (Tempmax - 980)*0.03/100;
  fcmax = fcT*(0.04 - (Tempmax - 980)*0.03/100);
  fcumax = fcuT*(0.04 - (Tempmax - 980)*0.03/100);  }
 else  {    opserr << "the temperature is invalid\n";  }
 // PK 2nd step is to determine compressice strength at ambient after cooling as shown in ANNEX C (EN1994-1-2:2005)
 if (Tempmax < 0) {
  opserr << "max temperature cannot be less than zero " << " " << Tempmax <<endln;}
 else if (Tempmax <= 80) {
  fcamb = kappa*fcT;
```

```
  fcuamb = kappa*fcuT;  }
 else if (Tempmax <= 280) {
  fcamb=(1-(0.235*(Tempmax-80)/200))* fcT;
  fcuamb=(1-(0.235*(Tempmax-80)/200))* fcuT;  }
 else if (Tempmax <= 1080) {
  fcamb = 0.9*kappa*fcT;
  fcuamb = 0.9*kappa*fcuT;  }
 else {    opserr << "the temperature is invalid\n";  }
  // Calculation of current compressive strength
 // linear interpolation between ambient and maximum compressive strength (after and before cooling)
 fc = fcmax - ((fcmax-fcamb)*(Tempmax-Temp)/Tempmax);
 fcu = fcumax - ((fcumax-fcuamb)*(Tempmax-Temp)/Tempmax);
  // Calculation of epsc0 for Tempmax and then keep it the same for all next time steps
 if (Tempmax < 0) {
  opserr << "max temperature cannot be less than zero " << " " << Tempmax <<endln;}
 else if (Tempmax <= 80) {
  epsc0max = -(0.0025 + (0.004-0.0025)*(Tempmax - 0)/(80 - 0));
  epscumax = -(0.0200 + (0.0225-0.0200)*(Tempmax - 0)/(80 - 0));  }
 else if (Tempmax <= 180) {
  epsc0max = -(0.0040 + (0.0055-0.0040)*(Tempmax - 80)/100);
  epscumax = -(0.0225 + (0.0225-0.0200)*(Tempmax - 80)/100);  }
 else if (Tempmax <= 280) {
  epsc0max = -(0.0055 + (0.0070-0.0055)*(Tempmax - 180)/100);
  epscumax = -(0.0250 + 0.0025*(Tempmax - 180)/100);  }
 else if (Tempmax <= 380) {
  epsc0max = -(0.0070 + (0.0100-0.0070)*(Tempmax - 280)/100);
  epscumax = -(0.0275 + 0.0025*(Tempmax - 280)/100);  }
 else if (Tempmax <= 480) {
  epsc0max = -(0.0100 + (0.0150-0.0100)*(Tempmax - 380)/100);
  epscumax = -(0.03 + 0.0025*(Tempmax - 380)/100);  }
 else if (Tempmax <= 580) {
  epsc0max = -(0.0150 + (0.0250-0.0150)*(Tempmax - 480)/100);
```

```
   epscumax = -(0.0325 + 0.0025*(Tempmax - 480)/100);  }
  else if (Tempmax <= 680) {
   epsc0max = -0.0250;
   epscumax = -(0.035 + 0.0025*(Tempmax - 580)/100);  }
  else if (Tempmax <= 780) {
   epsc0max = -0.0250;
   epscumax = -(0.0375 + 0.0025*(Tempmax - 680)/100);  }
  else if (Tempmax <= 880) {
   epsc0max = -0.0250;
   epscumax = -(0.04 + 0.0025*(Tempmax - 780)/100);  }
  else if (Tempmax <= 980) {
   epsc0max = -0.0250;
   epscumax = -(0.0425 + 0.0025*(Tempmax - 880)/100);  }
  else if (Tempmax <= 1080) {
   epsc0max = -0.0250;
   epscumax = -(0.045 + 0.0025*(Tempmax - 980)/100);  }
  else  {
   opserr << "the temperature is invalid\n";   }
  //make eps0 = eps0max
  epsc0 = epsc0max;
  // Calculating epscu
  epscu = epsc0 + ((epscumax-epsc0max)*fc/fcmax);
  ft=0;
  // Make thermal elongation zero during the cooling phase
 // Elong =0;  }
   if (Temp > 0) {
    //cooling=1;
          //opserr << "Heating,T,TP,Tmax " << Temp << " " << TempP << " " <<
Tempmax <<endln; }
  return 0;}
int
Concrete02ThermalSCC::commitState(void){
  ecminP = ecmin;
  deptP = dept;
```

```
    eP = e;
  sigP = sig;
  epsP = eps;
  TempP = Temp; //PK add set the previous temperature
  return 0;}
int
Concrete02ThermalSCC::revertToLastCommit(void)
{  ecmin = ecminP;;
  dept = deptP;
   e = eP;
  sig = sigP;
  eps = epsP;
  //Temp = TempP; //PK add set the previous temperature
  // NA ELENXW MIPWS EDW XANETAI TO TEMP LOGW MIN CONVERGENCE
  return 0;}
int
Concrete02ThermalSCC::revertToStart(void){
  ecminP = 0.0;
  deptP = 0.0;
  eP = 2.0*fc/epsc0;
  epsP = 0.0;
  sigP = 0.0;
  eps = 0.0;
  sig = 0.0;
  e = 2.0*fc/epsc0;
  return 0;}
int
Concrete02ThermalSCC::sendSelf(int commitTag, Channel &theChannel)
{  static Vector data(13);
  data(0) =fc;
  data(1) =epsc0;
  data(2) =fcu;
  data(3) =epscu;
  data(4) =rat;
```

```
  data(5) =ft;
  data(6) =Ets;
  data(7) =ecminP;
  data(8) =deptP;
  data(9) =epsP;
  data(10) =sigP;
  data(11) =eP;
  data(12) = this->getTag();
  if (theChannel.sendVector(this->getDbTag(), commitTag, data) < 0) {
    opserr << "Concrete02ThermalSCC::sendSelf() - failed to sendSelf\n";
    return -1;  }    return 0;}
int
Concrete02ThermalSCC::recvSelf(int commitTag, Channel &theChannel,
                FEM_ObjectBroker &theBroker)
{  static Vector data(13);
  if (theChannel.recvVector(this->getDbTag(), commitTag, data) < 0) {
    opserr << "Concrete02ThermalSCC::recvSelf() - failed to recvSelf\n";
    return -1;  }
  fc = data(0);
  epsc0 = data(1);
  fcu = data(2);
  epscu = data(3);
  rat = data(4);
  ft = data(5);
  Ets = data(6);
  ecminP = data(7);
  deptP = data(8);
  epsP = data(9);
  sigP = data(10);
  eP = data(11);
  this->setTag(data(12));
  e = eP;
  sig = sigP;    eps = epsP;
    return 0;}
```

```
void
Concrete02ThermalSCC::Print(OPS_Stream &s, int flag)
{  s << "Concrete02ThermalSCC:(strain, stress, tangent) " << eps << " " << sig <<
" " << e << endln;}
void
Concrete02ThermalSCC::Tens_Envlp (double epsc, double &sigc, double &Ect)
{/*-----------------------------------------------------------------------
! monotonic envelope of concrete in tension (positive envelope)
!   ft    = concrete tensile strength
!   Ec0   = initial tangent modulus of concrete
!   Ets   = tension softening modulus
!   eps   = strain
!   returned variables
!    sigc  = stress corresponding to eps
!    Ect  = tangent concrete modulus
!-----------------------------------------------------------------------*/
   double Ec0  = 2.0*fc/epsc0;
          // double Ec0  = 1.5*fc/epsc0;
  double eps0 = ft/Ec0;
  double epsu = ft*(1.0/Ets+1.0/Ec0);
  if (epsc<=eps0) {
    sigc = epsc*Ec0;
    Ect  = Ec0;
  } else {
    if (epsc<=epsu) {
      Ect  = -Ets;
      sigc = ft-Ets*(epsc-eps0);
    } else {
      //      Ect  = 0.0
      Ect  = 1.0e-10;
      sigc = 0.0;    }  }
  return;}
void
Concrete02ThermalSCC::Compr_Envlp (double epsc, double &sigc, double &Ect)
```

```
{/*----------------------------------------------------------------------
! monotonic envelope of concrete in compression (negative envelope)
!   fc    = concrete compressive strength
!   epsc0 = strain at concrete compressive strength
!   fcu   = stress at ultimate (crushing) strain
!   epscu = ultimate (crushing) strain
!   Ec0   = initial concrete tangent modulus
!   epsc  = strain
!   returned variables
!   sigc  = current stress
!   Ect   = tangent concrete modulus
----------------------------------------------------------------------*/
  double Ec0  = 2.0*fc/epsc0;
  //double Ec0  = 1.5*fc/epsc0;
  double ratLocal = epsc/epsc0;
  if (epsc>=epsc0) {
    sigc = fc*ratLocal*(2.0-ratLocal);
    Ect  = Ec0*(1.0-ratLocal);
  } else {
        //   linear descending branch between epsc0 and epscu
    if (epsc>epscu) {
      sigc = (fcu-fc)*(epsc-epsc0)/(epscu-epsc0)+fc;
      Ect  = (fcu-fc)/(epscu-epsc0);
    } else {
          // flat friction branch for strains larger than epscu
      sigc = fcu;
      Ect  = 1.0e-10;
      //       Ect  = 0.0    }  }
  return;}  int
Concrete02ThermalSCC::getVariable(const char *varName, Information &theInfo)
{  if (strcmp(varName,"ec") == 0) {
    theInfo.theDouble = epsc0;
    return 0;
  } else if (strcmp(varName,"ElongTangent") == 0) {
```

```
    Vector *theVector = theInfo.theVector;
    if (theVector != 0) {
      double tempT, ET, Elong, TempTmax;
      tempT = (*theVector)(0);
            ET = (*theVector)(1);
            Elong = (*theVector)(2);
      TempTmax = (*theVector)(3);
      this->getElongTangent(tempT, ET, Elong, TempTmax);
            (*theVector)(0) = tempT;
      (*theVector)(1) = ET;
      (*theVector)(2) = Elong;
            (*theVector)(3) = TempTmax;    }
    return 0;  }
  return -1;}
//this function is no use, just for the definiation of pure virtual function.
Int Concrete02ThermalSCC::setTrialStrain(double strain, double strainRate)
{     opserr << "Concrete02ThermalSCC::setTrialStrain(double strain, double strainRate) - should never be called\n";
  return -1;}
```